INVESTIGATING THE USE OF MULTIPOTENT ADULT PROGENITOR CELLS FOR TREATMENT OF DUCHENNE MUSCULAR DYSTROPHY: A TRANSLATIONAL APPROACH

A DISSERTATION
SUBMITTED TO THE FACULTY OF THE GRADUATE SCHOOL
OF THE UNIVERSITY OF MINNESOTA
BY

Sarah Anne Frommer

IN PARTIAL FULFILLMENT OF THE REQUIREMENTS
FOR THE DEGREE OF
DOCTOR OF PHILOSOPHY

Catherine M. Verfaillie, MD and Paul A. Iaizzo, PhD

August 2008

Acknowledgements

I would like to thank first and foremost my wonderful advisors, Dr. Verfaillie and Dr. Iaizzo, for their guidance and valuable knowledge. Next, I would like to thank Neda Shahghasemi, Andy McCullough, Dan Geoffrion, Jihan Jacobs, Dawn Qiu, Keriann Schulkers, David Abts, Erica Delin, Priya Muthu, Arjun Menon, Brendan McKnight, and Amanda Bartz, who were the many students who volunteered their time on my projects. Yves Heremans, PhD for his invaluable histology advice. Jonathan McCue, MD for his help with femoral artery ligations. Lucas Chase, PhD for his invaluable quantitative PCR advice. Additionally, Monica Mahre and Bill Gallagher from the Iaizzo lab and Lauri Andersen from the Verfaillie lab for their administrative support.

Lastly, I was very fortunate to receive funding from many sources. First I would like to thank Dr. John Day who granted funding to my project through the Nash Avery Search for Hope Fund. I would like to thank Dr. Dave Thomas who granted me the NIH Muscle Training Grant for my first two years. Dr. Denis Clohisy who granted me the NIH Musculoskeletal Training Grant for my last three years. And finally, the MD/PhD Program for funding my medical training.

Dedication

This dissertation is dedicated to my father, Robert Lee Frommer, PhD who laid the ground work for my scientific career and has always been there for me.

Sarah Anne Frommer

Word Count 338

Abstract

Taking a "translational" approach to developing clinical therapies is a two step process that requires: 1) Basic science research on clinical diseases; and 2) application of knowledge gained or resultant therapeutics from that research to patient care. The collaboration of basic sciences and clinical sciences will result in greater advancement of knowledge within each field. There are many diseases that have no cure, even with the tools that modern medicine has to offer. A good example of this is Duchenne muscular dystrophy (DMD). Unfortunately, there is no cure and no effective long-term treatment to delay the progression of DMD; modern medicine can only ameliorate the symptoms and attempt to give the patient the best quality of life possible.

It may one day be possible to cure patients if even one of the many experimental therapies for DMD, aimed at restoring dystrophin in skeletal muscle and shown to improve muscle function in dystrophic animals, could be developed clinically. One such therapy is stem cell therapy. The stem cells used in this work are multipotent adult progenitor cells (MAPC). MAPC were first discovered in the Verfaillie lab here at the University of Minnesota- Twin Cities. It was traditionally believed that adult stem cells like hematopoietic stem cells and mesenchymal stem cells could not differentiate into cells outside the mesodermal lineage; however there are currently numerous reports that challenge this thought.

This thesis presents the application of a three-step translational approach toward development of stem cell therapy for treatment of DMD. The three steps are: 1) *In vitro* study of MAPC myogenic potential; 2) *in vivo* study of MAPC myogenic potential; and 3) development of a system to measure functional effects of therapies. Chapter 2 describes multifactorial testing of different cytokines in an effort to develop a protocol aimed at directing myogenic induction. Chapter 3 describes methods developed and subsequently tested to enhance MAPC engraftment in the DMD model mouse upon intramuscular injection. Chapter 4 describes the development and testing of a system aimed at detecting functional differences due to therapy.

Table of Contents

Table of Figures

Table of Tables

INTRODUCTION

Taking a "translational" approach to developing clinical therapies is a two step process that requires: 1) Basic science research on clinical diseases; and 2) application of knowledge gained or resultant therapeutics from that research to patient care. The collaboration of basic sciences and clinical sciences will result in greater advancement of knowledge within each field. Many patients could benefit from translational research, such as those affected by Parkinson or diabetes mellitus type 1, and cancer patients; however it is patients with the incurable diseases that could benefit the most. There are many diseases that have no cure, even with the tools that modern medicine has to offer. Good examples of this are muscular dystrophies, which are a set of diseases that are genetically determined and result in abnormal and failing muscle function due to structural damage to the muscle tissue. The most common muscular dystrophy is Duchenne muscular dystrophy (DMD). It is an X-linked disease that affects approximately 1/3500 live male births of all ethnic groups. Patients typically present with muscle weakness by age 5, are wheelchair-bound by age 12, and die before age 30 due to respiratory and/or cardiac complications [1]. Unfortunately, there is no cure and no effective long-term treatment to delay the progression of DMD; modern medicine can only ameliorate the symptoms and attempt to give the patient the best quality of life possible.

It may one day be possible to cure patients if even one of the many experimental therapies for DMD, aimed at restoring dystrophin in skeletal muscle and shown to improve muscle function in dystrophic animals, could be developed clinically[2-4]. One such therapy is stem cell therapy. Stem cells have the potential to be the next great advance in medicine by providing doctors with a means to cure patients. Stem cells, for the treatment of DMD represent theoretically, an unlimited supply of cells that can be systemically delivered, could target all degenerating muscle cells, including cardiomyocytes, and hence provide a long-term cure for DMD. Although the widespread clinical use of stem cells is many years from being a reality, many investigators have shown proof of principle that stem cells have the potential to be clinically useful [4-7].

The stem cells used in this work are multipotent adult progenitor cells (MAPC). MAPC were first discovered in the Verfaillie lab here at the University of Minnesota- Twin Cities. Since their discovery, a landmark paper was published by Jiang et al. [8] from the Verfaillie lab describing the surprising potency of MAPC. Before this publication, pluripotency, the ability to form tissue from all three germ layers, was only associated with embryonic stem cells. It was traditionally believed that adult stem cells like hematopoietic stem cells and mesenchymal stem cells could not differentiate into cells outside the mesodermal lineage; however there are currently numerous reports that challenge this thought[9-16].

This thesis presents the application of a three-step translational approach toward development of stem cell therapy for treatment of DMD. The three steps are: 1) *In vitro* study of MAPC myogenic potential; 2) *in vivo* study of MAPC myogenic potential; and 3) development of a system to measure functional effects of therapies. Chapter 2 describes multifactorial testing of different cytokines in an effort to develop a protocol aimed at directing myogenic induction. Such a protocol would not only benefit

skeletal muscle development research but would benefit stem cell transplantation for DMD research, by allowing investigators to control the level of myogenic induction. Chapter 3 describes methods developed and subsequently tested to enhance MAPC engraftment in the DMD model mouse upon intramuscular injection. Chapter 4 describes the development and testing of a system aimed at detecting functional differences due to therapy. Finally, Chapter 1 provides background for understanding the disease processes associated with DMD, myogenesis and myogenic repair, skeletal muscle function and properties, stem cell involvement in muscle induction, and the different mechanisms of adult stem cell plasticity.

References

1. Emery, A. E. The muscular dystrophies. *Lancet* **359**, 687-95 (2002).
2. Alter, J. et al. Systemic delivery of morpholino oligonucleotide restores dystrophin expression bodywide and improves dystrophic pathology. *Nat Med* **12**, 175-7 (2006).
3. Lu, Q. L. et al. Functional amounts of dystrophin produced by skipping the mutated exon in the mdx dystrophic mouse. *Nat Med* **9**, 1009-14 (2003).
4. Sampaolesi, M. et al. Mesoangioblast stem cells ameliorate muscle function in dystrophic dogs. *Nature* **444**, 574-9 (2006).
5. Bittner, R. E. et al. Recruitment of bone-marrow-derived cells by skeletal and cardiac muscle in adult dystrophic mdx mice. *Anat Embryol (Berl)* **199**, 391-6 (1999).
6. Gussoni, E. et al. Dystrophin expression in the mdx mouse restored by stem cell transplantation. *Nature* **401**, 390-4 (1999).
7. LaBarge, M. A. & Blau, H. M. Biological progression from adult bone marrow to mononucleate muscle stem cell to multinucleate muscle fiber in response to injury. *Cell* **111**, 589-601 (2002).
8. Jiang, Y. et al. Pluripotency of mesenchymal stem cells derived from adult marrow. *Nature* **418**, 41-9 (2002).
9. Yoon, Y. S. et al. Clonally expanded novel multipotent stem cells from human bone marrow regenerate myocardium after myocardial infarction. *J Clin Invest* **115**, 326-38 (2005).
10. D'Ippolito, G. et al. Marrow-isolated adult multilineage inducible (MIAMI) cells, a unique population of postnatal young and old human cells with extensive expansion and differentiation potential. *J Cell Sci* **117**, 2971-81 (2004).
11. D'Ippolito, G., Howard, G. A., Roos, B. A. & Schiller, P. C. Isolation and characterization of marrow-isolated adult multilineage inducible (MIAMI) cells. *Exp Hematol* **34**, 1608-10 (2006).
12. Kogler, G. et al. A new human somatic stem cell from placental cord blood with intrinsic pluripotent differentiation potential. *J Exp Med* **200**, 123-35 (2004).
13. Kucia, M. et al. Morphological and molecular characterization of novel population of CXCR4+ SSEA-4+ Oct-4+ very small embryonic-like cells purified from human cord blood: preliminary report. *Leukemia* **21**, 297-303 (2007).
14. Kucia, M. et al. A population of very small embryonic-like (VSEL) CXCR4(+)SSEA-1(+)Oct-4+ stem cells identified in adult bone marrow. *Leukemia* **20**, 857-69 (2006).
15. Gupta, S. et al. Isolation and characterization of kidney-derived stem cells. *J Am Soc Nephrol* **17**, 3028-40 (2006).
16. Anjos-Afonso, F. & Bonnet, D. Nonhematopoietic/endothelial SSEA-1+ cells define the most primitive progenitors in the adult murine bone marrow mesenchymal compartment. *Blood* **109**, 1298-306 (2007).

CHAPTER 1: BACKGROUND

1.1 Duchenne Muscular Dystrophy

1.1.1 Clinical Presentation and Etiology

Muscular dystrophies are a set of diseases that are genetically determined and result in abnormal function due to structural damage to the muscle tissue. The prototypical disease is Duchenne Muscular Dystrophy (DMD). It is an X-linked recessive disease that affects approximately 1/3500 live male births of all ethnic groups. DMD characteristically follows a progressive degenerative course with patients usually presenting at 3-5 years with elevated creatine kinase (CK) levels, pseudohypertrophic calf muscles, decreased levels of physical ability, and sometimes mild, non-progressive mental retardation. Patients are usually wheelchair-bound by age 12 and typically die by their mid-twenties due to respiratory failure and/or cardiomyopathy. Throughout the lifetime of the patient, patients can develop aside from striated muscle and mental abnormalities, delayed gastric emptying[1] and abnormal retinal neurotransmission[2]. Interestingly, the intrinsic laryngeal muscle[3] and extraocular muscle[4] groups are spared for reasons which are still unclear. Presently, there is no definitive treatment for DMD. Treatment focuses on prolonging survival and improving quality of life. This includes weight management, physical therapy to promote mobility and to prevent contractures, monitoring and surgical intervention for orthopedic complications, and routine monitoring for cardiomyopathy [5]. Currently available treatments do little to improve muscle function or slow muscle degeneration.

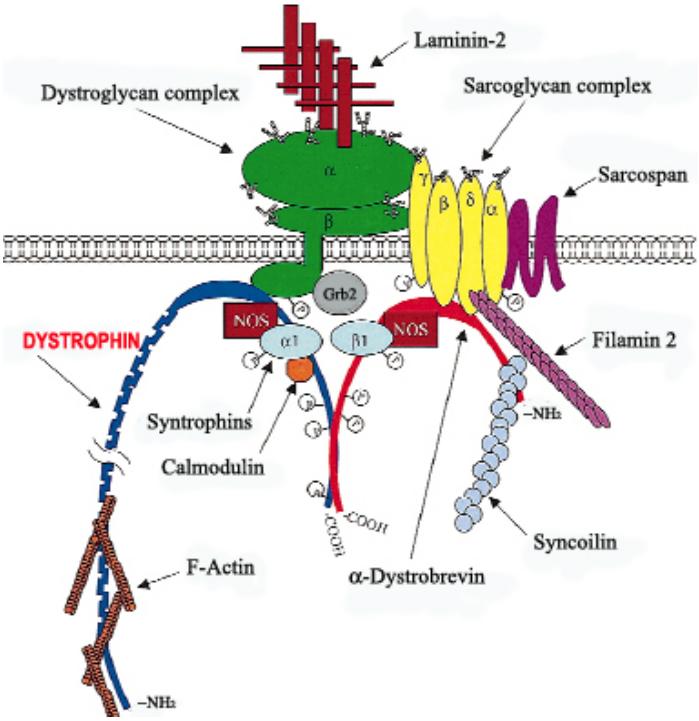

Figure 1.1. Dystrophin-Glycoprotein Complex. Adapted from Rando, Muscle & Nerve 2001

The etiology of this disease is a mutation in the dystrophin gene located on the X-chromosome. The dystrophin gene codes for a 427-kDa protein, dystrophin, as well as non-muscle isoforms, such as Dp260, Dp140, and the more common Dp71[6,7]. In skeletal muscle, dystrophin links F-actin to dystroglycan, a transmembrane protein consisting of a α- and β-subunit. All together dystrophin, the dystroglycans, the

dystrobrevins, the syntrophins, sarcospan, neuronal nitric oxide synthase (nNOS), and a four transmembrane complex of glycoproteins called the sarcoglycans (α, β, δ, γ), form the dystrophin-glycoprotein complex (DGC) [8]. The DGC is responsible for ultimately linking cytoskeletal F-actin to laminin-2, which is a structural protein in the extracellular matrix [9] (Figure 1.1). Mutations in the C-terminal region or DGC binding region, of dystrophin result in more severe phenotypes of DMD[10]. This evidence along with the observation that missing components of the DGC cause other forms of muscular dystrophies, initially suggested that destabilization of the DGC was the primary cause of muscle damage[11,12]. However, it was later found that stabilization of the DGC by Dp71 at the sarcolemma did not prevent the severe phenotype[13,14]. This new evidence shifted the theory that dystrophin had merely a static structural role to the thought of a dynamic role through signal transduction and DGC stabilization.

There are many hypotheses as to how dystrophin deficiency can lead to muscle deterioration. The most common hypothesis is that a loss of dystrophin causes instability of the cell membrane during contraction, thus causing microlesions in the cell membrane. Membrane instability has been supported by the use of low molecular weight dyes such as Procion orange and Evans Blue[15]. Through these microlesions, extracellular calcium can enter the muscle fiber to activate calpains. When activated, calpains cause cell membrane proteolysis, which then further causes an influx of calcium and ultimately muscle fiber death. Fiber necrosis marks the beginning of the degeneration cycle, which is followed by massive inflammation and fiber atrophy. The regeneration cycle begins when resident muscle stem cells, called satellite cells, are induced to proliferate and then fuse with each other and with the existing myofibers in order to repair the damage. Histologically, this is represented by the appearance of centralized nuclei and hypertrophic fibers. In normal animals, the satellite cell pool is sufficient to repair damage caused by daily wear and occasional muscle injury. However, in a dystrophic animal where there is a continual cycle of severe degeneration and regeneration, the satellite cell pool is insufficient and essentially "burns out," resulting in the replacement of muscle fibers by fat and connective tissue [16,17].

A second hypothesis addresses the observation that there is an associated loss of nNOS with dystrophin protein loss or truncation[8,18]. Nitric oxide synthase (NOS) is responsible for the production of nitric oxide (NO) from L-arginine. NO is an important signaling molecule and is best known for its role in vasodilation. In skeletal muscle, nNOS is anchored to the sarcolemma by dystrophin and α1-syntrophin. When there is a loss of either protein, nNOS moves from its membrane associated position to the cytoplasm and undergoes rapid degradation[8]. Reduction of NO is believed to cause a localized functional ischemia in the muscle tissue during increased physical exertion. Although loss of nNOS alone does not cause a dystrophic phenotype, it is argued that when added to the loss of the DGC there is an exacerbation of the phenotype[19].

The current therapy for DMD is to prescribe a regular administration of glucocorticoid corticosteroids, such as prednisone, prednisolone, and deflazacort. Studies have shown that there is some stabilization in muscle degeneration and increase in muscle strength; however it is only of short term benefit, and commonly lasts only for 6 months to 2 years before muscle degeneration resumes its

progression. In addition, the considerable side effects of corticosteroid use, such as weight gain, behavioral abnormalities, and bone demineralization, limit their clinical use [20,21].

1.1.2 Experimental Therapies

Current treatment for DMD patients is limited and ultimately does little for the patient in the long-term. Thus, research is being conducted to find better therapies and ideally a cure for DMD. One pharmacological strategy has focused on maintaining calcium homeostasis through the use of calcium channel blockers and calpain inhibitors, which have shown to be of some benefit [22-24]. Other pharmacological strategies that show potential have included the use of compounds to increase muscle strength, such as clenbutarol and creatine [25,26]; compounds that increase muscle mass, such as myostatin inhibitors, deacetylase inhibitors, and IGF-1 [27-30]; and compounds that decrease inflammation and fibrous tissue formation, such as cromolyn, the flurbiprofen derivative HCT 1026, and the TNF-α blocker Etanercept[31,32,33]. The use of pharmacologic agents is desirable because they can be delivered systemically; however they possess major therapeutic limitations because they are non-specific, often affecting non-target tissues, and they do not offer a long-term cure.

Because it is still unknown exactly how absence of dystrophin results in such a severe phenotype in humans, the only potential long-term cure currently is thought to require incorporation of dystrophin or a similar protein into the dystrophic fibers to correct structural and signaling deficiencies. Gene therapy and cell transplantation have been actively investigated as a method to accomplish this. Gene therapy research has mainly focused on three areas: 1) dystrophin gene replacement, 2) homologous gene up-regulation, and 3) exon skipping. In general, gene replacement research using non-viral and viral vectors has advanced greatly in the past few years; however for this therapy to be clinically useful, problems with efficient delivery, tissue specificity, long-term gene expression, and immune rejection have to be overcome.

Early studies using this technology have given some insights as to hurdles investigators will have to surmount to cure DMD. Full-length dystrophin cDNA is 14 kb long, which made it difficult to use adenoviral (AV) and adeno-associated viruses (AAV); previously shown to be the most effective in muscle[34-36]. Researchers investigated if a truncated dystrophin could ameliorate the dystrophic phenotype, as seen in the milder dystrophy Becker muscular dystrophy (BMD), and found that it was effective[36,37]. The truncated dystrophin products, mini-dystrophin (6.4 kb) and micro-dystrophin (3.7 kb) were created by deleting portions of the rod domain, which accounts for ~76% of the protein. Initial studies seemed promising in normal mice[38,39], but long-term dystrophin expression has been hampered by immune rejection of viral proteins and dystrophin in *mdx* mice[40].

Homologous gene up-regulation is another area of research that has shown some promise. It was observed that in dystrophin deficient animals, there was an up-regulation of utrophin. Utrophin, also known as dystrophin related protein (DRP), is a homologue of dystrophin that is up-regulated during muscle regeneration. Due to its similar structure to dystrophin, it is believed that in mice, utrophin can compensate for the loss of dystrophin, thus resulting in the milder phenotype of *mdx* mice, a mouse lacking

dystrophin[41]. This observation led to the hypothesis that up-regulation of utrophin may help protect the *mdx* mouse from sarcolemmal damage[42]. Indeed, it was shown that over-expression of utrophin did ameliorate the dystrophic phenotype in *mdx* mice [43-45].

An exciting area of gene therapy research is the use of antisense oligonucleotides (AON) to cause exon skipping. The dystrophin gene is the largest known gene in humans, containing 79 exons. As previously mentioned, BMD patients have a milder phenotype compared to DMD patients even though the same gene is affected. The difference between the two patient populations is that mutations in DMD patients disrupt the reading frame whereas BMD related mutations maintain it, resulting in a partially functional truncated protein. Researchers have shown in the *mdx* mouse which has a nonsense mutation on exon 23, that the use of AON targeted to skip exon 23 could restore significant levels of truncated dystrophin[46-48].

Cell therapies are another area being investigated as a treatment for muscular dystrophy. The different cell types tested thus far and their efficacy for transplantation will be addressed later in this chapter.

1.1.3 DMD models

Mammalian animal models for DMD include mice, cat, and dog. All three models exhibit a biochemical dystrophinopathy similar to humans, however the phenotype and resultant clinical progression of DMD is variable. Feline hypertrophic muscular dystrophy (FHMD) presents with an absence of dystrophin in skeletal muscle along with myofiber hypertrophy and elevated CK levels; however little muscle weakness is exhibited due to replacement of damaged fibers with regenerating hypertrophic fibers rather than by connective tissue [49,50]. The FHMD model is not widely used as a model for DMD due to the mild phenotype and the expense of using a large animal model.

The canine models (Golden retriever muscular dystrophy (GRMD) and German short-haired pointer (GSHP)), present with a more representative phenotype of clinical DMD, usually presenting with an absence of dystrophin in skeletal muscle, myofiber hypertrophy, elevated CK levels, and muscle weakness and fibrosis, resulting in early mortality due to cardiomyopathy and/or respiratory failure. Although the canine models are the most representative of DMD, their use as a model in DMD research has been limited by the variable phenotype from litter to litter, and the expense of breeding and maintaining colonies.

The most widely used model for DMD has been the C57BL/10ScSn-DMD$^{mdx/J}$ (*mdx*) mouse. The *mdx* mouse presents with an absence of dystrophin in skeletal muscle and elevated CK levels; however, like the FHMD model, the *mdx* model has a mild phenotype. A period of massive muscle degeneration begins at 3 weeks and continues to ~6-8 weeks of age. After this period, only mild myopathy and fibrosis can be seen, aside from the diaphragm [51], until ~15 months when degeneration resumes [52]. This observation suggests that murine muscle regeneration is more effective than human and canine muscle regeneration. Despite the mild phenotype, the *mdx* model has been an invaluable tool to investigate DMD therapies.

Gene and cell therapies can be readily evaluated by measuring expression of dystrophin through immunohistochemistry, as *mdx* mouse muscle lacks expression of dystrophin (other than the occasional revertant fiber). Although, the mice do not have severe muscle weakness, they do exhibit sarcolemmal instability as evidenced by low molecular weight dye assays, in addition to exhibiting susceptibility to muscle damage due to eccentric contractions [53,54].

To address problems with the traditional *mdx* model, other *mdx* models have been developed. As seen with human DMD, the *mdx* model will have occasional revertant fibers that express dystrophin. Although revertant fibers occur at a low frequencies (~1-7%), this interferes with the evaluation of the efficiency of gene and cell therapies [55]. To remedy this, the *mdx*^{2cv}, *mdx*^{3cv}, *mdx*^{4cv}, and *mdx*^{5cv} models were generated through ENU mutation [56]. Of these models, the *mdx*^{4cv} and *mdx*^{5cv} models had 10-fold fewer revertant fibers than traditional *mdx* mice. However, as the number of revertant fibers is insufficient to explain the mild phenotype of *mdx* mice, the *mdx*^{4cv} and *mdx*^{5cv} models still exhibit a mild phenotype. Additionally, immunodeficient models, such as *mdx*/nude and *mdx*/SCID, have been created to evaluate xenogeneic cell therapies and gene therapies, without the interfering problem of immunological rejection of the newly expressed gene products.

In an effort to create a murine model with a severe phenotype, different strategies have been used with the *mdx* mouse. Myotoxic agents such as cardiotoxin, notexin, and bupivacaine have been intramuscularly injected to cause reversible muscle damage. A second strategy is the use of high-dose radiation to stop satellite cell-mediated repair. A third strategy is to chronically exercise the *mdx* mouse through swimming or treadmill use[57]. Finally, the *mdx*/utrophin double knockout mouse was developed. The *mdx*/utrophin$^{-/-}$ mice are kyphotic, exhibit severe growth retardation, and typically die very early (~12-20 weeks) [58], making them good models for clinical DMD.

1.2 Skeletal Muscle Development and Regeneration

Skeletal muscle development has been investigated in many organisms; however as the representative model for vertebrate myogenesis, mouse skeletal muscle development will be mostly described. Mammalian myogenesis can be broken up into two phases, prenatal and postnatal. Prenatal myogenesis consists of three stages: 1) specification, 2) determination, and 3) differentiation. Myogenic specification is the stage when a somitic cell becomes a muscle progenitor cell (MPC) that is multipotent, or uncommitted to a muscle fate, and expresses the stage specific markers Pax3 and Pax7. At this stage, the MPC is not only capable of becoming skeletal muscle, but can become bone, cartilage, or dermis. Myogenic determination is the stage where the MPC loses its multipotency and commits to a muscle fate through the expression of Myf5 and MyoD; however it should be noted that this stage does not have to be irreversible, as previously thought. In fact Asakura et al.[59] and Wada et al.[60] demonstrated that primary myoblasts expressing MyoD, Myf5, and Pax7 could be induced to differentiate into osteocytes or adipocytes. Finally, myogenic differentiation is the stage where the determined muscle progenitor cells,

termed myoblasts, form a multinucleated myotube through fusion and express mature contractile proteins [61].

Postnatal myogenesis is also known as skeletal muscle regeneration. Regeneration occurs at very low levels with average physical activity; however under stressful conditions, for example strenuous exercise or myopathy, post-natal skeletal muscle has the capacity to renew itself through a pool of myogenic stem cells, called satellite cells. It is generally thought that regeneration follows a pathway very similar to that of prenatal myogenesis [62]. Both phases of myogenesis and important signaling pathways will be described further.

1.2.1 Prenatal Myogenesis

During embryonic development, the zygote undergoes cleavage and then gastrulation. The gastrulation process forms the three germ layers of the developing embryo; ectoderm, endoderm, and mesoderm. The ectoderm gives rise to structures like the brain, spinal cord, and outer epithelium of the body. The endoderm gives rise to structures like the liver, pancreas, and lung. It is the mesodermal layer that gives rise to skeletal muscle, in addition to structures such as heart, blood, dermis, and cartilage. There are five regions of the mesoderm: chordamesoderm, dorsal/paraxial mesoderm, intermediate mesoderm, lateral plate mesoderm, and head mesenchyme [63].

All skeletal muscle is formed from the dorsal/paraxial mesoderm, except the facial muscles that are derived from head mesenchyme. In the developing mesoderm, thick bands of paraxial mesoderm form along both sides of the notochord. Around 7.5-8 days post-coitus (d.p.c.), the primitive streak regresses, the neural folds begin to centralize, and the paraxial mesoderm begins to form blocks of cells called somites. Somitogenesis involves the "budding off" of new somites from the rostral paraxial mesoderm at regular intervals. The budding off interval as well as the number of somites formed is characteristic of a vertebrate species; for example mice form 65 somites and snakes form 500. Thus, somitogenesis plays an important role in how the bodies of different vertebrates are segmented or patterned. The exact mechanism for somite formation is not established, but what is known is that whorls of cells, called somitomeres, form in the paraxial mesoderm and as the somitomeres move anteriorly they compact into an epithelial somite that expresses fibronectin and N-cadherin [63].

As somites mature they can be divided into two regions, which demark their specification: sclerotome and dermomyotome. Cells in the sclerotome region are located nearest to the neural tube, which secretes sonic hedgehog (Shh) protein. Shh exposure induces the cells of the sclerotome to express Pax1 and Pax9, thus specifying the cells to a cartilage fate that later develop into vertebral and rib structures. Under the influence of neurotrophin 3 (NT-3) secreted by the neural tube, the cells located in the central dermomyotome region become specified for the formation of posterior dermis and express Msx1 and Dermo1. The medial and lateral parts of the dermomyotome give rise to specified MPC that express Pax3 and Pax7. The medial dermomyotome forms the epaxial muscles (back muscles). It is under the influence of Wnt proteins secreted from the neural tube and long-range Shh signaling from the notochord, which

causes a preferential expression of Myf5. The lateral dermomyotome forms the hypaxial muscles (body wall, limb, diaphragm, and tongue muscles). Under the influence of Wnts secreted by the dorsal ectoderm and BMP4 secreted from the lateral mesoderm; the cells of the lateral dermomyotome preferentially express MyoD, in addition to c-Met [61].

While in the dermomyotome, epaxial and hypaxial MPC undergo a first wave of proliferation and then migrate to a region just beneath the dermomyotome, called the myotome. Once in the myotome, the majority of MPC stop proliferating and begin to differentiate to form primary fibers. These primary fibers are responsible for defining a muscle's location, shape and type. The MPC that form the fore- and hindlimb muscles do not migrate into the myotome; they undergo an epithelio-mesenchymal transition and migrate as single cells into the limb mesenchyme where they form primary fibers [64]. When the dermomyotome disappears, there is a pool of mitotically competent MPC, which express the fibroblast growth factor (FGF) receptor, FGFR4 that migrate into the myotome. FGFR4 expressing MPC are associated with the second wave of proliferation, which is responsible for increasing skeletal muscle mass in the fetus [65].

Before myogenic differentiation can occur, the proliferating myoblasts must arrest in the G_1 phase of the cell cycle and then enter a G_0 state. This occurs when there is depletion or down regulation of mitotic factors, such as FGFs. After exiting the cell cycle, myoblasts align with each other, which is mediated by interaction with extracellular matrix components such as fibronectin, and begin to express the intermediate filaments, desmin and vimentin, as well as M-, N-, and R-Cadherins. Desmin and vimentin are important proteins for the alignment and elongation of pre-fusion myoblasts. The cadherins are a family of transmembrane cell adhesion glycoproteins, necessary for mediating migration, myoblast fusion, and connection of satellite cells to the myofiber [66]. The final step of differentiation involves innervation of the myofiber by a motoneuron.

1.2.2 Postnatal Myogenesis

Normal postnatal skeletal muscle undergoes very little daily cell turnover; it is believed that daily wear and tear only leads to replacement of ~1-2% myonuclei every week [67]. After birth, increases in muscle mass are largely attributed to muscle hypertrophy (addition of myonuclei to existing fibers); however, when a muscle experiences injury, it has the capacity for rapid and complete regeneration. Genetic defects, extensive physical activity, and chemical injury are just a few ways that induce injury, but regardless of the injury type the initial event of muscle degeneration involves necrosis of the myofiber. Necrosis is usually the result of increases in intracellular Ca^{++} due to either the influx of extracellular Ca^{++} following cell membrane disruption or sarcoplasmic reticulum damage. The primary consequence of increased intracellular Ca^{++} levels is activation of calpains, which are calcium-activated proteases that can break down structural and contractile proteins [68]. Within the first few hours of fiber necrosis, there is infiltration of neutrophils and then ~48 hours later there is infiltration of macrophages. Macrophages act to phagocytose cellular debris and secrete factors such as leukemia inhibitory factor (LIF) that activate satellite cells to begin proliferating. Satellite cells, which will be discussed more in depth later, are

myogenic stem cells capable of replenishing themselves and producing myoblastic progeny. These progeny can fuse to existing fibers or differentiate into new myofibers using a pathway that is very similar to embryonic differentiation; the myoblasts align with each other and then fuse to form new fibers. New fibers become functional within days and morphologically, they are indistinguishable from undamaged muscle [62].

1.2.3 Skeletal Muscle Signaling Pathways

In order to develop methodologies for skeletal muscle induction, it is necessary to evaluate the pathways involved in myogenesis. Myogenesis involves an intricate web of many signaling pathways; however there are a few specific pathways, which will be described that are highly involved in myogenesis.

1.2.3.1 Sonic Hedgehog

Sonic hedgehog (Shh) is a member of the Hedgehog (HH) family of signaling molecules. In vertebrates, Shh functions to mediate long-range and short-range signaling for dorso-ventral patterning in the specification of neural, mesodermal, and endodermal stem cell lineages, for limb patterning, for granular cell proliferation, and for suppression of tissue apoptosis. It has been shown that Shh plays a key role in epaxial myotome formation by targeting Myf5 via long-range signaling [69]. Shh acts by binding the Patched (Ptc) receptor which frees the transmembrane protein Smoothened (Smo) to activate the nuclear transduction of Gli, which is a zinc-finger transcription factor that binds to the Myf5 promoter to induce Myf5 expression (Figure 1.2).

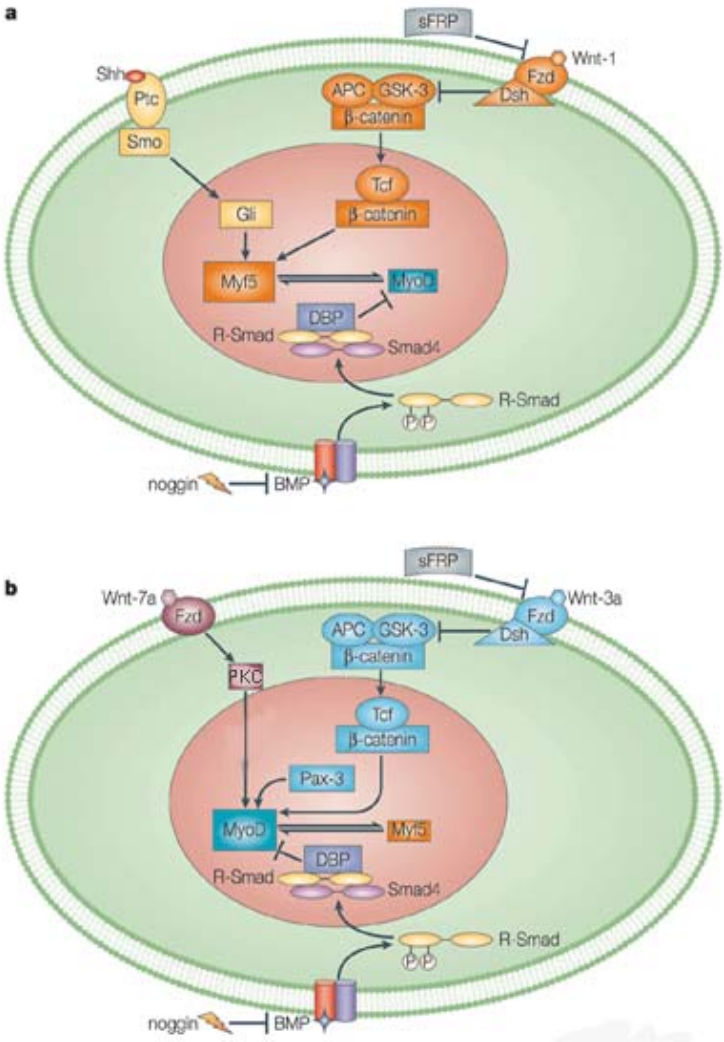

Figure 1.2. Pathways involved in (a) MyoD and (b) Myf5 activation. Modified from Parker et al., Nature Reviews Genetics 2003

1.2.3.2 Wnt Pathway

The Wnt family of genes encodes for over twenty cysteine-rich secreted glycoproteins that play a very important role in development. Wnt proteins have been implicated in axis formation, and kidney, CNS, hematopoietic, and skeletal muscle determination. For skeletal muscle determination, Wnt1 and Wnt3a act by binding to the Frizzled (Fzd) receptor on the cell membrane of target cells, which then activates Disheveled (Dvl), leading to the inactivation of glycogen synthase kinase-3β (GSK-3β). Inhibition of GSK-3β, along with the adenomatous polyposis of the colon (APC) protein, acts to stabilize β-catenin so it can translocate into the nucleus. Once in the nucleus, it associates with T-cell factor (Tcf) to bind to the Myf5 and MyoD genes, and induce their expression. Wnt1 and Wnt3a are secreted from the neural tube to activate Myf5 and MyoD, respectively[70]. Wnt7a is secreted from the dorsal ectoderm and activates MyoD through a pathway independent of β-catenin but dependent on Pax3 and protein kinase C (PKC) activity[71] (Figure 1.2).

1.2.3.3 TGF-β Superfamily

The TGF-β superfamily of proteins is divided into three groups: TGF-βs, bone morphogenetic proteins (BMPs) and activins. Cytokines from this family have important functions during embryonic development in pattern formation and tissue specification, in addition to functions in the adult such as tissue repair and immune modulation. The TGF-β superfamily of proteins acts on their target genes by binding to their respective receptors on the cell surface, which causes phosphorylation of receptor regulated-SMADs (R-SMADs). The phosphorylated R-SMADs form a complex with SMAD4, which is then translocated to the nucleus, bind to the promoters of MyoD and Myf5 and induce their expression [72]. At high concentrations, the TGF-β family of proteins acts to inhibit myogenesis and can even induce apoptosis, but at low concentrations they are required for muscle differentiation. TGF-β1 does not affect DNA binding or heterodimerization of the myogenic regulatory factors directly, but is believed to act on the co-factor, myocyte enhancing factor-2, to prevent it from being imported into the nucleus [73].

From the TGF-β superfamily, BMP4 and BMP7 have the most pronounced effects on myogenesis. BMP4 is initially expressed throughout the ectoderm and mesoderm regions of the late blastula, but is later restricted to the ventrolateral marginal zone. BMP4, along with BMP7 acts to ventralize the mesoderm, inducing the mesoderm to commit toward a hematopoietic fate rather than a skeletal muscle fate. Somites express noggin and follistatin which inhibit the ventralizing action of BMP4 and BMP7, respectively [63]. Although it would seem that BMP4 and BMP7 have negative effects on myogenesis, they do play an important regulatory role. BMP4 and BMP7 promote a proliferative state by inducing Pax3 expression, thus allowing for formation of enough MPC to constitute the muscles for the entire body [74]. In addition, BMP4 inhibits MyoD expression in the dermomyotome. By inhibiting MyoD expression, BMP4 signaling inhibits premature differentiation of myogenic cells from the somites; if BMP4 signaling is blocked, those cells do not migrate from the dermomyotome to the limbs [75].

The exact action of activins on myogenesis is less clear. However, during embryogenesis it is known that activins act to repress neural induction, but specify cells to an endodermal and mesodermal fate.

This was demonstrated by Kubo et al., using varying concentrations of Activin A in embryonic stem cell (ESC) differentiation cultures. They demonstrated that in the absence of Activin-A, cells allowed to differentiate in embryoid bodies (EBs) express neural markers. When Activin at concentrations <30ng/mL was added, skeletal muscle and hematopoietic genes became expressed whereas high concentrations of Activin-A (50-100ng/mL) induced endodermal gene expression [76]. Nevertheless, the exact action of Activin in the myogenic pathway needs to be further investigated.

Finally, myostatin is a TGF-β related factor that has an exclusive function during myogenesis. Myostatin is a skeletal muscle specific protein that is a negative regulator of muscle growth. Double negative mutations of the myostatin gene in mice and cows results in a significant increase of muscle mass through increased proliferation of MPC[77,78]. This makes myostatin blockade an alluring therapy for muscular dystrophies and AIDS wasting syndrome, where an increase in muscle mass would be desirable.

1.2.4 Key Genes involved in Myogenesis

There are many genes involved in myogenesis; however the most commonly associated genes will be described. A summary of gene roles during myogenesis is provided in table 1.1.

1.2.4.1 Pax3 and Pax7

Pax3 (*Splotch*, Sp) and Pax7 are paired-box-containing transcription factors important in the control of developmental processes. Pax3 is considered an early marker for myogenic specification due to its expression in pre-somitic mesoderm and in early somites. Pax3 has been shown to be important for migration from the dermomyotome and for proliferation of myogenic precursor cells; $Pax3^{-/-}$ mice do not survive to term and lack limb and diaphragm musculature due to impaired lateral migration from and reduced proliferation of the somitic dermomyotome. Interestingly, mice that are $Pax3/Myf5^{-/-}$ do not express MyoD, an important myogenic regulator, suggesting their parallel effect on MyoD regulation and their upstream actions in myogenesis [79]. The Pax3-FKHR fusion protein has been implicated in 60% of all alveolar rhabdomyosarcomas, an aggressive pediatric striated muscle cancer[80], suggesting a strong role for Pax3 as a muscle specification gene. In the embryonic carcinoma cell line, P19, overexpression of Pax3 induces expression of myogenic associated genes such as Mox1, Six1, Eya2, and MyoD; additionally Pax3 is necessary for expression of Six1, Eya2, and Lbx1[81,82].

Pax7, a homologue of Pax3, can be detected in the maturing somite along with Pax3. Pax7 is not essential for myogenic specification; however it is important for the formation of satellite cells in post-natal limb muscle. In $Pax7^{-/-}$ mice, there is a complete absence of satellite cells in the limbs. In addition, muscle-derived stem cells from $Pax7^{-/-}$ mice demonstrated an inability to differentiate into muscle suggesting that the satellite cell progenitor may come from an adult stem cell pool [83]. Overexpression of Pax7 in cultured myoblasts resulted in cell cycle exit and a down-regulation of MyoD with subsequent reduction in myogenin expression; suggesting a self-renewal role of Pax7 in satellite cells[84].

1.2.4.2 Myogenic Regulatory Factors

MyoD, Myf5, Myf6, and myogenin are part of the basic helix-loop-helix (bHLH) transcription factor family. Together they are termed myogenic regulatory factors (MRFs) due to their muscle specificity and ability to induce myogenesis in non-muscle cells [85]. bHLH proteins act by forming homo- and heterodimers that have an affinity for the DNA sequence CANNTG, which is referred to as the E-box. When MRFs form dimers with another bHLH protein, E2A, their affinity for the E-box increases 10-fold. E2A is required for myogenesis; however it can not commit a cell to a myogenic fate like MRFs can. When the MRF-E2A complex binds the E-box of skeletal muscle genes, it signals for that gene to be transcribed.

MyoD and Myf5 are important for muscle determination and are termed primary MRFs. Low levels of Myf5 are expressed along with Pax 3 and Pax 7 in myogenic precursor cells of the dermomyotome and their expression level increases in the maturing somite, but in particular in the epaxial myotome. Sonic hedgehog (Shh), produced in the notochord and the floor plate, is essential for Myf5 expression; Shh null mice show a reduction in Myf5 expression in the epaxial domain along with a deficiency in epaxial musculature. Signals from the neural tube and dorsal ectoderm induce MyoD expression in the hypaxial myotome through the Wnt3a-β-catenin pathway and through a β-catenin independent Wnt7a pathway. Originally, it was shown that mice deficient in either Myf5 or MyoD have little to no skeletal muscle deficiencies, but the combined deficiency of Myf5 and MyoD caused mice to die at birth due to a lack of skeletal myoblasts[79]. This suggested that there was some ability for MyoD and Myf5 to complement one another when there is a deficiency of only one factor. Myf6 (also known as MRF4 or herculin) is a secondary MRF, but this was revised after it was found that the Myf5:MyoD double knockout mouse had skeletal muscle if the Myf6 gene was not compromised; the previously described double knockouts did not take into account that the Myf6 and Myf5 genes are genetically linked. In addition to its role as a myogenic determination factor, Myf6 was shown to work with Myf5 to activate MyoD expression[88]. Myf6 is also involved in myofiber formation; however its expression seems less important than myogenin for terminal differentiation, as $Myf6^{-/-}$ mice have only minor defects in their musculature [89].Myogenin is a secondary MRF involved in terminal muscle differentiation, or formation of myofibers. Myogenin has been shown to be the necessary factor for myofiber formation since $myogenin^{-/-}$ mice have normal myoblast formation, but a failure of myofiber formation [86,87].

1.2.4.3 Mesenchyme Homeobox 1 and 2

Mesenchyme homeobox 1 (Mox1) and mesenchyme homeobox 2 (Mox2) are homeobox containing genes expressed in paraxial mesoderm. Initially, Mox1 and Mox2 are expressed together before somites divide into sclerotome and dermomyotome regions. Mox1 but not Mox2 is expressed in the dermomyotome, while both are expressed in the sclerotome. Mox1 is expressed following Pax3 expression and is important for normal formation of the axial skeleton[90]. Mox2 is expressed in migrating myoblasts along with Pax3 and is important for proper limb bud formation, as demonstrated in $Mox2^{-/-}$ mice in which Pax3 and Myf5 expression is decreased in the limb bud[91].

1.2.4.4 Myocyte Enhancing Factors

Since E-boxes can be found at a high degree throughout the genome, there should exist a mechanism to target the MRF-E2A heterodimer to the E-boxes located in muscle specific genes. It was found that the bHLH domain of all MRFs allow for a specific interaction with another family of DNA binding proteins, the myocyte enhancing factor 2 family (MEF2). The MEF2 family is a group of MADS-box (**M**CM1-**a**gamous **d**eficiens-**s**erum response factor) transcription factors, which consists of four genes: MEF2A-D. During embryogenesis, transcriptionally active MEF2 proteins are only seen in the brain, skeletal muscle, smooth muscle, and heart. Later, MEF2 proteins can be found ubiquitously in the developing fetus. Since there are multiple forms of MEF2s, researchers investigated how MEF disruption affects myogenesis in *Drosophila*, which only has one form of MEF2. It was found that loss of MEF2 caused normal formation of myoblasts, but a failure to develop myotubes [92]. In particular, there is a special relationship with myogenin and MEF2C; no other MRF is activated by MEF2C and vice versa. MEF2C interaction with myogenin is believed to cause proper spatio-temporal expression of myogenin; however, MEF2C null mice die at embryonic day 9.5 due to improper heart looping, not skeletal muscle defects [93].

1.2.4.5 Lady Bird-like Homeobox

Lady bird-like homeobox 1 (Lbx1) is another homeobox transcription factor linked to myogenesis. Lbx1 is important for MPC migration and proliferation[94,95]. Lbx1 knockout mice exhibit loss of hindlimb and extensor muscles of the forelimb. Interestingly, this pattern of muscle loss is opposite of that seen in Mox2-/- mice, suggesting opposing roles in MPC migration[91].

1.2.4.6 Muscle Segment Homeobox 1

Muscle segment homeobox (Msx1) is a gene associated with dedifferentiation. Ectopic expression of Msx1 in myotubes resulted in their dedifferentiation into mononucleated cells capable of redifferentiating into cells that express bone, cartilage, fat, or muscle markers[96].

	Specification	**Determination**	**Differentiation**	**Proliferation**	**Migration**	**Other**
Gene						
Pax3	**x**			**x**	**x**	
Pax7	**x**					**Self-renewal**
MyoD		**x**				
Myf5		**x**		**x**		
Myf6		**x**	**x**			
Myog			**x**			

Mox2					**x**	
Lbx1				**x**	**x**	
Msx1				**x**		**Dediff**
Mef2a			**x**			
Mef2c			**x**			

Table 1.1. Summary of Gene Roles in Myogenesis. Abbreviations: Dedifferentiation = Dediff

1.3 Skeletal Muscle Physiology

Skeletal muscle makes movement of the body possible through its highly integrated and organized structure, in addition to its ability to translate an electrical signal to a chemical one that results in contraction.

1.3.1 Sarcomere Structure

The hierarchy of muscle, from macroscopic to microscopic is muscle belly, muscle bundle, fascicle, myofiber, myofibril, and myofilament; without this hierarchy, coordinated movement would not be possible. It is within the myofibril that the contractile unit called the sarcomere, resides. As shown in figure 1.3, the sarcomere is composed of thick and thin myofilaments that are arranged into a regular and repeating matrix, which gives skeletal muscle its striated appearance. The borders of a sarcomeric unit are called the Z-lines, which bisect a region called the I-band. The I-band is the region of the sarcomere composed solely of thin filaments and the thin filaments anchor at the Z-line with the help of the actin-binding protein, α-actinin. Thick filaments anchor at the M-line which bisects the H-zone. The H-zone is the region of the sarcomere that is solely composed of thick filaments and it is contained within the A-band, which is composed of the overlapping thick and thin filaments. The thick filaments consist primarily of polymers of myosin. The myosin molecule is composed of two heavy chains and four light chains, which form a tail and two heads, respectively. The heads of the myosin molecule have two regions essential for contraction; the first is an ATPase region and the second is an actin binding site. The thin filament consists of an actin polymer backbone that forms a complex with

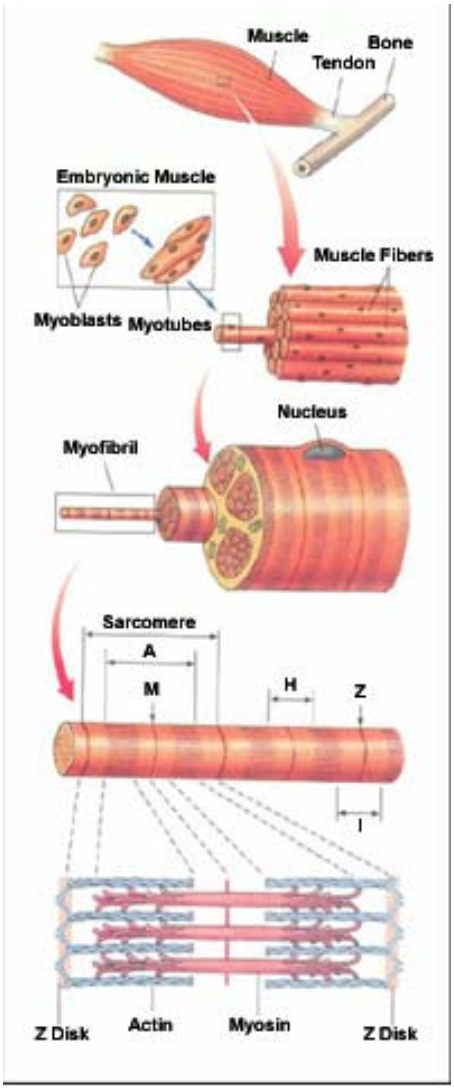

Figure 1.3. Skeletal muscle hierarchy and sarcomere architecture

the thin filament proteins, troponin and tropomyosin. The troponin-tropomyosin complex reacts to changes in intracellular Ca^{++} and is the regulatory unit of contraction [97]. In addition to thick and thin filaments, vertebrate striated muscle contains a third filament system that acts to confer structural stability and elasticity to the sarcomere. Titin, with a relative molecular mass of about 3,000 kD, is the main protein of this third system. Titin molecules extend from Z-discs to M-lines and acts as molecular rulers by setting the length of the sarcomere. The titin filament is also responsible for the resting tension in striated muscle due to spring-like properties [98]. Nebulin is another important giant filamentous protein found in skeletal muscle, which functions as a molecular ruler to determine thin filament length [99].

1.3.2 Skeletal Muscle Contraction

Excitation-contraction coupling (ECC) is the link between the depolarization of the muscle cell and release of Ca^{++} from the sarcoplasmic reticulum (SR) to cause contraction of the myocyte. When a motor neuron is stimulated, the action potential travels down its axon to the axon terminal located at the neuromuscular junction. The change in potential opens voltage-regulated Ca^{++} channels, which allows calcium ions to enter the axon terminal. The presence of calcium causes the already fused acetylcholine (Ach) vesicles of the axon terminal membrane to exocytose into the synaptic cleft. Ach interacts with the Ach receptor on the postsynaptic membrane to cause an influx of Na^{+} and a small efflux of K^{+}. This ion exchange causes a local depolarization of the motor end plate (MEP). This depolarization causes an action potential to propagate along the sarcolemma and down the T-Tubules, thus causing a release of Ca^{++} from the terminal cisternae into the cytosol. Ca^{++} binds to troponin, which is periodically located along the tropomyosin strand. When Ca^{++} is present, it binds to troponin and causes a conformational change in the troponin-tropomyosin complex. This results in the movement of the tropomyosin strand from the myosin binding sites on the actin filaments, thus exposing the binding sites. According to the cross-bridge model, the myosin head can then bind to actin, in addition to ATP, which it then hydrolyzes into ADP and P_i. This releases energy to cock the myosin head into a high-energy form. When myosin binds the actin filament, it causes the release of P_i from the myosin head. This release returns the myosin head to a low-energy state and produces the "power stroke." This action causes a sliding of the thin filaments inward toward the M-line. The myosin head releases from the actin filament when ATP binds and the process is started again.

1.3.3 Skeletal Muscle Fundamental Functional Properties

Evaluation of the progression and treatment of muscle disorders often involves force assessment methodologies. To understand how muscle injury can occur, it is important to understand the fundamental functional properties of skeletal muscle. Muscle injury can occur following mechanical contraction, which includes eccentric contraction (stretch), concentric contraction (shortening), and isometric contraction (contraction at a fixed length), when there is a greater external load compared to the internal contractile capacity of the muscle. Internal contractile capacity is dependent on the interaction of the actin and myosin filaments in the sarcomere. This is demonstrated by the isometric length-tension curve [100], which represents

the force a muscle is capable of generating while held at a series of discrete lengths. When tension at each length is plotted against sarcomere length, a relationship such as that shown in figure 1.4 is obtained. At point D, there is no cross-bridge interaction and thus no force generation. Force generation increases as the number of cross-bridge interactions increases (moving from point D to C). When all of the actin filaments interact with the myosin filaments (point C) without the actin filaments overlapping, maximum force will be generated. As the actin filaments begin to overlap (points B and A), the myosin filaments move closer to the Z-line during contraction, which ultimately acts to limit the strength of the contraction. Figure 1.4 also demonstrates that total force is derived from the addition of the passive and active forces. Passive force can be measured at sarcomere lengths exceeding the normal range (past point C) and increase as the sarcomere length increases. This force is the result of resistance against load from the muscle connective tissue. Therefore, it is not possible to measure active force directly in the presence of passive force; active force is found by subtracting passive force from total force.

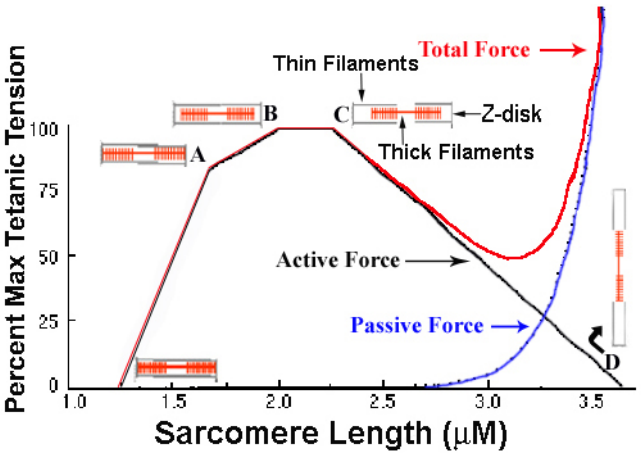

Figure 1.4. Length-Tension Plot

Another important functional property is fatigability of a muscle, which is mostly dependent on fiber type composition. Fiber types are categorized as type I (slow), type IIA (fast oxidative-glycolytic), and type IIB (fast glycolytic). A muscle fiber type is determined by the type of motoneuron innervating it. Most muscles of the body are composed of a mixed population of fiber types; for example, a mostly type I fiber muscle is the soleus, which primarily acts to support the body against gravity, and an example of a mixed type I and type IIB fiber muscle is the gastrocnemius muscle, which needs to be powerful, yet can withstand the demands of a long run.

A muscle fiber demonstrates fatigue when there is a decrease from initial force upon repeated stimulation. Type I fibers exhibit long twitch durations, low peak forces and a high resistance to fatigue. They are resistant to fatigue because they possess a high level of oxidative enzymes. They also possess characteristics that greatly aid in oxidative metabolism: 1) They have small diameters, which may be an adaptation to aid diffusion (absorption of oxygen and loss of carbon dioxide), 2) Have a large number of mitochondria to convert oxygen to ATP, 3) Have a more extensive blood supply, and 4) Contain high concentrations of myoglobin that acts to bind oxygen, which can help to buffer oxygen levels during high demand contractile periods. On the other spectrum, type IIB fibers exhibit short duration twitches, high peak forces, and a low resistance to fatigue. The primary function of these fibers is to generate a very large force of contraction rapidly. Characteristics of type IIB fibers that aid in their action are: 1) They have large

fiber diameters for greater strength of contraction, 2) Have an extensive sarcoplasmic reticulum for increased release of Ca^{++} to initiate contraction, and 3) Have increased levels of glycolytic enzymes for rapid energy release. Type IIA fibers tend to have characteristics of both type I and IIB fibers [101].

1.3.4 Evaluation of Skeletal Muscle Force

Evaluation of skeletal muscle force will be important in the assessment of different therapies for DMD. In the clinical setting, a patient's muscle force is subjectively evaluated on a scale of 0-4+. In animal studies, *in vitro* and *in vivo* methods are currently employed. The two traditional *in vitro* methods are whole muscle[102,103] and skinned fiber baths[104-106]. In whole muscle baths, dissected muscle is attached to a force transducer and stimulated by platinum electrodes while in an oxygenated electrolyte solution. This allows investigators to study the contractile properties of individual muscles rather than muscle groups and tension rather than torque; however investigators are limited to thinner muscles such as the extensor digitorum longus and the soleus due to limited diffusion of oxygen and nutrients *in vitro*. Skinned fiber baths are set up similarly to whole muscle baths; except muscle fibers are dissected from the muscle bundle and incubated with a detergent to remove the sarcolemma, allowing for easier diffusion of electrolytes and oxygen within the fiber. More recently this has been the preferred *in vitro* method to measure dystrophic muscle contractile properties because it has been shown that whole muscle baths are not sensitive enough to detect functional differences when dystrophic animals are compared to wild-type animals[107].

In vivo evaluation of force can be assessed in an alert or an anesthetized animal. Evaluation in an alert animal typically involves use of a force grip apparatus [108], or treadmill endurance protocols [109,110]. These methods are useful for long-term evaluation; however since measurements require voluntary effort from the animal, variance over time is increased which can decrease sensitivity of the test. Involuntary functional evaluation can be *in situ*[111-113] or *in vivo*[114-116]. *In situ* measurements are recorded from muscle that has one tendon dissected out and then attached to a force transducer. This method has the advantages of *in vitro* whole muscle baths and solves one of the disadvantages because larger muscle groups can be tested; however this method does not allow long-term evaluation because it is highly invasive. Involuntary *in vivo* force assessment has been described in humans[117], dogs[118], and mice[116]. In these studies, muscle groups were activated by percutaneous or motor-point stimulation and torque was measured. This method is useful for long-term studies; however whole muscle groups rather than individual muscles are evaluated.

1.4 Stem Cells

For a cell to be called a stem cell it must fulfill certain criteria such as, it is not differentiated, displays a capacity for self-renewal throughout the lifetime of an organism, and its progeny has the potential to differentiate into functional mature cells[119,120] upon tissue injury or during tissue maintenance. The ability to become multiple tissue types is described as potency. Stem cells can be multipotent, i.e. they give rise to a subset of cell lineages; pluripotent, i.e. can give rise to tissue derived from all three germ layers, as well as germ cells; or totipotent, i.e. in addition to forming all three germ layers and germ cells,

the stem cell can give rise to extra-embryonic structures. Early work with stem cells focused on using these cells as *in vitro* tools to investigate embryonic development and cell differentiation, but recently, there has been a shift in focus from their *in vitro* use to their potential *in vivo* use as a clinical therapy.

1.4.1 Embryonic Stem Cells and Skeletal Muscle Induction

Embryonic stem cells (ES cells), defined by stage specific embryonic antigen (SSEA; 1A for mouse ES cells; 3 and 4 for human ES cells), Oct-3/4, Nanog and Rex-1 expression and the presence of telomerase, were first described in 1981 by Evans and Kaufman when they cultured cells isolated from the inner cell mass (ICM) of murine blastocysts [121]. ES cells have also been isolated from human and non-human primates [122-124], in addition to rabbit [125], and pigs [126]. ES cells are considered the quintessential stem cell as they are pluripotent, can be maintained *in vitro* without senescence or loss of differentiation potential, and at least for mouse ES cells, pluripotency can be demonstrated by forming chimeric animals after introduction of ES cells into blastocysts [127,128], in addition to forming teratomas in post-natal animals [121]. *In vitro*, ES cells have been differentiated into cells possessing morphology and function similar to that of *in vivo* tissues, such as cardiomyocytes [129], hepatocytes [76], and neurons and glial cells [130] when allowed to form cellular aggregates, termed embryoid bodies (EBs) or through induction with specific cytokines. ES cell induction into skeletal muscle was initially shown through formation of EBs. This method is nonspecific for skeletal muscle so more directed approaches were developed by exposing EBs to dimethyl sulfoxide (DMSO) or treating EBs with activated MyoD[131], Pax3[82], or β-catenin[132] plus dimethyl sulfoxide (DMSO). Additionally, Kubo et al. demonstrated that the use of low concentrations of Activin A in murine EB cultures directed the cells toward a mesodermal fate, which included skeletal muscle[76]. More recently, reports have been made on directed differentiation protocols capable of producing non-teratoma forming myogenic cells *in vitro* and *in vivo* [133,134].

1.4.2 Adult Stem Cells and Skeletal Muscle Induction

Approximately 10 years ago, the potential of adult stem cells was believed to be limited to the tissue of origin; however many reports have suggested that adult stem cells exhibit plasticity[135-140]. Adult stem cells were known to exist in tissues which undergo continual turnover, such as skin, gut, and blood; as well as tissues where rapid regeneration upon injury would be of great benefit such as skeletal muscle, cornea, and liver. Presently, there are reports of stem cells in the majority of postnatal tissues[141-144]. The newly found potential of adult stem cells has changed the focus on the use of ES cells as clinical therapeutics to include adult stem cells as well. The possible use of stem cells as a therapy for DMD has led to the investigation of their homing and engraftment, as well as induction to skeletal muscle. There is a large body of publications regarding adult stem cells and skeletal muscle induction; however only the more established mesodermal stem cell lines will be described.

1.4.2.1 Satellite Cells and Myoblasts

Satellite cells are a small population of multipotent myogenic progenitors found in skeletal muscle that are required for postnatal muscle growth and repair [145]. Satellite cells are believed to be derived from somitic mesoderm; however there are reports that satellite cells could also be derived from a common myoendothelial progenitor cell [145,146]. Satellite cells are defined by morphology *in vivo*; residing in a space between the sarcolemma and the basal lamina. When muscle is uninjured, satellite cells are in a quiescent state and express Pax7, c-met, M-Cadherin, Myf5 and CD34 [147,148]. In the presence of injury and factors such as, IGF-1, bFGF, and HGF, satellite cells become activated to proliferate and begin to express MyoD, while they continue to express c-met, M-Cadherin, and Myf5 [145]. Satellite cells divide asymmetrically to maintain the satellite cell pool and to produce more differentiated progeny. This progeny, called myoblasts, undergoes further divisions and fuse together to make new myofibers, as well as fuse to existing fibers. Different populations of satellite cells have been described on the basis of morphology [149] or gene expression [150]. Difficulties encountered when considering use of satellite cells or myoblasts for transplantation include insufficient cells to be clinically useful, poor cell survival following transplantation [151], and inability to administer cells systemically as satellite cells appear not to colonize muscle tissue if delivered from the circulation [140]. Due to these problems, previous attempts to utilize satellite/myoblast cell therapy have been disappointing.

1.4.2.2 Mesenchymal Stem Cells

The term mesenchyme encompasses skeletal muscle, bone, blood, cartilage, adipose, and connective tissues. Any stem cell derived from these tissues is generically called a mesenchymal stem cells (MSCs). MSCs have been reported in all mesenchyme tissues; however MSCs are most commonly isolated from bone marrow. MSCs only represent a very small fraction of nucleated cells in marrow (0.001 - 0.01%)[152] and are characterized on the basis of morphology, plastic adherence, ability to differentiate into osteogenic, adipogenic, and chondrogenic lineages, as well as by particular cell surface markers[153,154]. MSC have been described by Wakitani et al. as plastic adherent bone marrow cells that are capable of many divisions and give rise to specialized mesenchymal tissues. The investigators demonstrated that 24 hour exposure to the hypomethylating agents, 5-Azacytidine and 5-Aza-2-Deoxycytidine, could commit rat MSC to a myogenic fate, although at low levels (~5%) [154]. In a different study, Phinney et al. induced mouse MSC to become cells capable of forming multinucleated myotubes after exposure to amphotericin B[155].

Ferrari et al. assessed the *in vivo* differentiation of bone marrow cells to muscle. Engraftment of transplanted unfractionated, adherent and non-adherent bone marrow cells was assessed in cardiotoxin injured tibialis anterior muscles of immunodeficient animals. Intramuscular and intravenous injections demonstrated that <1% donor derived nuclei were present in regenerating fibers. Level of engraftment was not found to be correlated with type of fractionation of transplanted bone marrow cells [140]. Bittner et al. obtained similar results with intravenous transplantation of unfractionated bone marrow in *mdx* mice. It was found that low levels of donor cells could be detected in skeletal muscle as well as cardiac muscle [156].

LaBarge et al. obtained slightly higher levels of engraftment (~3.5%) of unfractionated bone marrow in skeletal muscle after injection of cells into irradiation-exercise-induced injury SCID mice; notably, 12.89% of satellite cells were donor derived [57].

More recently, it has been shown that there is a resident population of cells present in bone marrow that express myogenic markers. Corti et al. demonstrated that a very small percentage of the bone marrow isolated cells express α-sarcomeric actin, desmin, slow myosin heavy chain, MyoD, Myf5, and Pax3 through immunohistochemistry and RT-PCR. The author noted that a higher percentage of muscle marker expressing cells could be found in the non-adherent population of the bone marrow. Transplantation of unfractionated and myogenic fractionated bone marrow into irradiated *mdx* mice revealed that the myogenic fraction of bone marrow engrafted slightly better (3.16%) compared to unfractionated bone marrow (2.25%) [157].

Additional specialized populations of adult stem cells with potential myogenic differentiation ability are described below and include muscle derived stem cells, hematopoietic stem cells, multipotent adult progenitor cells, and mesangioblasts.

1.4.2.3 Muscle Derived Stem Cells

Muscle derived stem cells (MDSC) are distinct from satellite cells. MDSC are defined as non-hematopoietic muscle derived cells isolated by the preplate method. This method involves isolating skeletal muscle and homogenizing the tissue into a single cell suspension and then serially plating the suspension on plastic flasks. The preplate method was originally described as a way to purify skeletal muscle isolates for myoblasts by removing adherent cells [158].

Late preplate cells express muscle markers such as desmin, MyoD, and myogenin without external induction, and express the hematopoietic stem cell markers CD34 and Sca-1. These late preplate MDSC were more resistant to apoptosis 48 hours post-injection into skeletal muscle compared to the earlier preplates [159], and late preplate cells could be detected 10 to 90 days post-injection[160]. Further evaluation of late preplate MDSC by the same group, revealed that these particular cells could be expanded up to 200 population doublings (PD) without indication of senescence or loss of the phenotypic markers, Sca1, CD34, and desmin[161].

Lee et al., demonstrated that a specific population of late preplate cells, called mc13 cells, express the myogenic markers desmin, c-met, MNF, and bcl-2. Following intramuscular and intravenous injection of mc13 cells into *mdx* mice, engraftment of donor cells in muscle was found with partial restoration of dystrophin in the skeletal muscle, but at very low levels [162].

1.4.2.4 Hematopoietic Stem Cells

The prototypical adult stem cell is the hematopoietic stem cell (HSC). HSCs are capable of extensive self-renewal and HSC progeny has the potential to fully repopulate the hematopoietic system in the presence or absence of injury[163-166]. Originally, it was thought that HSC were found only in the bone

marrow, where adult hematopoiesis primarily takes place; however there have been many reports of HSC pools found in non-marrow tissue, such as skeletal muscle, heart, brain, lung, and kidney [144]. In general, HSC have been described as cells that express CD45, Sca-1 (mouse), CD34, c-Kit, and/or have the ability to exclude Hoechst 33342 dye (termed side population cells).

The majority of articles regarding HSC contribution to skeletal muscle have focused on the use of side population (SP) cells. SP cells have been purified from multiple tissues by sorting for the population of cells that excludes Hoechst 33342 dye through the ABCG2 transporter[144]. This fraction of cells, when of myelomonocytic progenitor origin, have been shown to exhibit myogenic and hematopoietic potential, even at the clonal level, which suggests that there may be a common progenitor for myelomonocytic cells and skeletal muscle[167,168].

Gussoni et al., demonstrated that when SP cells were intravenously injected into irradiated *mdx* mice, there was reconstitution of the hematopoietic compartment, incorporation of donor nuclei into the host skeletal muscle, and partial restoration of dystrophin. Levels of engraftment and dystrophin expression were low, but most interestingly the investigators observed donor derived satellite cells [139]; suggesting that myogenic induction of donor cells may not be caused through fusion.

Asakura et al. also demonstrated the presence of donor derived satellite cells following intramuscular injection of muscle derived SP cells in regenerating muscles of SCID mice. The SP population was subfractionated in $CD45^+$ or $CD45^-$ fractions and co-cultured with myoblasts. Both $CD45^+$ and $CD45^-$ SP cells could fuse to form multinucleated myotubes with equal ability. Further studies demonstrated that SP cells were not direct progenitors for satellite cells because they maintained myogenic ability independent of the Pax7 pathway and were not co-purified with satellite cells during FACS/Hoechst isolation [169].

In 2003, two papers were published demonstrating that a single bone marrow derived SP cell can give rise to both blood and muscle [167,168]. In both studies, bone marrow depleted mice were injected with a single SP cell. Their bone marrow was allowed to reconstitute and animals were subjected to skeletal muscle injury to induce regeneration. Both studies detected incorporation of donor derived cells into host myofibers following injury, but at very low levels <0.1%.

Most recently, muscle-derived side population cells were delivered systemically into immunocompetent *mdx*5cv mice via the femoral artery; investigators reported an engraftment level and dystrophin expression approaching 5-8%[170].

Whether these studies demonstrate inherent ability of HSC to generate muscle, or that following fusion with muscle, myogeneic genes are expressed in HSC derived progeny is not clear. In many other tissues the question whether the apparent lineage switch is cell autonomous vs. following fusion with subsequent induction of gene expression consistent with the host cell can be addressed via Cre-Lox genetic tools, or by determining whether donor nuclei are present in host cells. As however muscle fibers are generated by fusion this cannot be addressed for HSC-muscle transdifferentiation. Few, if any studies have carefully examined whether satellite cells that would be of HSC donor origin are created in a cell

autonomous fashion or via fusion.

1.4.2.5 Mesangioblasts

De Angelis et al. described a multipotent cell derived from E9.5 dorsal aorta of MLC3F-nLacZ mice that had the potential to become skeletal muscle or endothelium. These cells, later termed mesangioblasts, expressed the myogenic markers MyoD, M-Cadherin, MNF, and desmin, as well as the endothelial markers VE-Cadherin, CD34, CD61, and P-Selectin under their culture conditions; demonstrating that there could be a common progenitor for endothelial and myogenic cells [146]. Sampaolesi et al. demonstrated that these mesangioblasts, when injected directly into the femoral artery of α-sarcoglycan (α-SG) null mice, could restore α-SG in more than 50% of the soleus muscle fibers 4 months after injection. When treated α-SG mice were compared to untreated α-SG animals, the investigators found that there was a decrease in Evans Blue dye uptake, a marked decrease in fibrosis (by Azan Mallory staining), and a significant increase in specific tension (force/cross-sectional area) of the skeletal muscle. More recently, canine mesangioblasts were isolated and subsequently transplanted arterially into a group of GRMD dogs. Heterologous and gene corrected autologous transplantation of mesangioblasts resulted in dystrophin expression and enhancement of contractile force in hindlimb muscles[118].

1.4.2.6 Multipotent Adult Progenitor Cells

The term pluripotent was originally reserved for defining embryonic stem cell lines; however, the work done by Reyes et al. and Jiang et al. in the Verfaillie Lab has demonstrated that a small population of pluripotent cells may be isolated from post-natal tissues of humans and rodents [136,171].

Multipotent adult progenitor cells (MAPC) have been isolated from bone marrow (rodent and human), brain (rodent), and skeletal muscle (rodent). Human and rodent MAPC were shown to express pluripotent markers such as Rex-1, Oct-4, and SSEAs. Additionally, human MAPC were $CD34^-$, $CD44^-$, $CD45^-$, HLA-class-I^- and class-II^-, and $cKit^-$ and rodent MAPC were $CD13^+$, $CD44^-$, $CD45^-$, class-I and class-II MHC $antigens^-$. Several populations have been cultured for > 100PDs, without telomere shortening or cytogenetic abnormalities, provided that low-density conditions were maintained [136,141,172].

Reyes et al. demonstrated that human MAPC (hMAPC) could be induced to a myogenic lineage, *in vitro*, following 24 hour treatment with 5-Azacytidine. After day 4, MyoD and myogenin could be detected by FACS analysis. On day 15, MyoD and myogenin were absent but sarcomeric actin and fast twitch myosin could be detected through FACS analysis. Additionally, at day 15 fast twitch myosin was detected in >80% of the treated culture when evaluated by immunohistochemistry [172]. *In vivo*, M. Reyes demonstrated that $2x10^5$ hMAPC and 5-Azacytidine pretreated hMAPC injected into the quadriceps of NOD/SCID mice, could be found in the skeletal muscle after 12 weeks and could express dystrophin. Interestingly, cells that had been pretreated appeared to contribute more significantly to the mouse muscle than undifferentiated MAPCs [173].

Jiang et al. demonstrated that rodent MAPC could contribute to most somatic tissues when injected into the developing blastocysts of mice. A single MAPC was found to contribute to >45% of the tissue in one animal after X-Gal staining for Lac-Z expressing donor derived cells. Tissues including the brain, retina, lung, cardiac and skeletal muscle, liver, intestine, kidney, spleen, BM, blood, and skin contained cells derived from the single transplanted MAPC. This study demonstrated that BM-derived single rodent MAPC could integrate into the developing mouse, give rise to cells of various fates, and form functional tissues [136].

Because of the tendency of mouse MAPC to acquire cytogenetic abnormalities, mouse and rat MAPC were isolated at 5% O_2 hypothesizing that this would lead to fewer cytogenetic changes. Although no significant effect was seen on the occurrence of polyploidy, culture at 5% O_2 resulted in the isolation of several clones of MAPCs with significantly higher levels of Oct4. Some mouse and rat MAPC clones obtained express Oct4 mRNA and protein at levels between 10 - 20% of mouse ES cells, which is >1,000 fold higher than in MAPC isolated under normoxic (21% O_2) conditions. However, transcripts for the other ES cell-specific TF, Nanog and Sox-2, were undetectable [174]. Although mouse MAPC express Oct4 mRNA at levels similar to ES cells, they do not form teratomas. We have evidence that high-Oct4-MAPC differentiate much more robustly into endothelium, hepatocytes and insulin-positive cells, and contribute more robustly to the hematopoietic system when transplanted in sublethally irradiated NOD/SCID mice [175]

1.4.2.7 Other Adult Stem Cells Populations With Greater Potential

Since the isolation of MAPC a number of cells with similar pluripotency have been isolated, including a number from bone marrow: human BM derived stem cells (hBMSCs), marrow isolated adult multilineage inducible (MIAMI) cells, multipotent renal progenitor cells (MRPCs) from kidney, and unrestricted somatic stem cells (USSCs) and very small embryonic-like (VESL) cells from cord blood.

Yoon et al. [176] reported the clonal isolation of hBMSCs from human BM that differentiate into the three germ layers and regenerate myocardium after myocardial infarction. hBMSCs have been expanded for more than 140 population doublings without telomere shortening in media containing 17% FBS and maintained at cell densities ranging from 4000-8000 cells/cm^2 on fibronectin coated plates. hBMSCs do not express Oct4, yet differentiate *in vitro* to cells with phenotype of neural and hepatic lineages and when grafted in an ischemic heart into cells with the phenotype of cardiomyocytes, endothelial cells and smooth muscle cells.

MIAMI cells are obtained by plating whole BM initially in media containing 5% FBS and subsequently maintained in media containing 2% FBS in fibronectin coated dishes, at 3% O2, and at cell densities between 1300-1400 cells/cm^2. MIAMI cells express telomerase and Oct4 and Rex-1 and can expand for more than 50 population doublings when cultured with 15% MIAMI cell conditioned medium. MIAMI cells differentiate into osteoblasts, chondroblasts and adipocytes as well as cells with phenotypic features of neural cells and spherical clusters expressing pancreatic genes[177,178] .

USSCs isolated from cord blood, are CD45, HLA class II-negative mononuclear cells with fibroblastic morphology, extended telomere length and *in vitro*/*in vivo* differentiation potential to osteoblasts, chondroblasts, adipocytes, hematopoietic, neural and hepatic cells. The cells were maintained for 40 population doublings without spontaneous differentiation [179] .

Another population of stem cells, VSEL cells, have been isolated from murine BM and human cord blood using multi-parameter cell sorting to obtain a highly enriched cell population with $CXCR4^+$, $Oct4^+$ and SSEA 1^+ (murine)/ SSEA-4^+ (human) characteristics [180,181]. VSEL cells express Oct4, Rex-1 and Nanog as well as markers of tissue committed stem cells like MyoD, GFAP and AFP. Murine VSEL cells are present in the side population of BM cells, enriched in BM of young mice, and differentiate into cells with phenotypic features of cardiomyocytes, neurons and pancreas in co-culture with fresh BM cells. Interestingly, these cells, like murine ES cells, respond by chemotaxis to SDF-1, HGF/SF and LIF gradients.

Using an approach similar to MAPC isolation MRPCs were isolated from rat kidneys. The Oct4 clones obtained, differentiated into cells with phenotypic features of endothelial, hepatic and neural lineages *in vitro* and into cells with the phenotype of renal tubular epithelium in both uninjured as well as injured kidneys *in vivo* [142] .

Recently, a non-hematopoietic/endothelial SSEA-1^{pos} (0.5-1% of all MSC) subpopulation from the mesenchymal compartment of BM was isolated based on negative depletion of CD45/CD11b from adherent cultures or Lin/CD45/CD31 from whole BM. These cells were termed pre-MSC. These SSEA-1^{pos} cells express Oct-3/4, Nanog, and Rex-1. The SSEA-1^{pos} cells could also be sorted from uncultured BM and also express Oct4 and Nanog mRNA and protein [182]. Like MAPC, these cells differentiate at the clonal level into cells of the three germ layers *in vitro* and to multiple mesodermal cell types *in vivo*. Of note, only when MAPC culture conditions were used could the cell phenotype and differentiation capabilities be maintained *in vitro*. Furthermore, SSEA-1^{pos} cells give rise to SSEA-1^{neg} fraction, which did not express pluripotency markers, but not vice-versa suggesting that the Oct4 expressing cells were not the result of re-programming by culture conditions.

Whether any of the cells with greater differentiation potential described above, aside from MAPC, can generate skeletal muscle has not been described.

1.5 Plasticity Mechanisms

An area of debate is the nature of adult stem cell plasticity. Traditionally it was believed that when the three germ layers form, the cells arising from a particular layer become specialized for a particular tissue lineage and that this specification is irreversible [183,184]. Plasticity suggests that a lineage committed cell has the ability to become a cell of another lineage. Four mechanisms have been described to explain plasticity: 1) dedifferentiation, 2) multiple stem cell pools, 3) a singular pluripotent stem cell, and 4) cell fusion. There is evidence to support all four mechanisms, which will be briefly described.

1.5.1 Dedifferentiation

The mechanism of dedifferentiation was demonstrated through the cloning of "Dolly" by Wilmut et al. [185]. They showed that when a nucleus from a somatic cell is inserted into an unfertilized egg, there is dedifferentiation of the nucleus to a pluripotent state and that this resultant egg can form a viable organism. Indeed other investigators have reported similar findings[186,187]. In nature, dedifferentiation can be demonstrated in the *Urodele* order of the class Amphibia. The *Urodele* order includes newts and salamanders, which have long been known to regenerate their limbs and tails, but have also demonstrated regeneration of the jaw, lens, retina and large parts of the heart. The mature cells at the edge of the wound dedifferentiate into a pool of pluripotent progenitor cells, called a blastema, that are capable of differentiating into cells that can reconstitute the damaged or missing tissue [188]. It has been demonstrated that the protein *msx1* participates in the dedifferentiation of mature muscle fibers into mononuclear cells, which are capable of redifferentiating into cells with characteristics of adipocytes, chondrocytes, myocytes, and osteocytes; this dedifferentiation mechanism was demonstrated in C2C12 myotubules [96].

In a recent study, Takahashi et al. demonstrated that forced expression of as few as four transcription factors, Oct4, Sox2, Klf4, and c-myc is necessary and sufficient to reprogram fibroblasts to a more pluripotent state. Such "iPS (Induced pluripotent stem cells)" form teratomas and EBs, and contribute to mouse chimeras [189].

1.5.2 Multiple Stem Cell Pools

A second mechanism for plasticity suggests that in a given tissue, stem cell pools for an unrelated tissue can reside. It has long been known that systemic infusion of granulocyte-colony stimulating factor (G-CSF) and/or stem cell factor (SCF) causes increased levels of peripheral blood progenitor cells (PBPC), which are hematopoietic stem cells that migrate out of the bone marrow into the circulation [190]. HSC can migrate and reside in other tissues; as shown in studies involving reconstitution of the BM with cells derived from skeletal muscle. Initially, reconstitution of the BM was believed to be caused by transdifferentiation of a skeletal muscle stem cell into a HSC [191]. However it was later proved that the BM was actually reconstituted by a progenitor of hematopoietic origins [192]. Another example is the presence of cells in the BM with the characteristics of oval cells, the progenitors for liver and biliary epithelial cells. Work by Oh et al. demonstrated the presence of alpha-fetoprotein and c-Met expressing bone marrow derived cells, which were induced to form hepatocyte-like cells [193]. Thus, studies demonstrating the ability of bone marrow cells to form liver could really be the result of this oval cell-like pool.

A similar finding was reported regarding CXCR4-positive stem cells residing in bone marrow. Investigators found that upon mobilization with G-CSF, a subset of $CXCR4^+$ PBPC expressed significant levels of mRNA for muscle, neural, and liver genes when normalized to PBSC from unmobilized blood[194,195]. This study suggested that bone marrow may house muscle, nerve and liver progenitor cells that become activated and mobilized upon injury, and contrarily does not house a pluripotent stem cell population; however clonal analysis of these cells has yet to be described.

1.5.3 Pluripotent Stem Cells

A third mechanism would be that a population of truly pluripotent cells resides in post-natal tissues. It is possible that a small set of pluripotent cells remains during embryological development that withdraw from further development and reside in post-natal tissues. Cells termed SKPs (skin derived progenitors) [196-198], were first isolated in culture cultures of juvenile and adult mouse dermis as multipotent, nestin-positive stem cells isolated from SKPs can be cultured long-term in suspension as small spheres of floating cells in the presence of EGF and FGF2. Spheres can be dissociated to single cells that can generate new spheres or cells can be allowed to differentiate into cells of both neuroectodermal and mesodermal lineages, including neurons, glia, smooth muscle cells and adipocytes. SKPs can be derived freshly, without preceding culture, from adult dermal skin during embryogenesis, as well as from adult mice adult mice where they appear to reside in a niche in the hair papillae and whisker follicles.

The study by Anjos-Afonso et al. [182] has shown that cells expressing the SSEA1 antigen, found on mouse embryonic stem cells can be isolated from mesenchymal stem cell cultures following 1 passage *in vitro*, express high levels of Oct4, and can differentiate following expansion into cells of mesodermal, endodermal and ectodermal lineage, and can contribute to hematopoiesis when grafted *in vivo*. This is consistent with the VSEL cells isolated by Kucia et al [181] . The latter studies suggest that rare cells exist in murine marrow that express Oct4 and SSEA1, phenotypic features of MAPCs, and to a greater or lesser extent of MIAMI cells, hBMSCs, USSCs, and the many other culture derived cells with greater potency. Whether the differentiation ability ascribed to MAPCs, MIAMI cells, hBMSCs, USSCs, or pre-MSC selected cells is already present in the primary selected, uncultured BM cells isolated by Anjos-Afonso and Kucia, and hence represent cells with greater potency persisting *in vivo* into postnatal life, or whether the differentiation ability is acquired once cells are culture expanded *in vitro*, and therefore represent de-differentiation of a rare Oct4 positive cell, is not known.

1.5.4 Cell Fusion

The last plasticity mechanism to be described is fusion. Cell fusion is a natural process that is readily demonstrated by macrophage mediated granuloma formation, but also occurs regularly in the liver and skeletal muscle. Heterokaryons formed by the fusion of a non-muscle human cell and a mouse muscle cell, demonstrated that it is possible to activate muscle specific genes through fusion of the two cell types [183]. ES cells have been shown to fuse *in vitro* with BM and brain-derived cells, thus conferring their pluripotency [199,200]. By using a Cre/lox recombination method, it was demonstrated that BM cells could fuse with purkinje neurons, cardiomyocytes, and hepatocytes and acquire the tissues' functional and morphological characteristics [201]. Wang et al., demonstrated that HSC contribute to liver tissue in response to injury primarily through fusion[202]. Additonally, Camargo et al., demonstrated through a LysM-Cre/ROSA$^{flox/STOP}$ system, that myeloid intermediates are incorporated into regenerating muscle primarily, and possibly solely, through fusion [168]. Fusion is particularly relevant for skeletal muscle differentiation,

since fusion is the cause of myofiber formation, therefore it could be argued that all *in vivo* skeletal muscle engraftment studies can be explained by fusion. Although studies have shown fusion of a donor nuclei to a host fiber with subsequent dystrophin expression [139], it should be noted that some investigators have also shown that a subpopulation of transplanted cells can become satellite cells [57,169]. Thus, fusion may not be the only mechanism by which muscle induction can take place. Whether stem cell plasticity is caused by one or more of the mechanisms discussed, the described mechanisms still need to be rigidly investigated and considered when planning future transplantation studies.

References

1. Barohn, R. J., Levine, E. J., Olson, J. O. & Mendell, J. R. Gastric hypomotility in Duchenne's muscular dystrophy. *N Engl J Med* **319**, 15-8 (1988).
2. Jensen, H., Warburg, M., Sjo, O. & Schwartz, M. Duchenne muscular dystrophy: negative electroretinograms and normal dark adaptation. Reappraisal of assignment of X linked incomplete congenital stationary night blindness. *J Med Genet* **32**, 348-51 (1995).
3. Marques, M. J., Ferretti, R., Vomero, V. U., Minatel, E. & Neto, H. S. Intrinsic laryngeal muscles are spared from myonecrosis in the mdx mouse model of Duchenne muscular dystrophy. *Muscle Nerve* (2006).
4. Khurana, T. S. et al. Absence of extraocular muscle pathology in Duchenne's muscular dystrophy: role for calcium homeostasis in extraocular muscle sparing. *J Exp Med* **182**, 467-75 (1995).
5. O'Brien, K. F. & Kunkel, L. M. Dystrophin and muscular dystrophy: past, present, and future. *Mol Genet Metab* **74**, 75-88 (2001).
6. Sarig, R. et al. Targeted inactivation of Dp71, the major non-muscle product of the DMD gene: differential activity of the Dp71 promoter during development. *Hum Mol Genet* **8**, 1-10 (1999).
7. Lidov, H. G. & Kunkel, L. M. Dp140: alternatively spliced isoforms in brain and kidney. *Genomics* **45**, 132-9 (1997).
8. Judge, L. M., Haraguchiln, M. & Chamberlain, J. S. Dissecting the signaling and mechanical functions of the dystrophin-glycoprotein complex. *J Cell Sci* **119**, 1537-46 (2006).
9. Straub, V. & Campbell, K. P. Muscular dystrophies and the dystrophin-glycoprotein complex. *Curr Opin Neurol* **10**, 168-75 (1997).
10. Rafael, J. A. et al. Forced expression of dystrophin deletion constructs reveals structure-function correlations. *J Cell Biol* **134**, 93-102 (1996).
11. Ervasti, J. M. & Campbell, K. P. Membrane organization of the dystrophin-glycoprotein complex. *Cell* **66**, 1121-31 (1991).
12. Matsumura, K. et al. Deficiency of dystrophin-associated proteins in Duchenne muscular dystrophy patients lacking COOH-terminal domains of dystrophin. *J Clin Invest* **92**, 866-71 (1993).
13. Leibovitz, S. et al. Exogenous Dp71 is a dominant negative competitor of dystrophin in skeletal muscle. *Neuromuscul Disord* **12**, 836-44 (2002).
14. Rafael, J. A. et al. Dystrophin and utrophin influence fiber type composition and post-synaptic membrane structure. *Hum Mol Genet* **9**, 1357-67 (2000).
15. Straub, V., Rafael, J. A., Chamberlain, J. S. & Campbell, K. P. Animal models for muscular dystrophy show different patterns of sarcolemmal disruption. *J Cell Biol* **139**, 375-85 (1997).
16. McArdle, A., Edwards, R. H. & Jackson, M. J. How does dystrophin deficiency lead to muscle degeneration?--evidence from the mdx mouse. *Neuromuscul Disord* **5**, 445-56 (1995).
17. Emery, A. E. The muscular dystrophies. *Lancet* **359**, 687-95 (2002).

18. Brenman, J. E. et al. Interaction of nitric oxide synthase with the postsynaptic density protein PSD-95 and alpha1-syntrophin mediated by PDZ domains. *Cell* **84**, 757-67 (1996).
19. Sander, M. et al. Functional muscle ischemia in neuronal nitric oxide synthase-deficient skeletal muscle of children with Duchenne muscular dystrophy. *Proc Natl Acad Sci U S A* **97**, 13818-23 (2000).
20. Manzur, A., Kuntzer, T., Pike, M. & Swan, A. Glucocorticoid corticosteroids for Duchenne muscular dystrophy. *Cochrane Database Syst Rev* **2**, CD003725 (2004).
21. Merlini, L. et al. Early prednisone treatment in Duchenne muscular dystrophy. *Muscle Nerve* **27**, 222-7 (2003).
22. De Backer, F., Vandebrouck, C., Gailly, P. & Gillis, J. M. Long-term study of Ca(2+) homeostasis and of survival in collagenase-isolated muscle fibres from normal and mdx mice. *J Physiol* **542**, 855-65 (2002).
23. Bertorini, T. E. et al. Effect of dantrolene in Duchenne muscular dystrophy. *Muscle Nerve* **14**, 503-7 (1991).
24. Badalamente, M. A. & Stracher, A. Delay of muscle degeneration and necrosis in mdx mice by calpain inhibition. *Muscle Nerve* **23**, 106-11 (2000).
25. Pulido, S. M. et al. Creatine supplementation improves intracellular Ca2+ handling and survival in mdx skeletal muscle cells. *FEBS Lett* **439**, 357-62 (1998).
26. Zeman, R. J., Zhang, Y. & Etlinger, J. D. Clenbuterol, a beta 2-agonist, retards wasting and loss of contractility in irradiated dystrophic mdx muscle. *Am J Physiol* **267**, C865-8 (1994).
27. Barton, E. R., Morris, L., Musaro, A., Rosenthal, N. & Sweeney, H. L. Muscle-specific expression of insulin-like growth factor I counters muscle decline in mdx mice. *J Cell Biol* **157**, 137-48 (2002).
28. Bogdanovich, S. et al. Functional improvement of dystrophic muscle by myostatin blockade. *Nature* **420**, 418-21 (2002).
29. Gregorevic, P., Plant, D. R., Leeding, K. S., Bach, L. A. & Lynch, G. S. Improved contractile function of the mdx dystrophic mouse diaphragm muscle after insulin-like growth factor-I administration. *Am J Pathol* **161**, 2263-72 (2002).
30. Minetti, G. C. et al. Functional and morphological recovery of dystrophic muscles in mice treated with deacetylase inhibitors. *Nat Med* **12**, 1147-50 (2006).
31. Granchelli, J. A., Avosso, D. L., Hudecki, M. S. & Pollina, C. Cromolyn increases strength in exercised mdx mice. *Res Commun Mol Pathol Pharmacol* **91**, 287-96 (1996).
32. Hodgetts, S., Radley, H., Davies, M. & Grounds, M. D. Reduced necrosis of dystrophic muscle by depletion of host neutrophils, or blocking TNFalpha function with Etanercept in mdx mice. *Neuromuscul Disord* **16**, 591-602 (2006).

33. Brunelli, S. et al. Nitric oxide release combined with nonsteroidal antiinflammatory activity prevents muscular dystrophy pathology and enhances stem cell therapy. *Proc Natl Acad Sci U S A* **104**, 264-9 (2007).
34. Howell, J. M. et al. High-level dystrophin expression after adenovirus-mediated dystrophin minigene transfer to skeletal muscle of dystrophic dogs: prolongation of expression with immunosuppression. *Hum Gene Ther* **9**, 629-34 (1998).
35. Ragot, T. et al. Efficient adenovirus-mediated transfer of a human minidystrophin gene to skeletal muscle of mdx mice. *Nature* **361**, 647-50 (1993).
36. Wang, B., Li, J. & Xiao, X. Adeno-associated virus vector carrying human minidystrophin genes effectively ameliorates muscular dystrophy in mdx mouse model. *Proc Natl Acad Sci U S A* **97**, 13714-9 (2000).
37. Yuasa, K. et al. Effective restoration of dystrophin-associated proteins in vivo by adenovirus-mediated transfer of truncated dystrophin cDNAs. *FEBS Lett* **425**, 329-36 (1998).
38. Kessler, P. D. et al. Gene delivery to skeletal muscle results in sustained expression and systemic delivery of a therapeutic protein. *Proc Natl Acad Sci U S A* **93**, 14082-7 (1996).
39. Xiao, X., Li, J. & Samulski, R. J. Efficient long-term gene transfer into muscle tissue of immunocompetent mice by adeno-associated virus vector. *J Virol* **70**, 8098-108 (1996).
40. Yuasa, K. et al. Adeno-associated virus vector-mediated gene transfer into dystrophin-deficient skeletal muscles evokes enhanced immune response against the transgene product. *Gene Ther* **9**, 1576-88 (2002).
41. Pearce, M. et al. The utrophin and dystrophin genes share similarities in genomic structure. *Hum Mol Genet* **2**, 1765-72 (1993).
42. Perkins, K. J. & Davies, K. E. The role of utrophin in the potential therapy of Duchenne muscular dystrophy. *Neuromuscul Disord* **12 Suppl 1**, S78-89 (2002).
43. Yamamoto, K. et al. Immune response to adenovirus-delivered antigens upregulates utrophin and results in mitigation of muscle pathology in mdx mice. *Hum Gene Ther* **11**, 669-80 (2000).
44. Rybakova, I. N., Patel, J. R., Davies, K. E., Yurchenco, P. D. & Ervasti, J. M. Utrophin binds laterally along actin filaments and can couple costameric actin with sarcolemma when overexpressed in dystrophin-deficient muscle. *Mol Biol Cell* **13**, 1512-21 (2002).
45. Tinsley, J. M. et al. Amelioration of the dystrophic phenotype of mdx mice using a truncated utrophin transgene. *Nature* **384**, 349-53 (1996).
46. Mann, C. J. et al. Antisense-induced exon skipping and synthesis of dystrophin in the mdx mouse. *Proc Natl Acad Sci U S A* **98**, 42-7 (2001).
47. Lu, Q. L. et al. Massive idiosyncratic exon skipping corrects the nonsense mutation in dystrophic mouse muscle and produces functional revertant fibers by clonal expansion. *J Cell Biol* **148**, 985-96 (2000).

48. Lu, Q. L. et al. Functional amounts of dystrophin produced by skipping the mutated exon in the mdx dystrophic mouse. *Nat Med* **9**, 1009-14 (2003).
49. Gaschen, F. & Burgunder, J. M. Changes of skeletal muscle in young dystrophin-deficient cats: a morphological and morphometric study. *Acta Neuropathol (Berl)* **101**, 591-600 (2001).
50. Carpenter, J. L. et al. Feline muscular dystrophy with dystrophin deficiency. *Am J Pathol* **135**, 909-19 (1989).
51. Stedman, H. H. et al. The mdx mouse diaphragm reproduces the degenerative changes of Duchenne muscular dystrophy. *Nature* **352**, 536-9 (1991).
52. Khurana, T. S. & Davies, K. E. Pharmacological strategies for muscular dystrophy. *Nat Rev Drug Discov* **2**, 379-90 (2003).
53. Petrof, B. J., Shrager, J. B., Stedman, H. H., Kelly, A. M. & Sweeney, H. L. Dystrophin protects the sarcolemma from stresses developed during muscle contraction. *Proc Natl Acad Sci U S A* **90**, 3710-4 (1993).
54. Moens, P., Baatsen, P. H. & Marechal, G. Increased susceptibility of EDL muscles from mdx mice to damage induced by contractions with stretch. *J Muscle Res Cell Motil* **14**, 446-51 (1993).
55. Crawford, G. E., Lu, Q. L., Partridge, T. A. & Chamberlain, J. S. Suppression of revertant fibers in mdx mice by expression of a functional dystrophin. *Hum Mol Genet* **10**, 2745-50 (2001).
56. Chapman, V. M., Miller, D. R., Armstrong, D. & Caskey, C. T. Recovery of induced mutations for X chromosome-linked muscular dystrophy in mice. *Proc Natl Acad Sci U S A* **86**, 1292-6 (1989).
57. LaBarge, M. A. & Blau, H. M. Biological progression from adult bone marrow to mononucleate muscle stem cell to multinucleate muscle fiber in response to injury. *Cell* **111**, 589-601 (2002).
58. Deconinck, A. E. et al. Utrophin-dystrophin-deficient mice as a model for Duchenne muscular dystrophy. *Cell* **90**, 717-27 (1997).
59. Asakura, A., Komaki, M. & Rudnicki, M. Muscle satellite cells are multipotential stem cells that exhibit myogenic, osteogenic, and adipogenic differentiation. *Differentiation* **68**, 245-53 (2001).
60. Wada, M. R., Inagawa-Ogashiwa, M., Shimizu, S., Yasumoto, S. & Hashimoto, N. Generation of different fates from multipotent muscle stem cells. *Development* **129**, 2987-95 (2002).
61. Tajbakhsh, S. in *Vertebrate Myogenesis* (ed. B.Brand-Saberi) 61-79 (Springer-Verlag, Berlin, 2002).
62. Charge, S. B. & Rudnicki, M. A. Cellular and molecular regulation of muscle regeneration. *Physiol Rev* **84**, 209-38 (2004).
63. Gilbert, S. F. (ed.) *Developmental Biology* (Sinauer Associates, Inc, Sunderland, Massachusetts, 1997).
64. Patel, K., Christ, B. & Stockdale, F. in *Vertebrate Myogenesis* (ed. Brand-Saberi, B.) 163-186 (Springer, Berlin, 2002).
65. Marcelle, C., Lesbros, C. & Linker, C. in *Vertebrate Myogenesis* (ed. B.Brand-Saberi) 81-108 (Springer, Berlin, 2002).

66. Waibler, Z. & Starzinski-Powitz, A. in *Vertebrate Myogenesis* (ed. B.Brand-Saberi) 188-198 (Springer-Verlag, Berlin, 2002).
67. Schmalbruch, H. & Lewis, D. M. Dynamics of nuclei of muscle fibers and connective tissue cells in normal and denervated rat muscles. *Muscle Nerve* **23**, 617-26 (2000).
68. Belcastro, A. N., Shewchuk, L. D. & Raj, D. A. Exercise-induced muscle injury: a calpain hypothesis. *Mol Cell Biochem* **179**, 135-45 (1998).
69. Gustafsson, M. K. et al. Myf5 is a direct target of long-range Shh signaling and Gli regulation for muscle specification. *Genes Dev* **16**, 114-26 (2002).
70. Cossu, G. & Borello, U. Wnt signaling and the activation of myogenesis in mammals. *Embo J* **18**, 6867-72 (1999).
71. Brunelli, S., Relaix, F., Baesso, S., Buckingham, M. & Cossu, G. Beta catenin-independent activation of MyoD in presomitic mesoderm requires PKC and depends on Pax3 transcriptional activity. *Dev Biol* (2007).
72. Heldin, C. H., Miyazono, K. & ten Dijke, P. TGF-beta signalling from cell membrane to nucleus through SMAD proteins. *Nature* **390**, 465-71 (1997).
73. De Angelis, L. et al. Inhibition of myogenesis by transforming growth factor beta is density-dependent and related to the translocation of transcription factor MEF2 to the cytoplasm. *Proc Natl Acad Sci U S A* **95**, 12358-63 (1998).
74. Zhao, P. & Hoffman, E. P. Embryonic myogenesis pathways in muscle regeneration. *Dev Dyn* **229**, 380-92 (2004).
75. Pourquie, O. et al. Lateral and axial signals involved in avian somite patterning: a role for BMP4. *Cell* **84**, 461-71 (1996).
76. Kubo, A. et al. Development of definitive endoderm from embryonic stem cells in culture. *Development* **131**, 1651-62 (2004).
77. McPherron, A. C. & Lee, S. J. Double muscling in cattle due to mutations in the myostatin gene. *Proc Natl Acad Sci U S A* **94**, 12457-61 (1997).
78. McPherron, A. C., Lawler, A. M. & Lee, S. J. Regulation of skeletal muscle mass in mice by a new TGF-beta superfamily member. *Nature* **387**, 83-90 (1997).
79. Parker, M. H., Seale, P. & Rudnicki, M. A. Looking back to the embryo: defining transcriptional networks in adult myogenesis. *Nat Rev Genet* **4**, 497-507 (2003).
80. Khan, J. et al. cDNA microarrays detect activation of a myogenic transcription program by the PAX3-FKHR fusion oncogene. *Proc Natl Acad Sci U S A* **96**, 13264-9 (1999).
81. Mennerich, D., Schafer, K. & Braun, T. Pax-3 is necessary but not sufficient for lbx1 expression in myogenic precursor cells of the limb. *Mech Dev* **73**, 147-58 (1998).
82. Ridgeway, A. G. & Skerjanc, I. S. Pax3 is essential for skeletal myogenesis and the expression of Six1 and Eya2. *J Biol Chem* **276**, 19033-9 (2001).

83. Seale, P. & Rudnicki, M. A. A new look at the origin, function, and "stem-cell" status of muscle satellite cells. *Dev Biol* **218**, 115-24 (2000).

84. Olguin, H. C. & Olwin, B. B. Pax-7 up-regulation inhibits myogenesis and cell cycle progression in satellite cells: a potential mechanism for self-renewal. *Dev Biol* **275**, 375-88 (2004).

85. Davis, R. L., Weintraub, H. & Lassar, A. B. Expression of a single transfected cDNA converts fibroblasts to myoblasts. *Cell* **51**, 987-1000 (1987).

86. Hasty, P. et al. Muscle deficiency and neonatal death in mice with a targeted mutation in the myogenin gene. *Nature* **364**, 501-6 (1993).

87. Nabeshima, Y. et al. Myogenin gene disruption results in perinatal lethality because of severe muscle defect. *Nature* **364**, 532-5 (1993).

88. Kassar-Duchossoy, L. et al. Mrf4 determines skeletal muscle identity in Myf5:Myod double-mutant mice. *Nature* **431**, 466-71 (2004).

89. Patapoutian, A. et al. Disruption of the mouse MRF4 gene identifies multiple waves of myogenesis in the myotome. *Development* **121**, 3347-58 (1995).

90. Stamataki, D., Kastrinaki, M., Mankoo, B. S., Pachnis, V. & Karagogeos, D. Homeodomain proteins Mox1 and Mox2 associate with Pax1 and Pax3 transcription factors. *FEBS Lett* **499**, 274-8 (2001).

91. Mankoo, B. S. et al. Mox2 is a component of the genetic hierarchy controlling limb muscle development. *Nature* **400**, 69-73 (1999).

92. Lodish, H. et al. *Molecular Cell Biology* (W.H. Freeman and Company, New York, 2000).

93. Li, H. & Capetanaki, Y. An E box in the desmin promoter cooperates with the E box and MEF-2 sites of a distal enhancer to direct muscle-specific transcription. *Embo J* **13**, 3580-9 (1994).

94. Martin, B. L. & Harland, R. M. A novel role for lbx1 in Xenopus hypaxial myogenesis. *Development* **133**, 195-208 (2006).

95. Brohmann, H., Jagla, K. & Birchmeier, C. The role of Lbx1 in migration of muscle precursor cells. *Development* **127**, 437-45 (2000).

96. Odelberg, S. J., Kollhoff, A. & Keating, M. T. Dedifferentiation of mammalian myotubes induced by msx1. *Cell* **103**, 1099-109 (2000).

97. Craig, R. in *Myology* (ed. Andrew G. Engel, B. Q. B.) 73-123 (McGraw-Hill, New York, 1986).

98. Labeit, S. & Kolmerer, B. Titins: giant proteins in charge of muscle ultrastructure and elasticity. *Science* **270**, 293-6 (1995).

99. Labeit, S. & Kolmerer, B. The complete primary structure of human nebulin and its correlation to muscle structure. *J Mol Biol* **248**, 308-15 (1995).

100. Gordon, A. M., Huxley, A. F. & Julian, F. J. The variation in isometric tension with sarcomere length in vertebrate muscle fibres. *J Physiol* **184**, 170-92 (1966).

101. Guyton, A. & Hall, J. (eds.) *Textbook of Medical Physiology* (W.B. Saunders Company, Philadelphia, 1996).

102. Lynch, G. S., Hinkle, R. T., Chamberlain, J. S., Brooks, S. V. & Faulkner, J. A. Force and power output of fast and slow skeletal muscles from mdx mice 6-28 months old. *J Physiol* **535**, 591-600 (2001).

103. Anderson, J. E., Bressler, B. H. & Ovalle, W. K. Functional regeneration in the hindlimb skeletal muscle of the mdx mouse. *J Muscle Res Cell Motil* **9**, 499-515 (1988).

104. Williams, D. A., Head, S. I., Lynch, G. S. & Stephenson, D. G. Contractile properties of skinned muscle fibres from young and adult normal and dystrophic (mdx) mice. *J Physiol* **460**, 51-67 (1993).

105. Torrente, Y. et al. Human circulating AC133(+) stem cells restore dystrophin expression and ameliorate function in dystrophic skeletal muscle. *J Clin Invest* **114**, 182-95 (2004).

106. Sampaolesi, M. et al. Cell therapy of alpha-sarcoglycan null dystrophic mice through intra-arterial delivery of mesoangioblasts. *Science* **301**, 487-92 (2003).

107. Duclos, F. et al. Progressive muscular dystrophy in alpha-sarcoglycan-deficient mice. *J Cell Biol* **142**, 1461-71 (1998).

108. Smith, J. P., Hicks, P. S., Ortiz, L. R., Martinez, M. J. & Mandler, R. N. Quantitative measurement of muscle strength in the mouse. *J Neurosci Methods* **62**, 15-9 (1995).

109. Burdi, R. et al. First evaluation of the potential effectiveness in muscular dystrophy of a novel chimeric compound, BN 82270, acting as calpain-inhibitor and anti-oxidant. *Neuromuscul Disord* **16**, 237-48 (2006).

110. Yang, B. et al. Skeletal muscle function and water permeability in aquaporin-4 deficient mice. *Am J Physiol Cell Physiol* **278**, C1108-15 (2000).

111. Sacco, P., Jones, D. A., Dick, J. R. & Vrbova, G. Contractile properties and susceptibility to exercise-induced damage of normal and mdx mouse tibialis anterior muscle. *Clin Sci (Lond)* **82**, 227-36 (1992).

112. Lovering, R. M. & De Deyne, P. G. Contractile function, sarcolemma integrity, and the loss of dystrophin after skeletal muscle eccentric contraction-induced injury. *Am J Physiol Cell Physiol* **286**, C230-8 (2004).

113. Dangain, J. & Vrbova, G. Muscle development in mdx mutant mice. *Muscle Nerve* **7**, 700-4 (1984).

114. Lesniewski, L. A., Miller, T. A. & Armstrong, R. B. Mechanisms of force loss in diabetic mouse skeletal muscle. *Muscle Nerve* **28**, 493-500 (2003).

115. Ingalls, C. P., Warren, G. L., Lowe, D. A., Boorstein, D. B. & Armstrong, R. B. Differential effects of anesthetics on in vivo skeletal muscle contractile function in the mouse. *J Appl Physiol* **80**, 332-40 (1996).

116. Ashton-Miller, J. A., He, Y., Kadhiresan, V. A., McCubbrey, D. A. & Faulkner, J. A. An apparatus to measure in vivo biomechanical behavior of dorsi- and plantarflexors of mouse ankle. *J Appl Physiol* **72**, 1205-11 (1992).

117. Hong, J. B. & Iaizzo, P. A. Force assessment of the stimulated arm flexors: quantification of contractile properties. *J Med Eng Technol* **26**, 28-35 (2002).
118. Sampaolesi, M. et al. Mesoangioblast stem cells ameliorate muscle function in dystrophic dogs. *Nature* **444**, 574-9 (2006).
119. Verfaillie, C. M., Pera, M. F. & Lansdorp, P. M. Stem cells: hype and reality. *Hematology (Am Soc Hematol Educ Program)*, 369-91 (2002).
120. Rippon, H. J. & Bishop, A. E. Embryonic stem cells. *Cell Prolif* **37**, 23-34 (2004).
121. Evans, M. J. & Kaufman, M. H. Establishment in culture of pluripotential cells from mouse embryos. *Nature* **292**, 154-6 (1981).
122. Thomson, J. A. et al. Isolation of a primate embryonic stem cell line. *Proc Natl Acad Sci U S A* **92**, 7844-8 (1995).
123. Shamblott, M. J. et al. Derivation of pluripotent stem cells from cultured human primordial germ cells. *Proc Natl Acad Sci U S A* **95**, 13726-31 (1998).
124. Thomson, J. A. et al. Embryonic stem cell lines derived from human blastocysts. *Science* **282**, 1145-7 (1998).
125. Graves, K. H. & Moreadith, R. W. Derivation and characterization of putative pluripotential embryonic stem cells from preimplantation rabbit embryos. *Mol Reprod Dev* **36**, 424-33 (1993).
126. Li, M. et al. Isolation and culture of embryonic stem cells from porcine blastocysts. *Mol Reprod Dev* **65**, 429-34 (2003).
127. Bradley, A., Evans, M., Kaufman, M. H. & Robertson, E. Formation of germ-line chimaeras from embryo-derived teratocarcinoma cell lines. *Nature* **309**, 255-6 (1984).
128. Keller, G. M. In vitro differentiation of embryonic stem cells. *Curr Opin Cell Biol* **7**, 862-9 (1995).
129. Maltsev, V. A., Rohwedel, J., Hescheler, J. & Wobus, A. M. Embryonic stem cells differentiate in vitro into cardiomyocytes representing sinusnodal, atrial and ventricular cell types. *Mech Dev* **44**, 41-50 (1993).
130. Nakayama, T., Momoki-Soga, T., Yamaguchi, K. & Inoue, N. Efficient production of neural stem cells and neurons from embryonic stem cells. *Neuroreport* **15**, 487-91 (2004).
131. Dinsmore, J. et al. Embryonic stem cells differentiated in vitro as a novel source of cells for transplantation. *Cell Transplant* **5**, 131-43 (1996).
132. Petropoulos, H. & Skerjanc, I. S. Beta-catenin is essential and sufficient for skeletal myogenesis in P19 cells. *J Biol Chem* **277**, 15393-9 (2002).
133. Kamochi, H. et al. Transplantation of myocyte precursors derived from embryonic stem cells transfected with IGFII gene in a mouse model of muscle injury. *Transplantation* **82**, 516-26 (2006).
134. Bhagavati, S. & Xu, W. Generation of skeletal muscle from transplanted embryonic stem cells in dystrophic mice. *Biochem Biophys Res Commun* **333**, 644-9 (2005).

135. Cao, B. et al. Muscle stem cells differentiate into haematopoietic lineages but retain myogenic potential. *Nat Cell Biol* **5**, 640-6 (2003).

136. Jiang, Y. et al. Pluripotency of mesenchymal stem cells derived from adult marrow. *Nature* **418**, 41-9 (2002).

137. Lagasse, E. et al. Purified hematopoietic stem cells can differentiate into hepatocytes in vivo. *Nat Med* **6**, 1229-34 (2000).

138. Zhao, L. R. et al. Human bone marrow stem cells exhibit neural phenotypes and ameliorate neurological deficits after grafting into the ischemic brain of rats. *Exp Neurol* **174**, 11-20 (2002).

139. Gussoni, E. et al. Dystrophin expression in the mdx mouse restored by stem cell transplantation. *Nature* **401**, 390-4 (1999).

140. Ferrari, G. et al. Muscle regeneration by bone marrow-derived myogenic progenitors. *Science* **279**, 1528-30 (1998).

141. Jiang, Y. et al. Multipotent progenitor cells can be isolated from postnatal murine bone marrow, muscle, and brain. *Exp Hematol* **30**, 896-904 (2002).

142. Gupta, S. et al. Isolation and characterization of kidney-derived stem cells. *J Am Soc Nephrol* **17**, 3028-40 (2006).

143. Oyama, T. et al. Cardiac side population cells have a potential to migrate and differentiate into cardiomyocytes in vitro and in vivo. *J Cell Biol* **176**, 329-41 (2007).

144. Asakura, A. & Rudnicki, M. A. Side population cells from diverse adult tissues are capable of in vitro hematopoietic differentiation. *Exp Hematol* **30**, 1339-45 (2002).

145. Seale, P., Asakura, A. & Rudnicki, M. A. The potential of muscle stem cells. *Dev Cell* **1**, 333-42 (2001).

146. De Angelis, L. et al. Skeletal myogenic progenitors originating from embryonic dorsal aorta coexpress endothelial and myogenic markers and contribute to postnatal muscle growth and regeneration. *J Cell Biol* **147**, 869-78 (1999).

147. Seale, P. et al. Pax7 is required for the specification of myogenic satellite cells. *Cell* **102**, 777-86 (2000).

148. Beauchamp, J. R. et al. Expression of CD34 and Myf5 defines the majority of quiescent adult skeletal muscle satellite cells. *J Cell Biol* **151**, 1221-34 (2000).

149. Hashimoto, N., Murase, T., Kondo, S., Okuda, A. & Inagawa-Ogashiwa, M. Muscle reconstitution by muscle satellite cell descendants with stem cell-like properties. *Development* **131**, 5481-90 (2004).

150. Relaix, F., Rocancourt, D., Mansouri, A. & Buckingham, M. A Pax3/Pax7-dependent population of skeletal muscle progenitor cells. *Nature* **435**, 948-53 (2005).

151. Gussoni, E., Blau, H. M. & Kunkel, L. M. The fate of individual myoblasts after transplantation into muscles of DMD patients. *Nat Med* **3**, 970-7 (1997).

152. Pittenger, M. F. et al. Multilineage potential of adult human mesenchymal stem cells. *Science* **284**, 143-7 (1999).

153. Phinney, D. G. et al. Donor variation in the growth properties and osteogenic potential of human marrow stromal cells. *J Cell Biochem* **75**, 424-36 (1999).

154. Wakitani, S., Saito, T. & Caplan, A. I. Myogenic cells derived from rat bone marrow mesenchymal stem cells exposed to 5-azacytidine. *Muscle Nerve* **18**, 1417-26 (1995).

155. Phinney, D. G., Kopen, G., Isaacson, R. L. & Prockop, D. J. Plastic adherent stromal cells from the bone marrow of commonly used strains of inbred mice: variations in yield, growth, and differentiation. *J Cell Biochem* **72**, 570-85 (1999).

156. Bittner, R. E. et al. Recruitment of bone-marrow-derived cells by skeletal and cardiac muscle in adult dystrophic mdx mice. *Anat Embryol (Berl)* **199**, 391-6 (1999).

157. Corti, S. et al. A subpopulation of murine bone marrow cells fully differentiates along the myogenic pathway and participates in muscle repair in the mdx dystrophic mouse. *Exp Cell Res* **277**, 74-85 (2002).

158. Rando, T. A. & Blau, H. M. Primary mouse myoblast purification, characterization, and transplantation for cell-mediated gene therapy. *J Cell Biol* **125**, 1275-87 (1994).

159. Qu, Z. et al. Development of approaches to improve cell survival in myoblast transfer therapy. *J Cell Biol* **142**, 1257-67 (1998).

160. Qu-Petersen, Z. et al. Identification of a novel population of muscle stem cells in mice: potential for muscle regeneration. *J Cell Biol* **157**, 851-64 (2002).

161. Deasy, B. M. et al. Long-term self-renewal of postnatal muscle-derived stem cells. *Mol Biol Cell* **16**, 3323-33 (2005).

162. Lee, J. Y. et al. Clonal isolation of muscle-derived cells capable of enhancing muscle regeneration and bone healing. *J Cell Biol* **150**, 1085-100 (2000).

163. Blomberg, M. et al. Repetitive bone marrow transplantation in nonmyeloablated recipients. *Exp Hematol* **26**, 320-4 (1998).

164. Uchida, N., Aguila, H. L., Fleming, W. H., Jerabek, L. & Weissman, I. L. Rapid and sustained hematopoietic recovery in lethally irradiated mice transplanted with purified Thy-1.1lo Lin-Sca-1+ hematopoietic stem cells. *Blood* **83**, 3758-79 (1994).

165. Osawa, M., Hanada, K., Hamada, H. & Nakauchi, H. Long-term lymphohematopoietic reconstitution by a single CD34-low/negative hematopoietic stem cell. *Science* **273**, 242-5 (1996).

166. McKenzie, J. L., Gan, O. I., Doedens, M., Wang, J. C. & Dick, J. E. Individual stem cells with highly variable proliferation and self-renewal properties comprise the human hematopoietic stem cell compartment. *Nat Immunol* **7**, 1225-33 (2006).

167. Corbel, S. Y. et al. Contribution of hematopoietic stem cells to skeletal muscle. *Nat Med* **9**, 1528-32 (2003).

168. Camargo, F. D., Green, R., Capetenaki, Y., Jackson, K. A. & Goodell, M. A. Single hematopoietic stem cells generate skeletal muscle through myeloid intermediates. *Nat Med* **9**, 1520-7 (2003).

169. Asakura, A., Seale, P., Girgis-Gabardo, A. & Rudnicki, M. A. Myogenic specification of side population cells in skeletal muscle. *J Cell Biol* **159**, 123-34 (2002).

170. Bachrach, E. et al. Muscle engraftment of myogenic progenitor cells following intraarterial transplantation. *Muscle Nerve* **34**, 44-52 (2006).

171. Reyes, M. & Verfaillie, C. M. Characterization of multipotent adult progenitor cells, a subpopulation of mesenchymal stem cells. *Ann N Y Acad Sci* **938**, 231-3; discussion 233-5 (2001).

172. Reyes, M. et al. Purification and ex vivo expansion of postnatal human marrow mesodermal progenitor cells. *Blood* **98**, 2615-25 (2001).

173. Muguruma, Y. et al. In vivo and in vitro differentiation of myocytes from human bone marrow-derived multipotent progenitor cells. *Exp Hematol* **31**, 1323-30 (2003).

174. Breyer, A. et al. Multipotent adult progenitor cell isolation and culture procedures. *Exp Hematol* **34**, 1596-601 (2006).

175. Serafini, M. et al. Hematopoietic reconstitution by multipotent adult progenitor cells: precursors to long-term hematopoietic stem cells. *J Exp Med* **204**, 129-39 (2007).

176. Yoon, Y. S. et al. Clonally expanded novel multipotent stem cells from human bone marrow regenerate myocardium after myocardial infarction. *J Clin Invest* **115**, 326-38 (2005).

177. D'Ippolito, G. et al. Marrow-isolated adult multilineage inducible (MIAMI) cells, a unique population of postnatal young and old human cells with extensive expansion and differentiation potential. *J Cell Sci* **117**, 2971-81 (2004).

178. D'Ippolito, G., Howard, G. A., Roos, B. A. & Schiller, P. C. Isolation and characterization of marrow-isolated adult multilineage inducible (MIAMI) cells. *Exp Hematol* **34**, 1608-10 (2006).

179. Kogler, G. et al. A new human somatic stem cell from placental cord blood with intrinsic pluripotent differentiation potential. *J Exp Med* **200**, 123-35 (2004).

180. Kucia, M. et al. Morphological and molecular characterization of novel population of CXCR4+ SSEA-4+ Oct-4+ very small embryonic-like cells purified from human cord blood: preliminary report. *Leukemia* **21**, 297-303 (2007).

181. Kucia, M. et al. A population of very small embryonic-like (VSEL) CXCR4(+)SSEA-1(+)Oct-4+ stem cells identified in adult bone marrow. *Leukemia* **20**, 857-69 (2006).

182. Anjos-Afonso, F. & Bonnet, D. Nonhematopoietic/endothelial SSEA-1+ cells define the most primitive progenitors in the adult murine bone marrow mesenchymal compartment. *Blood* **109**, 1298-306 (2007).

183. Blau, H. M. et al. Plasticity of the differentiated state. *Science* **230**, 758-66 (1985).

184. Wagers, A. J. & Weissman, I. L. Plasticity of adult stem cells. *Cell* **116**, 639-48 (2004).

185. Wilmut, I., Schnieke, A. E., McWhir, J., Kind, A. J. & Campbell, K. H. Viable offspring derived from fetal and adult mammalian cells. *Nature* **385**, 810-3 (1997).

186. Kishigami, S., Wakayama, S., van Thuan, N. & Wakayama, T. Cloned mice and embryonic stem cell establishment from adult somatic cells. *Hum Cell* **19**, 2-10 (2006).

187. Inoue, K. et al. Differential developmental ability of embryos cloned from tissue-specific stem cells. *Stem Cells* (2007).

188. Brockes, J. P. & Kumar, A. Plasticity and reprogramming of differentiated cells in amphibian regeneration. *Nat Rev Mol Cell Biol* **3**, 566-74 (2002).

189. Takahashi, K. & Yamanaka, S. Induction of pluripotent stem cells from mouse embryonic and adult fibroblast cultures by defined factors. *Cell* **126**, 663-76 (2006).

190. McNiece, I. K., Briddell, R. A., Hartley, C. A. & Andrews, R. G. The role of stem cell factor in mobilization of peripheral blood progenitor cells: synergy with G-CSF. *Stem Cells* **11 Suppl 3**, 83-8 (1993).

191. Jackson, K. A., Mi, T. & Goodell, M. A. Hematopoietic potential of stem cells isolated from murine skeletal muscle. *Proc Natl Acad Sci U S A* **96**, 14482-6 (1999).

192. McKinney-Freeman, S. L. et al. Muscle-derived hematopoietic stem cells are hematopoietic in origin. *Proc Natl Acad Sci U S A* **99**, 1341-6 (2002).

193. Oh, S. H. et al. Hepatocyte growth factor induces differentiation of adult rat bone marrow cells into a hepatocyte lineage in vitro. *Biochem Biophys Res Commun* **279**, 500-4 (2000).

194. Kucia, M., Ratajczak, J., Reca, R., Janowska-Wieczorek, A. & Ratajczak, M. Z. Tissue-specific muscle, neural and liver stem/progenitor cells reside in the bone marrow, respond to an SDF-1 gradient and are mobilized into peripheral blood during stress and tissue injury. *Blood Cells Mol Dis* **32**, 52-7 (2004).

195. Ratajczak, M. Z. et al. Stem cell plasticity revisited: CXCR4-positive cells expressing mRNA for early muscle, liver and neural cells 'hide out' in the bone marrow. *Leukemia* **18**, 29-40 (2004).

196. Toma, J. G., McKenzie, I. A., Bagli, D. & Miller, F. D. Isolation and characterization of multipotent skin-derived precursors from human skin. *Stem Cells* **23**, 727-37 (2005).

197. Toma, J. G. et al. Isolation of multipotent adult stem cells from the dermis of mammalian skin. *Nat Cell Biol* **3**, 778-84 (2001).

198. Fernandes, K. J. et al. A dermal niche for multipotent adult skin-derived precursor cells. *Nat Cell Biol* **6**, 1082-93 (2004).

199. Terada, N. et al. Bone marrow cells adopt the phenotype of other cells by spontaneous cell fusion. *Nature* **416**, 542-5 (2002).

200. Ying, Q. L., Nichols, J., Evans, E. P. & Smith, A. G. Changing potency by spontaneous fusion. *Nature* **416**, 545-8 (2002).

201. Alvarez-Dolado, M. et al. Fusion of bone-marrow-derived cells with Purkinje neurons, cardiomyocytes and hepatocytes. *Nature* **425**, 968-73 (2003).

202. Wang, X. et al. Cell fusion is the principal source of bone-marrow-derived hepatocytes. *Nature* **422**, 897-901 (2003).

CHAPTER 2

DEVELOPMENT OF AN IN VITRO PROTOCOL TO DIRECT MURINE MULTIPOTENT ADULT PROGENITOR CELLS TOWARD A MYOGENIC FATE

Sarah A. Frommer[1,2], Saswati Mahapatra[1], Yuehua Jiang[1], and Catherine M. Verfaillie[1]

Stem Cell Institute[1] and Biomedical Engineering Department[2], University of Minnesota, Minneapolis, Minnesota

Abstract

Stem cells have long been studied as *in vitro* models for development[1-3]. Currently, investigators are taking the next step by directing differentiation of stem cells towards a particular tissue fate. Studies have been done for endocrine pancreatic, neuronal, hepatic, and myocardial tissues[4-6] in an effort to create differentiated cells that can be used as therapies and/or tools for pharmacological testing. One disease that would benefit greatly from such studies is Duchenne muscular dystrophy, a degenerative and fatal muscle disorder[7]; however little, if any, work has been done to develop specific protocols for skeletal muscle induction. In an effort to address this, we developed a protocol for myogenic induction using multipotent adult progenitor cells (MAPC); cells that can generate progeny of the three germ layers. After review of embryonic myogenesis and post-natal muscle regeneration[8-15], we targeted 11 different cytokines to test; of those, combined addition of Activin-A, insulin-like growth factor-I (IGF-I), and basic fibroblast growth factor (bFGF), appeared to most consistently induce early myogenic transcription factors. By using quantitative RT-PCR as a screening tool, we detected that for the majority of the combinations tested, we observed an average >10-fold increase in Pax7 and MyoD, and >100-fold increase for Pax3 transcripts. This suggests that this cytokine combination is an effective method for directing pluripotent cells toward an early myogenic fate.

Introduction

The use of stem cells as models for development and potential therapeutics has created a need for protocols aimed at directing cells toward a specific tissue or cell type. As models for development, stem cells offer investigators a means to control experimental conditions thus facilitating their study of a specific tissue. As cell therapies, stem cells can only be useful if a therapeutic number of cells can be obtained, stem cell-derived tissues are appropriately functional, and there is long-term persistence of functional tissue. Numerous populations of stem cells have been described; however embryonic stem (ES) cells have been the most popular cell to study development due to their extensive self-renewal capabilities, ease of expansion, and established pluripotentiality. The very characteristics that make ES cells attractive for studying development make them potentially dangerous as a cell therapy due to teratoma formation; however, investigators have been developing protocols to direct differentiation in an effort to address this issue. Extensive work has been done on directing stem cells towards an endocrine pancreatic, neuronal, hepatic, and cardiomyocyte fate[4-6,16].

Duchenne muscular dystrophy (DMD) is a disease where cell therapies would be clinically useful. DMD is characterized by progressive muscle deterioration which results in early patient mortality[7]. The etiology of this disease is a mutation of the dystrophin gene, which results in a loss of functional dystrophin protein[17]. This functional protein loss increases muscle fiber susceptibility to injury. Despite the potential therapeutic potential of stem cells for DMD, few studies have addressed induction of skeletal myoblasts from stem cells. Many of the reported methods involve the use of toxic chemicals, such as demethylating agents[18] or dimethyl sulfoxide (DMSO)[19]. Additionally, co-culture with myogenic cells, overexpression of myogenic genes, or formation of embryoid bodies have been reported[18-23]. These induction methods are inefficient (< 5% induction) or not desirable for cells intended for transplantation; yet prove that stem cells can be induced to a skeletal muscle fate.

Our goal was to develop a skeletal muscle induction protocol that does not require co-culture with other cells, toxic chemicals, or addition of sera, but by taking cues from normal embryonic myogenesis and post-natal skeletal muscle regeneration. Using a multifactorial analysis, cytokines known to be involved in myogenesis such as, Activin-A, fibroblast growth factor-8 (FGF-8), basic FGF (bFGF), and insulin-like growth factor-I (IGF-I) were added to MAPC cultures and mRNA levels for the early myogenic transcription factors, Pax3, Pax7, MyoD, Myf5, and Myf6 were assessed by qRT-PCR.

Materials and Methods

MAPC Expansion Media

Murine MAPC expansion media consisted of 60% low glucose DMEM (LG-DMEM) (Gibco, Carlsbad, CA), 40% MCDB-201 (Sigma, St. Louis, MO), 1% selenium, insulin, transferrin, and ethanolamine (SITE; Sigma, St. Louis, MO), 0.2mg/mL linoleic acid bovine serum albumin (LA-BSA), 10^{-4} M ascorbic acid 2-phosphate (Sigma, St. Louis, MO), 100U penicillin, 1000U streptomycin, 10ng/mL mouse epidermal growth factor (mEGF; R&D Systems, Minneapolis, MN), 10ng/mL platelet derived growth factor (PDGF-BB; R&D Systems, Minneapolis, MN), 2% fetal calf serum (FCS; Hyclone, Logan, UT), 1mg/mL cell culture grade bovine serum albumin (Sigma, St. Louis, MO), 1% chemically defined lipid concentrate (Gibco, Carlsbad, CA), 0.1% β-Mercaptoethanol (Gibco, Carlsbad, CA), and 1000U/mL leukemia inhibitory factor (LIF; Chemicon, Temecula, CA) modified from Jiang et al., 2002[24] and published in Breyer et al [25].

MAPC Isolation and Culture

1 to 3 week old C57Bl/6J mice were euthanized. The hindlimbs were removed and the muscles detached. Bones were minced into very small pieces and placed into a 50mL conical tube with 20-30mL of 0.2% collagenase in Media 199. The tube was incubated at 37°C for 45-60 minutes while being gently shaken. A single cell suspension was obtained by triturating the digested bone with a 23-gauge needle attached to a 10mL syringe 5-10 times. Then the cell suspension was passed through a 40μM nylon mesh filter and 10% FBS was added to inactivate the collagenase. Cells were washed 3 times with 10-15mLs PBS + 0.5% BSA or MAPC expansion medium; in between washes cells were centrifuged at 1800 rpm for 6 minutes. After final PBS wash, cells were plated at 6 x 10^6/well on 100ng/mL human fibronectin (FN; Sigma, St. Louis, MO) coated 6-well plates (NUNC, Rochester, NY) in 2mLs media/well. Cells were incubated at 37°C, 5% CO_2, and 5% O_2. On day 3, 5, and 7, 1 mL of expansion media was added to each well (no media was removed). During the second week, ½ volume of media was changed every other day. During the third week, cells were replated at ~80% confluence (~2x10^4 cells/cm^2). Once cells had grown to 100% confluence, they were replated at 80%. Replating occurred for about one month, after which, $CD45^+$ and $Terr119^+$ cells were removed using a MACS column (Miltenyi Biotec Inc., Auburn, CA). $CD45^-$/$Terr119^-$ cells were then plated on FN coated 96-well plates at 1 cell, 2 cells, 5 cells and 10 cells/well to obtain clones. Two thirds of the media was changed every three days. As clones grew they were transferred to progressively larger plates. Clones meeting quality control standards (see testing below) were cultured on FN coated 10cm plates at seeding density 10,000 cells/plate and split every 36-38 hours. MAPC were maintained at pH ~7.2, 5.5 - 6% CO_2, 5% O_2, and 37ºC conditions. Populations derived from initial subcloning at >1 cell/well, were re-subcloned at 1 cell/well to obtain clonal lines.

Quality Control Testing

Tri-lineage Differentiation (Modified from Jiang et al., 2002[24]) was evaluated using quantitative RT-PCR (qRT-PCR) as previously described[26].

Endothelial differentiation.

4.5 x 10^4 cells/cm^2 were plated on a FN coated 24-well plate in MAPC expansion medium for 12-18 hours. Expansion media was removed and cells washed twice with PBS. Base MAPC medium (expansion media without cytokines and FCS) with 10ng/mL vascular endothelial growth factor (VEGF; R&D Systems, Minneapolis, MN) was added. ~80% media was changed after three days and then every other day onwards. Differentiation was confirmed by qRT-PCR for endothelial transcripts as described in Serafini et al[26].

Neural differentiation

2-3 X 10^3 cells/cm^2 were plated on a FN coated 24-well plate in MAPC expansion medium for 12-18 hours. Expansion media was removed and cells washed twice with PBS. Base MAPC medium with 100ng/mL basic fibroblast growth factor (bFGF; R&D Systems, Minneapolis, MN), 100ng/mL noggin, 2% B27 supplement, 10ng/mL brain-derived neurotrophic factor (BDNF; R&D Systems, Minneapolis, MN), and 20nM retinoic acid. ~80% media was changed after three days and then every other day onwards. Differentiation was confirmed by qRT-PCR for neuroectodermal transcripts as described in Serafini et al[26].

Hepatocyte differentiation

5.5 x 10^4 cells/cm^2 were plated on a 2% Matrigel (BD Biosciences, San Jose, CA) coated 24-well plate in MAPC expansion medium for 12-18 hours. Expansion media was removed and cells washed twice with PBS. Base MAPC medium with 10ng/mL fibroblast growth factor-4 (FGF-4; R&D Systems, Minneapolis, MN) and 10ng/mL hepatocyte growth factor (HGF; R&D Systems, Minneapolis, MN) was added. ~80% media was changed after three days and then every other day onwards. Differentiation was confirmed by qRT-PCR for hepatic transcripts as described in Serafini et al[26].

Additional Quality Testing

In addition to tri-lineage differentiation every month, further quality control tests were conducted on MAPC. Cytogenetics and qRT-PCR for Oct4 mRNA (Oct4 primers listed in table 2.2) were tested once a week. Once a month, FACS was used to assess cell surface morphology for the following markers Sca-1, c-kit, Thy1, CD44, MHC-I^b, MHC-II^b, as previously described[26]. Mycoplasma testing was conducted once a month. Cell morphology was evaluated daily.

Skeletal Muscle Induction

MAPC were plated at 2 x 10^4 cells/well on 1μg/mL FN coated 6-well plates (Corning, Lowell, MA) for 24 hours in MAPC expansion medium. Expansion medium was removed and cells were washed one time with Hams/F12 medium (Mediatech, Herndon, VA). Medium consisting of 1% SITE and 1mg/mL BSA in Hams/F12 medium (called base medium) was added for 48 hours. Base medium was then removed and 1.5mLs of induction medium was added. Induction medium components are listed in Tables 2.1A-C. Media was changed in full every other day until RNA was isolated. Cultures were maintained at 5.5 - 6% CO_2, 5%

O_2, and 37ºC conditions. All cytokines were obtained from R&D Systems (Minneapolis, MN). Fetal calf and horse serum were obtained from Hyclone (Logan, UT), and chick serum from Invitrogen (Carlsbad, CA).

MAPC Co-Culture with C2C12 Cells

MAPC were plated at 2 x 10^4 cells/well on 1μg/mL FN coated 6-well plates (Corning, Lowell, MA) for 24 hours in MAPC expansion medium. Expansion media was removed and cells were washed one time with Hams/F12 media. Base medium was added for 48 hours. 24 hours before co-culture with MAPC, 2 x 10^4 C2C12 cells (ATCC, Manassas, VA) were seeded on 0.45μM transwells (Corning, Lowell, MA) and treated with 10 μg/mL Mitomycin C (Sigma, St. Louis, MO) for 3 hours to arrest cell proliferation. C2C12 loaded transwells were then placed above the MAPC and maintained in base medium with media exchanges every other day until RNA isolation. Cultures were maintained at 5.5 - 6% CO_2, 5% O_2, and 37ºC conditions.

Total RNA Isolation and qRT-PCR

RNA was extracted and isolated from day 0 MAPC and MAPC induced to differentiate to skeletal muscle using the RNeasy Mini kit (Qiagen, Valencia, CA) following the kit protocol for animal cells. The mRNA was reverse transcribed according to instructions from the Superscript III® First-Strand Synthesis System for RT-PCR kit (Invitrogen, Carlsbad, CA) and cDNA was amplified as follows: 40 cycles of a two-step PCR (95°C for 15 seconds, 58 or 60°C for 60 seconds) after initial denaturation (95°C for 10 minutes) with 1 μl DNA solution, 1× TaqMan® SYBR green universal PCR mix (Applied Biosystems, Boston, MA), and with a 100nM primer concentration, using an ABI PRISM 7700 (Applied Biosystems, Boston, MA). Primers used for amplification are listed in Table 2.2. The mRNA levels were normalized using the Gapdh housekeeping gene and RNA from 10-12 day mouse embryo (Ambion, Austin, TX) was used as the positive control. PCR products were verified by running a 1.8% agarose gel (0.5μg/mL ethidium bromide). With exception of Gapdh primers, all primers were purchased through the Microchemical Facility at the University of MN, Minneapolis.

A

A	I	BF	SH	V	H	P	E	F8	W3	B4	NG
20	10	10									
20	20	10									
20	20	10						10			
20	20	10								5	
20	20	10						10		5	
20	20	10									5
20	20	10							10		
10	10	10									
10	20	10									
10	40	10									
10	100	10									
10	10	20									
10	10	40									
10	10	10	10								
10	10	10		10							
10	10	10			10						
10	10	10				10					
10	10	10					10				

C

A	I	BF	F8	W3	NG	BS	CS	HS
2.5	20	10						
2.5	20	10					2	
2.5	20	10						2
2.5	20	10	25					
2.5	20	10	25				2	
2.5	20	10	25					2
0	20	10						
0	20	10					2	
0	20	10						2
0	20	10	25					
0	20	10	25				2	
0	20	10	25					2
0	20	10			5			
0								
0						10		
0							2	
0								2

B

A	I	BF	SH	V	H	P	E	F8	W3	B4	NG	BS	CS	HS
5												10		
5	10													
5		10												
5						10								
5							10							
5	10	10												
5	10					10								
5	10						10							
5		10				10								
5		10					10							
5	20	10												
5	20	10										2		
5	20	10											2	
5	20	10												2
5	20	10							10					
5	20	10						25						
5	20	10						25	10					
5	20	10							10				2	
5	20	10						25					2	
5	20	10						25	10				2	
5	20	10							10					2
5	20	10						25						2
5	20	10						25	10					2
5	20	10								5				
5	20	10							25	5				
5	20	10									5			

Table 2.1 Induction Conditions. A) Conditions with Activin A concentrations of 10-20 ng/mL; B) conditions with Activin A concentrations of 5 ng/mL; C) conditions with Activin A concentrations of 0-2.5 ng/mL. Abbreviations: Activin A (A); Insulin-like Growth Factor-I (I); Basic Fibroblast Growth Factor (BF); Sonic Hedgehog (SH); Vascular Endothelial Growth factor (V); Hepatocyte Growth Factor (H); Platelet-Derived Growth Factor (P); Epidermal Growth Factor (E); Fibroblast Growth Factor-8 (F8); Wnt3A (W3); Bone Morphogenetic Protein-4 (B4); Noggin (NG); Fetal Bovine Serum (BS); Chick Serum (CS); and Horse Serum (HS). All numeric values in the tables represent concentrations in ng/mL with the exception of numeric values for BS, CS, and HS, which represent percentages.

	GENE	Forward Primer 5’ – 3’	Reverse Primer 5’ – 3’	Product Size (bp)
Muscle	Pax3	AAACCCAAGCAGGTG ACAAC	CTAGATCCGCCTCCT CCTCT	205
	Pax7	CTAGAGACCTGCTTG GGAGAAA	CCCAAACAAGGCTG AGTTTTAC	195
	MyoD	CGACTGCCTGTCCAGC ATAG	AAATCGCATTGGGGT TTGAG	200
	Myf5	GACGGCATGCCTGAA TGTAA	CGGATGGCTCTGTAG ACGTG	169
	Myf6	TGCTAAGGAAGGAGG AGCAA	CCTGCTGGGTGAAGA ATGTT	166
	Dystrophin	GAGCAGGTCAGGGTC AACTC	AACAATCCAGCGGTC TTCAG	153
	Mox1	GCTCCAAAGACCAAA ACCAA	AAGGGGCTGCTGAG ATGTAA	195
	Mox2	AGAAGTGGCAGCAAA AGGAA	TGGAACCACACTTTC ACCTG	224
	MEF2A	CAGCAGCACCATCTA GGACA	TGGACAAATTTGAAC CCTGAG	83
	LBX	AAGACCTTTAAGGGG CTGGA	GAAAGCGTTTCTCCA ACTCG	154
	MSX	GGCCTCTCTTTTCCTC TTGG	GGTGACTCTGGACCC ACCTA	164
Bone	Runx2	GGACGAGGCAAGAGT TTCAC	TGAGGCGATCAGAG AACAAA	166
Cartilage	Sox9	AGCTCACCAGACCCT GAGAA	TCCCAGCAATCGTTA CCTTC	199
Dermis	Twist2	AGAGCGACGAGATGG ACAAT	AGATGTGCAGGTGG GTCCT	175

Endothelium	Flk1	TCTGTGGTTCTGCGTG GAGA	GTATCATTTCCAACC ACCCT	270
Smooth Muscle	Sm22	CCACAAACGACCAAG CCTTCT	CGGCTCATGCCGTAG GAT	65
Liver	AFP	GCCCTACAGACCATG AAACAAG	GTGAAACAGACTTCC TGGTCCT	149
	Albumin	AGACTGCCTTGTGTGG AAGACT	TCAACTGTCAGAGCA GAGAAGC	149
Neural	Sox1	CACAACTCGGAGATC AGCAA	TGTAATCCGGGTGTT CCTTC	127
	Sox2	AGGAAGGAGTTTATT CGGATTTG	ACGATATCAACCTGC ATGGAC	181
Wnts	Wnt3a	ATGGCTCCTCTCGGAT ACCT	GGGCATGATCTCCAC GTAGT	204
	Wnt1	ACAGCAACCACAGTC GTCAG	GAATCCGTCAACAG GTTCGT	192
Pluripotency	Oct4	CCAATCAGCTTGGGCT AGAG	CCTGGGAAAGGTGTC CTGTA	129
Housekeeping	Gapdh	Taqman® Rodent GAPDH Control Kit (Applied Biosystems)		177

Table 2.2. Primers Used

Results

In one experiment, MAPC were co-cultured with the myoblast cell line C2C12 plated on 0.45μm transwell plates for 12 days, and mRNA expression levels in MAPC-progeny were measured for the Pax3, Pax7, MyoD, Myf5, and Myf6 genes on days 0, 1, 3, 6, 9, and 12 (Figure 2.1). Expression levels were normalized to day 0 MAPC transcript levels. The expression levels for all transcription factors (TFs) increased by >10 fold between days 3 and 9, except for Myf5 which was not induced and MyoD which increased >100 fold by day 6.

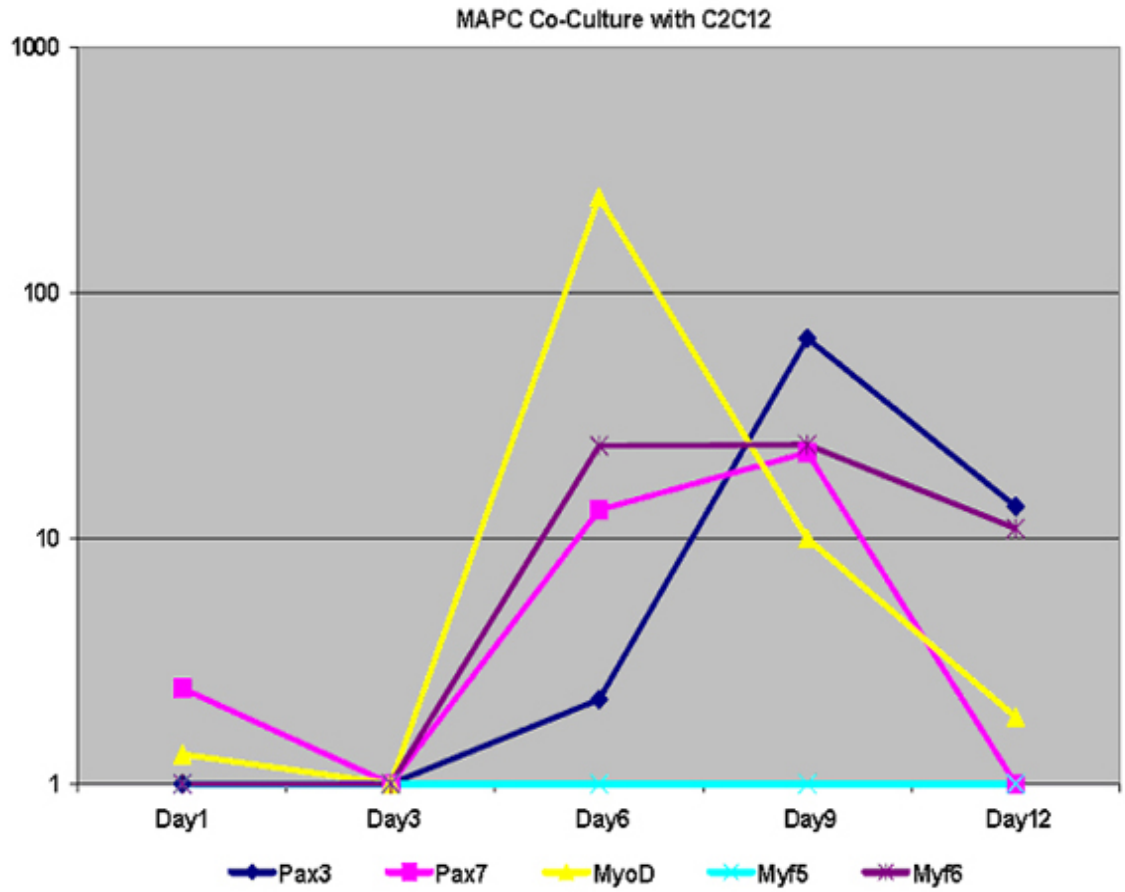

Figure 2.1. MAPC expression levels for Pax3, Pax7, MyoD, Myf5, and Myf6 mRNA when normalized to baseline MAPC levels. Y-axis is on a logarithmic scale

In a multivariate analysis (n=1-9 for each condition), we next evaluated the influence of the many growth factors that have been suggested to play a role in muscle development and regeneration, including Wnt3A, Activin-A, BMP4, FGF-8, VEGF, EGF, PDGF, Noggin, HGF, SHH, bFGF, and IGF-I, alone, in combination, or sequentially, and with or without horse serum, chick serum, or fetal calf serum. Of the conditions tested, the best and most consistent response for skeletal muscle induction was seen with low concentrations of Activin-A (see figure 2.3), 20ng/mL IGF-I, and 10ng/mL bFGF.

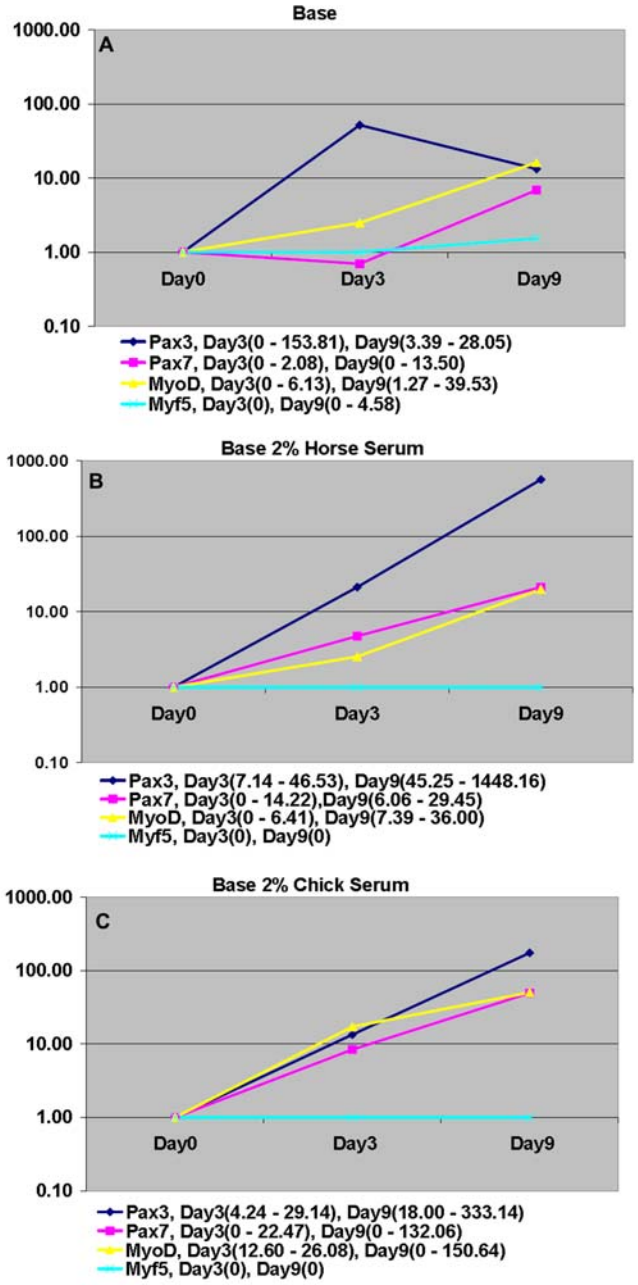

Figure 2.2. Effect of serum on skeletal muscle gene expression. A) Base media, B) base media with 2% horse serum, and C) base media with 2% chick serum conditions were compared using q-RT-PCR for the early muscle genes Pax3, Pax7, MyoD, and Myf5 at three time points. Y-axis is fold increase/decrease compared to day 0 MAPC expression levels on a logarithmic scale. Fold averages are represented in each graph and fold ranges are given for each gene in the figure legends. mRNA for day 0 was from MAPC before plating for induction cultures; day3 and 9 are timepoints beyond the 48 hour base media exposure, as described in methods section

To further assess these conditions, MAPC were cultured in base medium or base medium with 0, 2.5 or 5ng/mL Activin A, 20ng/mL IGF-I, and 10ng/mL bFGF, and with or without 2% horse serum or 2% chick serum (n=3-9 for each condition); FCS was not further assessed because we observed that even low amounts of FCS (0.5-2%) in our induction culture conditions was preferentially adipogenic. In addition, conditions containing cytokines were evaluated when 25ng/mL FGF-8 was present.

Figure 2.2 is a graphical representation of the effect addition of sera to base medium has on muscle gene expression. These studies demonstrate that simple addition of sera increased gene expression for Pax3 and Pax7 as compared to base medium alone.

We evaluated the effect of Activin-A at different concentrations combined with 20ng/mL IGF-I and 10ng/mL bFGF (Figure 2.3). Although significant variability was seen, these studies suggest that lower concentrations of Activin-A were preferential for skeletal muscle induction and that low concentrations of Activin-A are needed for Myf5 expression (can be observed in figures 2.5 and 2.6 as well).

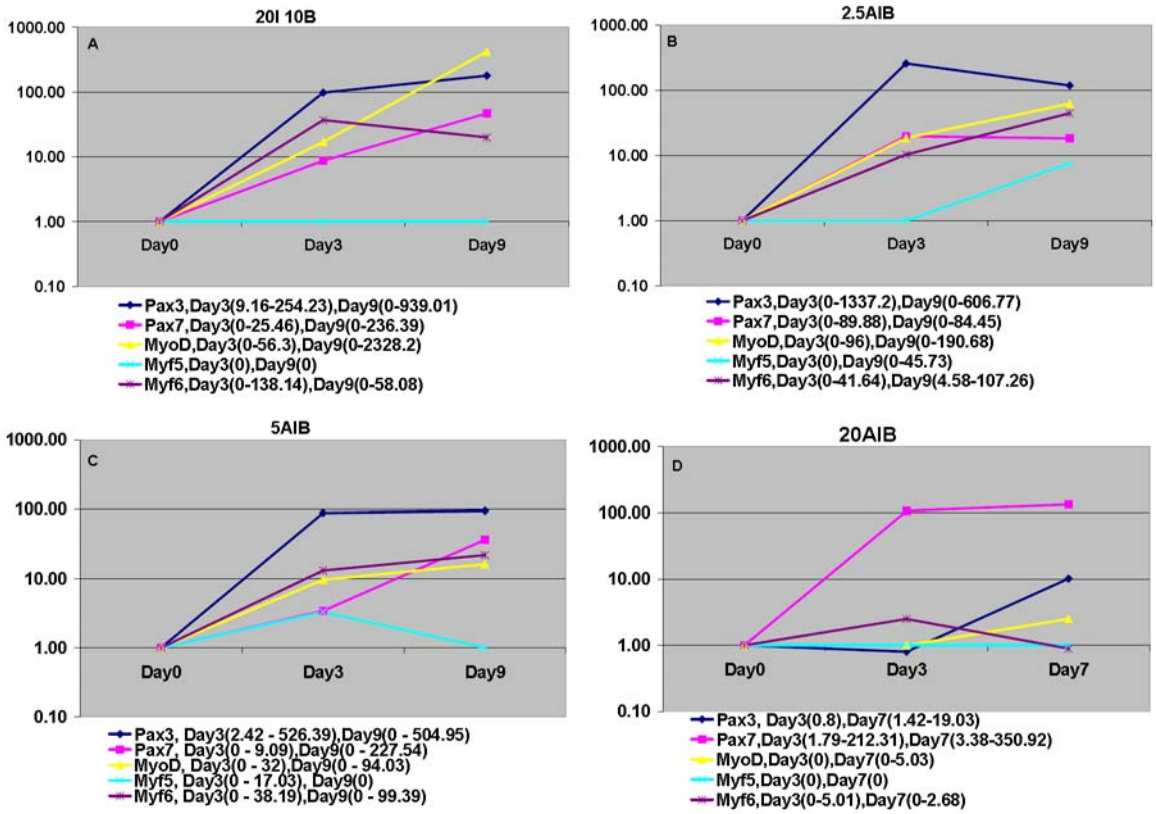

Figure 2.3. Effects of different concentrations of Activin A. Conditions were compared using q-RT-PCR for the muscle transcription factors Pax3, Pax7, MyoD, Myf5, and Myf6 at three time points. Y-axis is fold increase/decrease compared to day 0 MAPC expression levels on a logarithmic scale. Fold averages are represented in each graph and fold ranges are given for each gene in the figure legends. mRNA for day 0 was from MAPC before plating for induction cultures; day3, 7 and 9 are timepoints beyond the 48 hour base media exposure, as described in methods section. Abbreviations: 20ng/mL IGF-I (20I), 10ng/mL bFGF (10B), 2.5ng/mL Activin-A, 20ng/mL IGF-I, 10ng/mL bFGF (2.5AIB), 5ng/mL Activin-A, 20ng/mL IGF-I, 10ng/mL bFGF (5AIB), 20ng/mL Activin-A, 20ng/mL IGF-I, 10ng/mL bFGF (20AIB).

We next tested whether addition of horse serum, chick serum or 25ng/mL FGF-8 to the induction medium containing 0, 2.5, or 5ng/mL Activin-A combined with 20ng/mL IGF-I and 10ng/mL bFGF would increase the robustness of the induction conditions (Figures 2.4-6). Despite significant variability between the different individual experiments, it is unclear whether addition of horse serum, chick serum, or

25ng/mL FGF-8 further enhanced the differentiation ability of MAPC to the myogenic lineage; however the addition of chick serum seemed to preferentially enhance Pax7 expression over addition of horse serum on day 3.

In a final set of experiments we evaluated whether addition of FGF-8 together with serum would have a synergistic effect on myogenic commitment. As shown in figure 2.7, no significant additional effect of FGF-8 was seen when added to induction cultures; although addition of FGF-8 may enhance the effect horse serum conditions have on Pax7 expression at day 3.

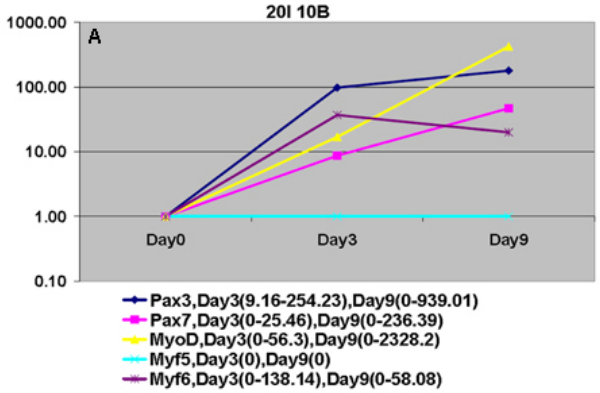

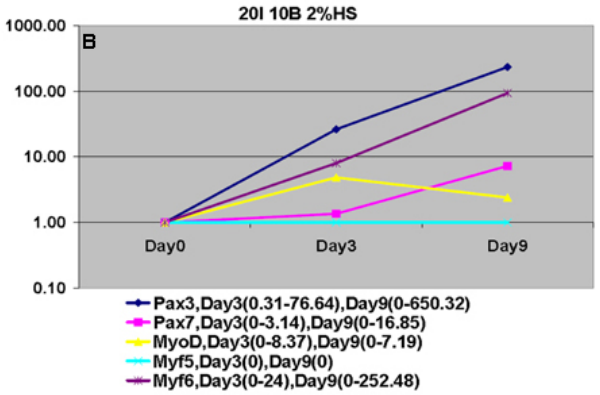

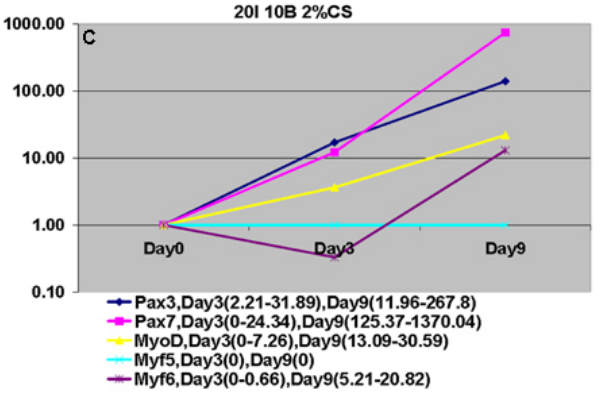

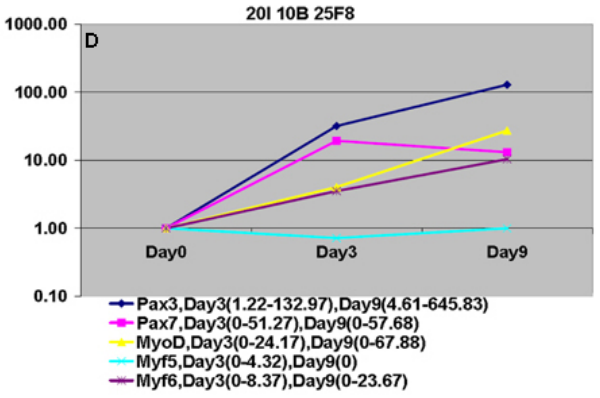

Figure 2.4. Effects of serum or FGF-8 without Activin A on skeletal muscle induction. Conditions were compared using q-RT-PCR for the muscle transcription factors Pax3, Pax7, MyoD, Myf5, and Myf6 at three time points. Y-axis is fold increase/decrease compared to day 0 MAPC expression levels on a logarithmic scale. Fold averages are represented in each graph and fold ranges are given for each gene in the figure legends. mRNA for day 0 was from MAPC before plating for induction cultures; day3 and 9 are timepoints beyond the 48 hour base media exposure, as described in methods section. Abbreviations: 20ng/mL IGF-I (20I), 10ng/mL bFGF (10B), horse serum (HS), chick serum (CS), and 25ng/mL FGF-8 (25F8).

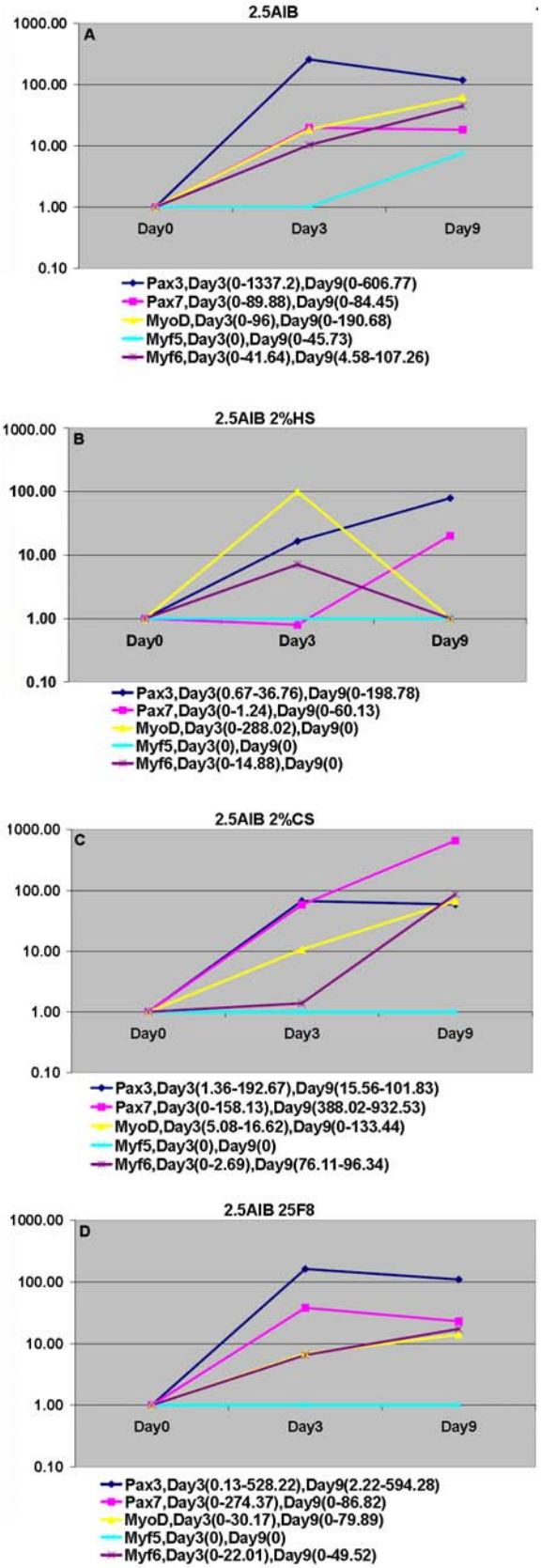

Figure 2.5. Effects of serum or FGF-8 with 2.5ng/mL Activin A on skeletal muscle induction. Conditions were compared using q-RT-PCR for the muscle transcription factors Pax3, Pax7, MyoD, Myf5, and Myf6 at three time points. Y-axis is fold increase/decrease compared to day 0 MAPC expression levels on a logarithmic scale. Fold averages are represented in each graph and fold ranges are given for each gene in the figure legends. mRNA for day 0 was from MAPC before plating for induction cultures; day3 and 9 are timepoints beyond the 48 hour base media exposure, as described in methods section. Abbreviations: 20ng/mL IGF-I (20I), 10ng/mL bFGF (10B), 2.5ng/mL Activin-A, 20ng/mL IGF-I, 10ng/mL bFGF (2.5AIB), horse serum (HS), chick serum (CS), and 25ng/mL FGF-8 (25F8).

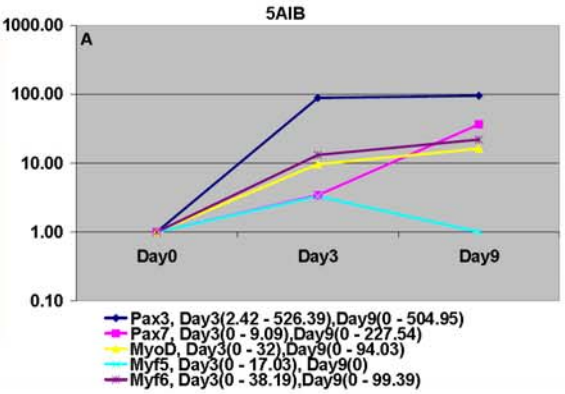

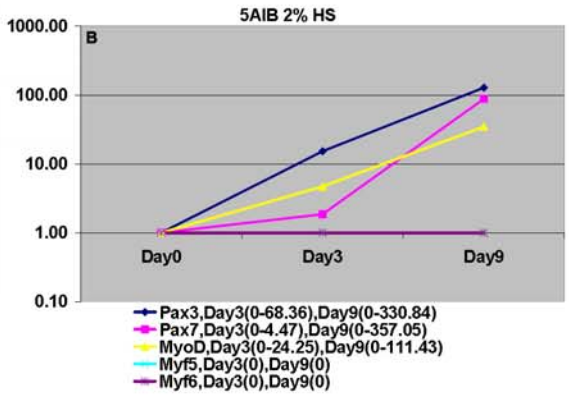

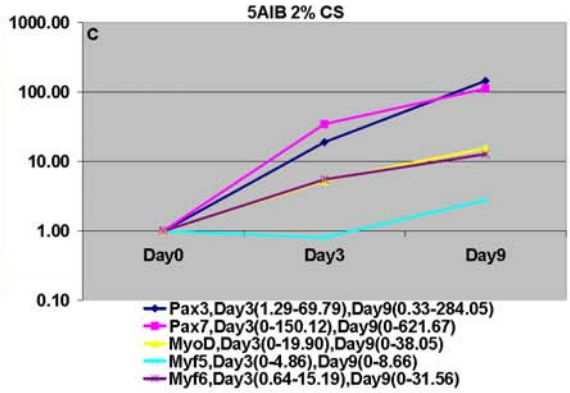

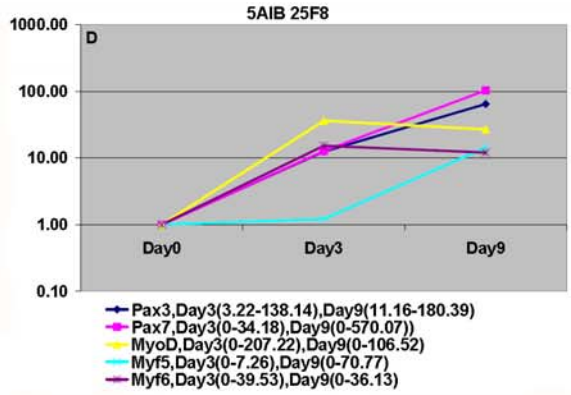

Figure 2.6. Effects of serum or FGF-8 with 5ng/mL Activin A on skeletal muscle induction. Conditions were compared using q-RT-PCR for the muscle transcription factors Pax3, Pax7, MyoD, Myf5, and Myf6 at three time points. Y-axis is fold increase/decrease compared to day 0 MAPC expression levels on a logarithmic scale. Fold averages are represented in each graph and fold ranges are given for each gene in the figure legends. mRNA for day 0 was from MAPC before plating for induction cultures; day3 and 9 are timepoints beyond the 48 hour base media exposure, as described in methods section. Abbreviations: 20ng/mL IGF-I (20I), 10ng/mL bFGF (10B), 5ng/mL Activin-A, 20ng/mL IGF-I, 10ng/mL bFGF (5AIB), horse serum (HS), chick serum (CS), and 25ng/mL FGF-8 (25F8).

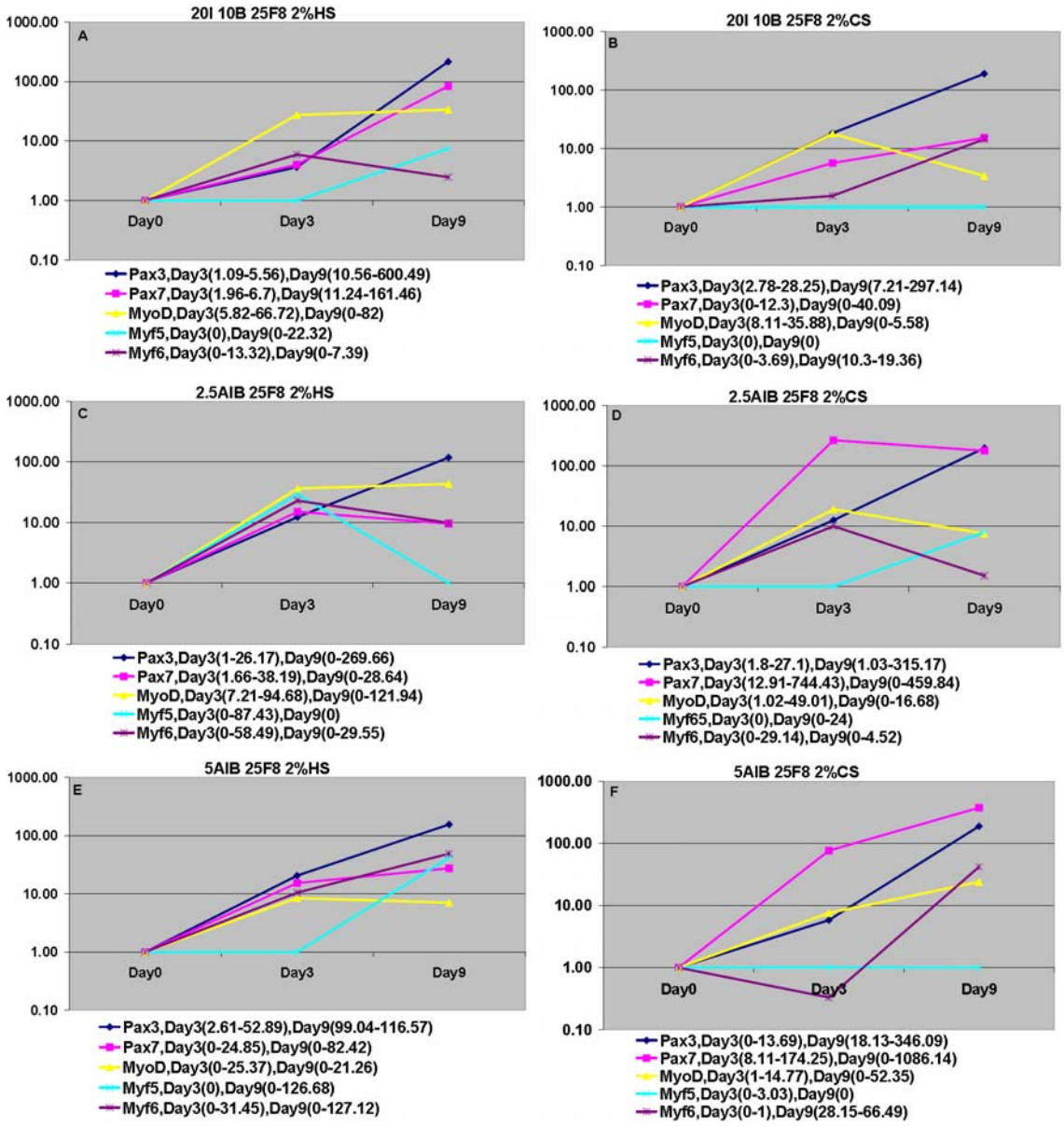

Figure 2.7.Conditions with FGF-8 and serum. Conditions were compared using q-RT-PCR for the early muscle genes Pax3, Pax7, MyoD, Myf5, and Myf6 at three time points. Y-axis is fold increase/decrease compared to day 0 MAPC expression levels on a logarithmic scale. Fold averages are represented in each graph and fold ranges are given for each gene in the figure legends. mRNA for day 0 was from MAPC before plating for induction cultures; day3 and 9 are timepoints beyond the 48 hour base media exposure as described in methods section. Abbreviations: 20ng/mL IGF-I (20I), 10ng/mL bFGF (10B), 2.5ng/mL Activin-A, 20ng/mL IGF-I, 10ng/mL bFGF (2.5AIB), 5ng/mL Activin-A, 20ng/mL IGF-I, 10ng/mL bFGF (5AIB), horse serum (HS), chick serum (CS), 25ng/mL FGF-8 (25F8).

We also evaluated whether the induction was specific, i.e. whether transcripts found in other tissues would also be induced by the presumed myogenic induction schema. Tables 2.3-5 display expression levels of select mesoderm (Dystrophin, Lbx, Msx, Mox1, Mox2, Mef2A, Runx2, Sox9, Flk1, Sm22, and Twist2), endoderm (AFP and Albumin), and neuroectoderm (Sox1 and Sox2) genes for base medium alone, base medium supplemented with 5ng/mL Activin-A, 20ng/mL IGF-I and 10ng/mL bFGF, and base medium supplemented with 5ng/mL Activin-A, 20ng/mL IGF-I and 10ng/mL bFGF with 2% HS. Values are given as fold increases/decreases when expression levels were normalized to baseline MAPC expression levels.

BASE	**Dystrophin**	**LBX**	**MSX**	**MOX1**	**MOX2**	**MEF2A**
Day3 AVG	0	49.464	6.225	14.602	0	13.737
Day3 Range	-	7.81 - 100.78	1.4-15.08	6.48 - 26.17	-	3.99 - 31.78
Day7 AVG	41.212	12.212	12.524	114.045	0	19.229
Day7 Range	0 - 164.85	0 - 47.18	0 - 45.73	0 - 311.91	-	5.94 - 54.00
Day9 AVG	9.818	17.956	13.639	4.567	0	18.019
Day9 Range	0 - 19.29	0 - 47.51	1.89 – 29.96	0 - 11.20	-	10.59 - 31.67
5AIB	**Dystrophin**	**LBX**	**MSX**	**MOX1**	**MOX2**	**MEF2A**
Day3 AVG	56.299	358.701	3.33	4.196	0.766	9.851
Day3 Range	8.54 - 165.42	3.86 – 286	1.09 - 8.06	0 - 14.62	0 - 4.60	4.44 - 18.64
Day7 AVG	35.39	1446.968	8.884	0	0	21.908
Day7 Range	18.25 - 52.53	1342-1552	1.88 – 15.89	-	-	7.19 - 36.63
Day9	109.812	305.562	14.023	36.517	0	18.156

AVG						
Day9 Range	0 - 301.29	0 - 1740	3.40 – 39.26	0 - 103.25	-	7.97 - 35.75
5AIB HS	**Dystrophin**	**LBX**	**MSX**	**MOX1**	**MOX2**	**MEF2A**
Day3 AVG	14.034	70.492	6.378	42.223	0.73	5.362
Day3 Range	5.03 - 33.01	10.12 - 153.28	1.51 - 8.46	0 - 128.89	0 - 2.92	2.72 - 9.32
Day7 AVG	21.432	126.263	13.465	78.271	0	13.224
Day7 Range	6.61 - 36.25	75.85 - 176.68	12.51 – 14.42	71.51 - 85.04	-	4.36 - 22.09
Day9 AVG	62.045	138.459	24.979	79.349	0	10.277
Day9 Range	0 - 226.76	7.29 - 321.8	8.43 - 36	0 - 239.69	-	7.16 - 15.14

Table 2.3. Analysis of additional myogenic genes. Day 3, 7 and 9 are timepoints beyond the 48 hour base media exposure, as described in methods section. Abbreviations: Average (AVG); 5ng/mL Activin A, 20ng/mL IGF-I, and 10ng/mL bFGF (5AIB); and horse serum (HS).

Table 2.3 is a summary of expression for genes associated with myogenesis that were tested in addition to Pax3, Pax7, MyoD, Myf5, and Myf6. Again, expression was highly variable however there appears to be increased expression of dystrophin and Lbx in the presence of Activin-A; additionally horse serum appears to decrease the effect of Activin-A on expression of these genes.

BASE	**FLK1**	**SM22**	**RUNX2**	**SOX9**	**TWIST2**
Day3 AVG	2.199	20.979	9.695	67.634	0
Day3 Range	0.16 - 5.01	1.68 - 59.1	2.51 - 23.51	55.72 - 79.07	-
Day7 AVG	3.422	20.34	21.711	932.177	0
Day7 Range	1.11 - 7.73	0.37 - 48.84	2.61 - 60.34	0 - 3666.02	-

Day9 AVG	5.854	17.435	43.173	60.893	0.79
Day9 Range	3.51 - 9.06	8.17 - 33.36	10.20 - 100.43	46.36 - 72.25	0 - 1.67
5AIB	**FLK1**	**SM22**	**RUNX2**	**SOX9**	**TWIST2**
Day3 AVG	1.234	11.229	21.938	244.022	0
Day3 Range	0.23 - 1.87	0.75 - 26.17	0.05 - 96.67	0 - 989.1	-
Day7 AVG	2.955	6.299	267.83	1178.786	0
Day7 Range	1.56 - 4.35	2.61 - 9.99	0.06 - 535.6	162.6 - 2195	-
Day9 AVG	2.146	2.974	96.963	506.602	0
Day9 Range	0.88 - 3.52	1.88 - 9.45	0 - 496.28	15.14 - 1808	-
5AIB HS	**FLK1**	**SM22**	**RUNX2**	**SOX9**	**TWIST2**
Day3 AVG	0.862	6.395	83.217	97.484	0
Day3 Range	0.21 - 1.48	3.27 - 10.2	1.63 - 249	4.42 - 233.94	-
Day7 AVG	0.648	17.494	251.334	756.813	0
Day7 Range	0.21 - 1.08	15.08 - 19.9	233.94 - 268.73	381.36 - 1132.27	-
Day9 AVG	0.638	134.399	75.392	349.63	0
Day9 Range	0.05 - 1.3	14.32 - 294.07	7.97 - 141.04	61.18 - 768.02	-

Table 2.4. Analysis of somitic mesodermal gene expression. Day 3, 7 and 9 are timepoints beyond the 48 hour base media exposure, as described in methods section. Abbreviations: Average (AVG); 5ng/mL Activin A, 20ng/mL IGF-I, and 10ng/mL bFGF (5AIB); and horse serum (HS).

Table 2.4 is a summary of non-muscle mesodermal gene expression. Our tested induction conditions appear to affect osteocyte and chondrocyte gene expression most extensively and again, the presence of Activin-A had a positive effect on expression of these genes.

BASE	**AFP**	**Albumin**	**SOX1**	**SOX2**

Day3 AVG	0.322	3.024	3.626	3.758
Day3 Range	0.03 – 0.78	1.31 - 5.96	2.78 – 4.68	2.01 - 6.61
Day7 AVG	0.512	20.529	14.226	8.338
Day7 Range	0.08 – 1.49	2.88 - 43.41	2.92 – 25.11	0.99 - 16.51
Day9 AVG	1.784	16.671	12.363	15.144
Day9 Range	0.13 – 4.91	3.19 - 42.67	1.51 – 30.38	1.46 - 36.89
5AIB	**AFP**	**Albumin**	**SOX1**	**SOX2**
Day3 AVG	0.104	21.525	1.0729	1.251
Day3 Range	0.02 – 0.18	3.17 - 45.41	0.61 – 1.68	0.8 - 1.91
Day7 AVG	0.445	3.936	1.496	2.177
Day7 Range	0.09 - 0.8	3.39 - 4.48	0.57 – 2.42	0.96 - 3.4
Day9 AVG	2.336	82.546	3.124	19.161
Day9 Range	0.07 – 8.69	5.56 - 168.31	0.86 – 4.61	1 - 67.42
5AIB HS	**AFP**	**Albumin**	**SOX1**	**SOX2**
Day3 AVG	0.445	9.695	1.311	1.508
Day3 Range	0.18 - 1.1	2.2 - 28.34	0.71 – 2.94	0.94 - 2.19
Day7 AVG	2.002	49.167	1.871	2.788
Day7 Range	1.46 – 2.54	28.54 - 69.79	1.73 – 2.01	2.47 - 3.11
Day9 AVG	8.413	196.505	1.373	3.425
Day9 Range	1.95 – 14.37	13.64 - 548.75	0.3 - 3.75	0.59 - 9.51

Table 2.5. Analysis of hepatic and neuronal gene expression. Day 3, 7 and 9 are timepoints beyond the 48 hour base media exposure, as described in methods section. Abbreviations: Average (AVG); 5ng/mL Activin A, 20ng/mL IGF-I, and 10ng/mL bFGF (5AIB); and horse serum (HS).

Table 2.5 summarizes results for hepatic and neuronal gene expression. Average AFP and albumin expression levels were increased when the induction condition included Activin-A. By contrast, neuronal gene expression decreased when Activin-A was included.

Lastly, cytogenetics, passage number, and Oct4 mRNA expression were evaluated as potential factors influencing level of induction. Figure 2.8 represents the plot of Oct4 mRNA expression for Day 0 (undifferentiated) MAPC as a percentage of ES cell Oct4 expression versus passage number. The percent of diploid cells is also plotted versus passage number in figure 2.8. No definite correlation between gene expression and cytogenetics, passage number, or Oct4 expression could be deduced.

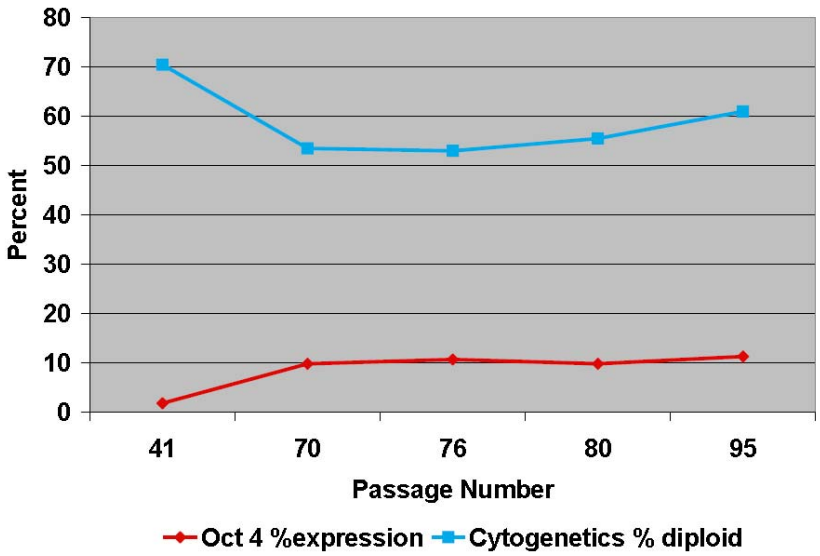

Figure 2.8. Oct4 Expression and Cytogenetics Versus Passage Number for Undifferentiated MAPC

Discussion

Quantitative real-time PCR (q-RT-PCR) is a useful and efficient screening tool to assess gene expression when a large number of variable conditions are being tested. We tested over 60 different induction schemes for myogenic gene expression on at least two different time points. The tested induction schemes were derived after studying cytokines involved in embryonic myogenesis and post-natal skeletal muscle regeneration. Of those tested induction schemes a subset, wherein Activin-A, bFGF, IGF-I and FGF-8 were added singly or in combination to MAPC differentiation cultures, stood out and were further evaluated for myogenic induction potential.

Stem cell co-culture with myogenic cells is a proven method for inducing skeletal muscle. We used this culture system to determine whether MAPC could be induced to express genes found in primitive muscle progenitors. To be able to separate the MAPC progeny from C2C12 cells and avoid the complication of potential MAPC-C2C12 cell fusion, we elected to co-culture our cells with C2C12 cells using transwell plates. Previously reported co-culture protocols typically co-culture so that there is direct cell-cell contact and at least one report noted that direct contact was necessary for induction[27]. This may explain why the increases in gene expression in MAPC co-cultured with C2C12 cells are not as dramatic as those reported. It should however be noted that fusion had not been ruled out as the reason for the observed muscle induction in the previously published studies. Our observation in the MAPC/C2C12 co-culture is indicative that soluble factors secreted by C2C12 cells can initiate muscle induction and the transwell co-culture system wherein C2C12 cells are also treated with Mitomycin C definitively rules out that the induction is the result of fusion. Interestingly, we observed a spike and subsequent drop in MyoD expression between days 7 and 9 in some of our cytokine-mediated culture conditions (data not shown), which is similar to that seen between days 6 and 9 for the co-culture experiment (figure 2.1). This observation indicates that transcription factor expression may peak at a day earlier than day 9, and may account for some of the variability in levels detected for the various transcription factors in our cultures where we evaluated expression only on day 3 and day 9.

Our goal was to determine a defined, non-toxic, preferentially serum-free culture system for skeletal muscle induction. The co-culture with C2C12 cells, however, provided us with a time course of myogenic gene expression. Compared with the co-culture system, our defined protocol can equally induce early myogenic gene expression, specifically induction of Pax3, Pax7, MyoD, Myf6, and in some instances Myf5. These particular transcription factors were chosen as screening genes because of their known role during embryonic myogenesis. Pax3 and Pax7 are early markers of skeletal muscle specification and can be detected in the developing somite[28]. MyoD, Myf5, and Myf6 are myogenic regulatory factors that are involved in myogenic determination[29].

Although a serum free culture condition was desired, the use of serum was investigated for any significant effects on induction. FBS had a strong adipogenic effect on our cultures, which correlates with reported findings [30,31]. Horse and chick serum have been well established as low mitogenic media supplements used to cause myoblast differentiation (formation of myotubules), so we chose to evaluate

their use in our induction cultures. Adipogenesis was still observed with the use of horse and chick serum, but to a lesser extent than with the use of FBS, therefore their use was further evaluated in combination with cytokines. Addition of serum did not have a dramatic effect on our induction cultures; however a possible link between chick serum exposure and up-regulation of Pax7 expression was observed.

MAPC have characteristics of pluripotent cells such as Oct4 expression and extensive renewal capabilities[24,26,32]; therefore we chose the use of Activin-A to direct differentiation away from ectoderm and toward mesoderm. Kubo et al. demonstrated that low concentrations of Activin-A (1-10ng/mL) were preferential for skeletal muscle induction, which supports two of our findings[2]; 1) concentrations of lower than 20ng/mL of Activin-A were needed, and 2) the observed up-regulation of Myf5 required Activin-A exposure.

Proper embryonic myogenesis requires a delicate balance of phasic exposures to and gradients of a number of different cytokines[8,12,15,33-35]. Use of bFGF and IGF-I in our induction cultures was derived from testing a number of growth factors involved in myogenesis. Lower concentrations of all tested cytokines (5-10ng/mL) were initially chosen because our goal was to induce myogenesis and not to cause proliferation, which would likely block induction of differentiation. After we determined that from among the many choices, IGF-I and bFGF induced the most pronounced expression of myogenic transcription factors, higher concentrations were tested for one cytokine in combination with lower concentration of the second cytokine. As expected, the higher concentrations of IGF-I (40 and 100ng/mL) and bFGF (20 and 40ng/mL) appeared to decrease myogenic gene expression (data not shown); however increasing IGF-I from 10ng/mL to 20ng/mL had a positive effect and thus this concentration was chosen for our future studies. Addition of 25ng/mL FGF-8 did not obviously affect myogenic gene expression. Different concentrations of FGF-8 were not tested and future testing will need to address whether increased or decreased concentrations of FGF-8 might have a more pronounced effect.

To verify appropriate gene expression, a subset of our experiments was further evaluated for expression of the myogenic genes, Lbx, dystrophin, Msx, Mef2A, Mox1, and Mox2. There was a noticeable increase in Lbx expression which correlates with published reports on a link between Lbx and Pax3 expression[36]. All other myogenic genes tested, aside from Mox2, showed on average a >10-fold increase in gene expression above baseline MAPC levels for at least one of the days tested; further supporting our observation that our induction conditions are myogenic.

From our studies, we also determined that the induction was not limited to skeletal myogenesis as early somitic transcription factors known to be required for osteoblast[37] and chondroblast[38] differentiation were also induced. Interestingly, there was no observed dermis gene expression, which correlates to previous reports that Runx2 expression is inhibited by Twist2[39]; suggesting a preferential induction of somite-derived mesenchymal tissues by the use of our culture conditions. We also observed to a lesser extent increases in endodermal gene expression using our defined conditions. Although Kubo et al. [2] demonstrated that high concentrations of Activin-A (100ng/mL) were best for inducing definitive endoderm, they also reported that low levels of hepatic gene expression could still be detected with lower

concentrations of Activin-A. Finally, the virtual absence of neuroectoderm gene expression was observed in our induction cultures, which was expected with the use of Activin-A.

The myogenic induction conditions described here are an initial step towards creating a defined protocol to induce myogenesis in pluripotent stem cells. The induction of MAPC to an early myogenic fate, as we have shown here, may yield a useful population of cells for transplantation. Indeed, levels of Pax3 and Pax7 consistently, albeit variably, increased during the culture period and such cells could prove useful for transplantation in dystrophic models where donor-derived satellite cells will be necessary for long-term treatment[40]. However future studies should further verify transcription factor protein expression, prior to testing the cells in *in vivo* models. In addition, the finding that the cultures remain mixed will need to be addressed, as transplantation of osteoblast and / or chondroblast committed cells may lead to calcified lesions when grafted in an inflammatory environment *in vivo*. Furthermore, the current conditions could be applied to defining protocols for osteoblast and chondroblast development as Runx2 and Sox9 expression was robust using our conditions.

Finally, cells generated using our induction protocols are obviously not mature myoblasts. Additional manipulations such as co-culture with myoblasts following initial induction, and delayed addition of sera could be used to determine if differentiation to a more mature fate can be obtained. If that would be possible, undefined induction protocols could then be replaced by defined serum free conditions using a multivariate analysis study as was done here to define conditions to induce initial myogenic commitment.

Acknowledgements

The authors would like to thank David Abts, Brendan McKnight, and Arjun Menon for their work on this project. Additionally, the authors thank Lucas Chase for his invaluable quantitative PCR advice. SAF was funded by a NASH Grant, NIH Muscle Training Grant, and NIH Musculoskeletal Training Grant. The work was also supported by R01 DK58295 to CMV.

References

1. Nakayama, T., Momoki-Soga, T., Yamaguchi, K. & Inoue, N. Efficient production of neural stem cells and neurons from embryonic stem cells. *Neuroreport* **15**, 487-91 (2004).
2. Kubo, A. et al. Development of definitive endoderm from embryonic stem cells in culture. *Development* **131**, 1651-62 (2004).
3. Maltsev, V. A., Rohwedel, J., Hescheler, J. & Wobus, A. M. Embryonic stem cells differentiate in vitro into cardiomyocytes representing sinusnodal, atrial and ventricular cell types. *Mech Dev* **44**, 41-50 (1993).
4. Yin, Y. et al. AFP(+), ESC-derived cells engraft and differentiate into hepatocytes in vivo. *Stem Cells* **20**, 338-46 (2002).
5. Klug, M. G., Soonpaa, M. H., Koh, G. Y. & Field, L. J. Genetically selected cardiomyocytes from differentiating embronic stem cells form stable intracardiac grafts. *J Clin Invest* **98**, 216-24 (1996).
6. Kim, J. H. et al. Dopamine neurons derived from embryonic stem cells function in an animal model of Parkinson's disease. *Nature* **418**, 50-6 (2002).
7. O'Brien, K. F. & Kunkel, L. M. Dystrophin and muscular dystrophy: past, present, and future. *Mol Genet Metab* **74**, 75-88 (2001).
8. Gilbert, S. F. (ed.) *Developmental Biology* (Sinauer Associates, Inc, Sunderland, Massachusetts, 1997).
9. Buckingham, M. Skeletal muscle formation in vertebrates. *Curr Opin Genet Dev* **11**, 440-8 (2001).
10. Buckingham, M. et al. The formation of skeletal muscle: from somite to limb. *J Anat* **202**, 59-68 (2003).
11. Charge, S. B. & Rudnicki, M. A. Cellular and molecular regulation of muscle regeneration. *Physiol Rev* **84**, 209-38 (2004).
12. Cossu, G. & Borello, U. Wnt signaling and the activation of myogenesis in mammals. *Embo J* **18**, 6867-72 (1999).
13. Konigsberg, I. R. in *Myology* (ed. Engel, A. G.) 39-71 (McGraw-Hill, Inc, New York, 1986).
14. Sabourin, L. A. & Rudnicki, M. A. The molecular regulation of myogenesis. *Clin Genet* **57**, 16-25 (2000).
15. Zhao, P. & Hoffman, E. P. Embryonic myogenesis pathways in muscle regeneration. *Dev Dyn* **229**, 380-92 (2004).
16. D'Amour, K. A. et al. Production of pancreatic hormone-expressing endocrine cells from human embryonic stem cells. *Nat Biotechnol* **24**, 1392-401 (2006).
17. Straub, V. & Campbell, K. P. Muscular dystrophies and the dystrophin-glycoprotein complex. *Curr Opin Neurol* **10**, 168-75 (1997).
18. Wakitani, S., Saito, T. & Caplan, A. I. Myogenic cells derived from rat bone marrow mesenchymal stem cells exposed to 5-azacytidine. *Muscle Nerve* **18**, 1417-26 (1995).

19. Dinsmore, J. et al. Embryonic stem cells differentiated in vitro as a novel source of cells for transplantation. *Cell Transplant* **5**, 131-43 (1996).
20. Ridgeway, A. G. & Skerjanc, I. S. Pax3 is essential for skeletal myogenesis and the expression of Six1 and Eya2. *J Biol Chem* **276**, 19033-9 (2001).
21. Petropoulos, H. & Skerjanc, I. S. Beta-catenin is essential and sufficient for skeletal myogenesis in P19 cells. *J Biol Chem* **277**, 15393-9 (2002).
22. Asakura, A., Seale, P., Girgis-Gabardo, A. & Rudnicki, M. A. Myogenic specification of side population cells in skeletal muscle. *J Cell Biol* **159**, 123-34 (2002).
23. Guan, K. et al. Pluripotency of spermatogonial stem cells from adult mouse testis. *Nature* **440**, 1199-203 (2006).
24. Jiang, Y. et al. Pluripotency of mesenchymal stem cells derived from adult marrow. *Nature* **418**, 41-9 (2002).
25. Breyer, A. et al. Multipotent adult progenitor cell isolation and culture procedures. *Exp Hematol* **34**, 1596-601 (2006).
26. Serafini, M. et al. Hematopoietic reconstitution by multipotent adult progenitor cells: precursors to long-term hematopoietic stem cells. *J Exp Med* **204**, 129-39 (2007).
27. Salvatori, G. et al. Myogenic conversion of mammalian fibroblasts induced by differentiating muscle cells. *J Cell Sci* **108 (Pt 8)**, 2733-9 (1995).
28. Tajbakhsh, S. in *Vertebrate Myogenesis* (ed. B.Brand-Saberi) 61-79 (Springer-Verlag, Berlin, 2002).
29. Kassar-Duchossoy, L. et al. Mrf4 determines skeletal muscle identity in Myf5:Myod double-mutant mice. *Nature* **431**, 466-71 (2004).
30. Smith, P. J., Wise, L. S., Berkowitz, R., Wan, C. & Rubin, C. S. Insulin-like growth factor-I is an essential regulator of the differentiation of 3T3-L1 adipocytes. *J Biol Chem* **263**, 9402-8 (1988).
31. Huang, H., Lane, M. D. & Tang, Q. Q. Effect of serum on the down-regulation of CHOP-10 during differentiation of 3T3-L1 preadipocytes. *Biochem Biophys Res Commun* **338**, 1185-8 (2005).
32. Jiang, Y. et al. Multipotent progenitor cells can be isolated from postnatal murine bone marrow, muscle, and brain. *Exp Hematol* **30**, 896-904 (2002).
33. Gustafsson, M. K. et al. Myf5 is a direct target of long-range Shh signaling and Gli regulation for muscle specification. *Genes Dev* **16**, 114-26 (2002).
34. Brunelli, S., Relaix, F., Baesso, S., Buckingham, M. & Cossu, G. Beta catenin-independent activation of MyoD in presomitic mesoderm requires PKC and depends on Pax3 transcriptional activity. *Dev Biol* (2007).
35. Heldin, C. H., Miyazono, K. & ten Dijke, P. TGF-beta signalling from cell membrane to nucleus through SMAD proteins. *Nature* **390**, 465-71 (1997).

36. Mennerich, D., Schafer, K. & Braun, T. Pax-3 is necessary but not sufficient for lbx1 expression in myogenic precursor cells of the limb. *Mech Dev* **73**, 147-58 (1998).
37. Stein, G. S. et al. Runx2 control of organization, assembly and activity of the regulatory machinery for skeletal gene expression. *Oncogene* **23**, 4315-29 (2004).
38. Kawakami, Y. et al. Transcriptional coactivator PGC-1alpha regulates chondrogenesis via association with Sox9. *Proc Natl Acad Sci U S A* **102**, 2414-9 (2005).
39. Bialek, P. et al. A twist code determines the onset of osteoblast differentiation. *Dev Cell* **6**, 423-35 (2004).
40. Montarras, D. et al. Direct isolation of satellite cells for skeletal muscle regeneration. *Science* **309**, 2064-7 (2005).

CHAPTER 3

TRANSPLANTATION OF MURINE MULTIPOTENT ADULT PROGENITOR CELLS INTO MYOPATHIC MICE

Sarah A. Frommer[1,2], Amanda Bartz[1], Marta Serafini[1], Beatriz Pelacho[1], Aernout Luttun[1], Saswati Mahapatra[1], Yuehua Jiang[1], Molly Nelson-Holte[1] and Catherine M. Verfaillie[1]

Stem Cell Institute[1] and Biomedical Engineering Department[2], University of Minnesota, Minneapolis, Minnesota

Abstract

Duchenne muscular dystrophy (DMD) is a genetic disease caused by a mutation of the dystrophin gene, which results in a functional loss of protein. The dystrophin protein is associated with stabilization of the muscle membrane upon contraction[1] as well as anchoring important signaling enzymes[2,3]. Functional loss of dystrophin leads to a constant degeneration and regeneration cycle in DMD patients until the resident muscle stem cells, satellite cells,"burn out" [4], upon which muscle tissue is replaced by fat and connective tissue. DMD patients typical die in their mid-twenties and currently there are no effective therapies that will increase the patient's life span or cure them; however experimental therapies aimed at restoring functional dystrophin expression have been promising[5-7].

One such therapy is the use of stem cells. Here we investigate the use of a specific stem cell, multipotent adult progenitor cells (MAPC), as therapy for DMD. Additionally, we investigate a number of muscle injury strategies using *mdx*5cv mice in an effort to increase engraftment levels. Our studies reveal that MAPC do not contribute to skeletal muscle in a model without muscle injury, however there is the potential for MAPC to be a systemically delivered therapy for DMD. Analysis of tissue from different injury models revealed that MAPC can contribute to muscle fibers using some of our developed strategies; however no co-localization of donor fibers and dystrophin was detected.

Introduction

Muscular dystrophies are a set of genetic diseases that affect striated muscle. The most common dystrophy is Duchenne muscular dystrophy (DMD). Caused by the functional loss of dystrophin, this disease is characterized by progressive deterioration of striated muscle resulting in early mortality of the patients[8]. Within skeletal muscle, dystrophin provides a link between the cellular cytoskeleton and the basal lamina, thereby conferring stability during contraction. Loss of this stability is believed to cause a cascade that ultimately leads to myofiber necrosis[9].

This devastating disease occurs in 1/3500 live male births and is diagnosed in early childhood (3-5 years). Patients are typically wheel-chair bound by age 12 and die in their mid-twenties from respiratory and/or cardiac complications[10]. Unfortunately, there is still no cure or effective treatment to slow the progression of DMD. Many researchers have been working to develop potential curative therapies. The most promising therapies for long-term amelioration of DMD are exon skipping[6,11,12], gene therapy[13,14], and/or cell therapy[7,15-19]. All three therapies aim to introduce functional dystrophin; however only cell therapies have the potential for long-term effects through donor-derived satellite cells.

A number of different cells types have been tested for treatment of DMD in mouse models, however levels of engraftment have been low (<10%)[15,16,18,20-22]. Here we investigate the use of MAPC as a cell therapy for DMD and test different injury induction methods in an effort to increase engraftment levels. Previously reported methods such as high dose limb irradiation and use of the myotoxic agent, cardiotoxin were tested. In addition, we developed injury induction protocols utilizing forced exertion through swimming and femoral artery ligations.

Materials and Methods

Animal Models

All experimental protocols were approved by, and were performed in accordance with guidelines of the Institutional Animal Care Usage Committee at the University of Minnesota. B6Ros.Cg-DMD*mdx*-5cv (*mdx*5cv), C57Bl/6, and NOD/LtSz-*scid/scid* (NOD/SCID) mice were originally obtained from Jackson Laboratories (Bar Harbor, ME). NOD/SCID and *mdx*5cv mouse colonies were established at the University of Minnesota and all animals were housed in specific pathogen-free Research Animal Resources facilities. The ages of the *mdx*5cv mice used in this study ranged from 3-8 weeks.

MAPC Isolation and Culture

1 to 3 week old C57Bl/6TgN(act-EGFP) (a kind gift by Dr. M. Okabe, Osaka University, Japan) mice were euthanized. The hindlimbs were removed and the muscles detached. Bones were minced into very small pieces and placed into a 50mL conical tube with 20-30mL of 0.2% collagenase in Media 199. The tube was incubated at 37°C for 45-60 minutes while being gently shaken. A single cell suspension was obtained by triturating the digested bone with a 23-gauge needle attached to a 10mL syringe 5-10 times. Then the cell suspension was passed through a 40μM nylon mesh filter and 10% FBS was added to inactivate the collagenase. Cells were washed 3 times with 10-15mLs PBS + 0.5% BSA or MAPC expansion medium; in between washes cells were centrifuged at 1800 rpm for 6 minutes. After final PBS wash, cells were plated at 6 x 10^6/well on 100ng/mL human fibronectin (FN; Sigma, St. Louis, MO) coated 6-well plates (NUNC, Rochester, NY) in 2mLs media/well. Cells were incubated at 37°C, 5% CO_2, and 5% O_2. On day 3, 5, and 7, 1 mL of expansion media were added to each well (no media was removed). During the second week, ½ volume of media were changed every other day. During the third week, cells were replated at ~80% confluence (~2x10^4 cells/cm^2). Once cells had grown to 100% confluence, they were replated at 80%. Replating occurred for about one month, after which, $CD45^+$ and $Terr119^+$ cells were removed using a MACS column (Miltenyi Biotec Inc., Auburn, CA). $CD45^-$/$Terr119^-$ cells were then plated on FN coated 96-well plates at 1 cell, 2 cells, 5 cells and 10 cells/well to obtain clones. Two thirds of the media were changed every three days. As clones grew they were transferred to progressively larger plates. Clones meeting quality control standards (see testing below) were cultured on FN coated 10cm plates at seeding density 10,000 cells/plate and split every 36-38 hours. MAPC were maintained at pH ~7.2, 5.5 - 6% CO_2, 5% O_2, and 37ºC conditions. Populations derived from initial subcloning at >1 cell/well, were re-subcloned at 1 cell/well to obtain clonal lines.

Quality Control Testing

Tri-lineage Differentiation (Modified from Jiang et al., 2002[23]) was evaluated using quantitative RT-PCR (q-RT-PCR) as previously described[24].

Endothelial differentiation.

4.5 x 10^4 cells/cm^2 were plated on a FN coated 24-well plate in MAPC expansion medium for 12-18 hours. Expansion media was removed and cells washed twice with PBS. Base MAPC medium (expansion media without cytokines and FCS) with 10ng/mL vascular endothelial growth factor (VEGF; R&D Systems, Minneapolis, MN) was added. ~80% media was changed after three days and then every other day onwards. Differentiation was confirmed by qRT-PCR for endothelial transcripts as described in Serafini et al[24].

Neural differentiation

2-3 X 10^3 cells/cm^2 were plated on a FN coated 24-well plate in MAPC expansion medium for 12-18 hours. Expansion media was removed and cells washed twice with PBS. Base MAPC medium with 100ng/mL basic fibroblast growth factor (bFGF; R&D Systems, Minneapolis, MN), 100ng/mL noggin, 2% B27 supplement, 10ng/mL brain-derived neurotrophic factor (BDNF; R&D Systems, Minneapolis, MN), and 20nM retinoic acid. ~80% media were changed after three days and then every other day onwards. Differentiation was confirmed by qRT-PCR for neuroectodermal transcripts as described in Serafini et al[24].

Hepatocyte differentiation

5.5 x 10^4 cells/cm^2 were plated on a 2% Matrigel (BD Biosciences, San Jose, CA) coated 24-well plate in MAPC expansion medium for 12-18 hours. Expansion media was removed and cells washed twice with PBS. Base MAPC medium with 10ng/mL fibroblast growth factor-4 (FGF-4; R&D Systems, Minneapolis, MN) and 10ng/mL hepatocyte growth factor (HGF; R&D Systems, Minneapolis, MN) was added. ~80% media was changed after three days and then every other day onwards. Differentiation was confirmed by qRT-PCR for hepatic transcripts as described in Serafini et al[24].

Additional Quality Control Testing

In addition to tri-lineage differentiation every month, further quality control tests were conducted on MAPC. Cytogenetics and q-RT-PCR for Oct4 mRNA (Forward: 5'-CCAATCAGCTTGGGCTAGAG-3'; Reverse: 5'- CCTGGGAAAGGTGTCCTGTA-3') were tested once a week, as previously described[24]. Approximately once a month, FACS was used to assess cell surface morphology for the following markers Sca-1, c-kit, Thy1, CD44, MHC-I^b, MHC-II^b, as previously described[24]. Mycoplasma testing was conducted once a month. Cell morphology was evaluated daily.

NOD/SCID Transplantations

6-8 week old NOD/SCID mice were irradiated with 275cGy/min at 57 cGy/min. Four hours before injection of mouse MAPC (mMAPC), NOD/SCID mice were treated with an intraperitoneal injection of anti-asialo GM1 antibody (20μL of the stock solution diluted in 380μL of 1x PBS; Wako, Richmond, VA). Animals also received anti-asialo GM1 antibody on days 11 and 22 after transplantation. Transplantation of mMAPC was via tail vein injection and occurred 12-24 hours after irradiation. Further experimental protocols can be found in Serafini and Dylla et al [24].

Muscle Injury Procedures

Cardiotoxin Damage

Mice were anesthetized with 2.5 - 3% isoflurane at a 2 L/min flow rate prior to injecting cardiotoxin. The injection site was sterilized by wiping the area with alcohol three times. Cardiotoxin (Sigma, St. Louis, MO) 25ng suspended in 25μL sterile PBS was injected intramuscularly into the gastrocnemius muscle 24-48 hours prior to intramuscular (IM) injection of 500,000 mMAPC.

X-Ray mediated limb injury

Mice were anesthetized by 100 mg/kg of ketamine and 10 mg/kg of xylazine. Animals were then placed in a pie-shaped plexiglass holder, and covered with a 4-mm-thick lead shield. The hindleg was extended from under the lead shielding into the center of the holder, taped into place, and the foot was protected with a small, 4-mm-thick lead shield. The legs were then exposed to X-rays at a dose rate of 1.4 Gy/min generated by a Philips 250-kV orthovoltage machine (Philips Medical Systems, Brookfield, WI) for a total dose of 10Gy. Directly following limb irradiation, mice were IM injected with 500,000 mMAPC.

Exertion by swimming

A counter-current swimming pool, made specifically for rodents, was filled with distilled water and pre-warmed to 32°C. Mice swam for 30 min on three consecutive days. The current was adjusted for each mouse so that voluntary maximum effort was achieved. Animals were watched closely for fatigue and the current was adjusted accordingly to allow the animals to finish the 30 min swim time. IM injection of 500,000 mMAPC was performed ~24 hours after the last swim day; except for two animals which were injected directly following the last swim time.

5-fluorouracil treatment

5-Fluorouracil (5-FU, Sigma, St. Louis, MO) was diluted in distilled sterile water to stock concentration of 10mg/mL and was given at a dosage of 150mg/kg intraperitoneally. 5-FU was given at least 24-36 hours before IM injection of 500,000 mMAPC.

Femoral Artery Ligation

Hindlimb ischemia was induced by permanent ligation of the left common femoral artery just proximal to the deep femoral artery in C57Bl/6 and *mdx*5cv mice. Surgical procedures were performed in a laminar flow hood. Animals were anesthetized with 2.5 - 3% isoflurane with a flow of 2 L/min using 100% O_2. The left groin area was shaved with an electric shaver (Oster, McMinnville, TN) and sterilized with alcohol. The femoral artery was exposed and the area intended for ligation was delicately dissected out with great care not to injury the nerve or vein. An Ethilon 9-0 suture attached to a 3/8 circular needle (Ethicon product code 2890G, Piscataway, NJ) was used to ligate the artery; two ligations were performed on the same artery to ensure complete ligation. Directly following ligation, 500,000 mMAPC were IM injected into the gastrocnemius muscle.

Animal Perfusion and Tissue Harvest

At ~3-6 weeks (mdx5cv) or ~8-21 weeks (NOD/SCID) after mMAPC injection, transplanted animals were anesthetized and perfused intracardially with 10ml of 10 mM EDTA/1xPBS, followed by 10 ml 1x Z-Fix

(Anatech, Battle Creek, MI). After systemic perfusion with PBS and Z-Fix, muscles were removed, post-fixed in Z-Fix for 8-24 hours at 4°C and processed for routine paraffin embedding. In some instances, fixed tissues were washed with 1x PBS, cryoprotected by overnight incubation in 30% sucrose and subsequently quick-frozen in optimum cutting temperature (OCT; Sakura, Torrance, CA) compound and stored at -80°C.

Immunohistology for eGFP$^+$ cells

Frozen muscle was sectioned at 10 μM, rehydrated with PBS, counterstained with Hoechst, and then mounted. Muscle embedded in paraffin was sectioned at 6μM. After dewaxing and rehydration, antigen retrieval was done by steaming for 20 minutes in 0.01M citrate buffer pH 6.0. Endogenous peroxidase was blocked by 5 minute incubations with 1.8% H_20_2 (Sigma, St. Louis, MO) and 2.5% periodic acid (Sigma, St. Louis, MO), both in water. After a wash with water, slides were incubated for 2 minutes with 0.02% sodium borohydride (Sigma, St. Louis, MO) in water. Endogenous biotin was blocked by sequential 15 minute incubations with avidin and biotin (Biotin Blocking System, DakoCytomation, Carpinteria, CA). Non-specific binding sites were blocked by incubation for 30 minutes with 0.4% fish skin gelatin (Sigma, St. Louis, MO) in PBS. Blocking buffer was removed, rabbit anti-GFP (Abcam, Cambridge, MA) diluted 1:350 was added and incubated overnight at 4°C. After primary antibody incubation, slides were washed and subsequently incubated with AlexaFluor 488 anti-rabbit diluted 1:500 (Invitrogen, Carlsbad, CA), then counterstained with Hoechst and mounted in fluorescent mounting media (Dakocytomation, Carpinteria, CA) or incubated with diaminobenzidine (DAB; Dakocytomation, Carpinteria, CA), counterstained with hematoxilyn, then dehydrated and mounted. Fluorescence was visualized and recorded using an Axiovert 200M microscope and AxioVision 4.3 software (Carl Zeiss, Inc., Thornwood, NY). DAB staining was visualized and recorded using an Olympus microscope (Model BX41; Center Valley, PA) with a Nikon (Coolpix 995 model; Tokyo, Japan) digital camera attached.

Lectin, Dystrophin, and CD45 Staining

Frozen sections (10μm) were incubated with biotin conjugated BS-I lectin (Sigma, St. Louis, MO), diluted 1:100 for 1 hour at room temperature, washed with TBS, and then incubated with strepavidin-PE (BD Pharmingen, San Diego, CA), diluted 1:500 for 45 min and Hoechst. Slides were mounted in Fluorescence Mounting Medium (DakoCytomation, Carpinteria, CA). Frozen sections or deparaffinized, rehydrated, and antigen retrieved paraffin sections (see above for protocol) were incubated overnight with rabbit anti-dystrophin diluted 1:500 ("Rabbit 3" raised against human dystrophin middle rod actin binding domain, a kind gift from Dr. J. Ervasti, University of Wisconsin Medical School, Madison) and subsequently incubated with anti-rabbit AlexaFluor 594 diluted 1:500 (Invitrogen, Carlsbad, CA) and Hoechst. For CD45 staining, rat anti-CD45 (Biolegend, San Diego, CA) diluted 1:250 was used as the primary antibody and anti-rat Cy3 (Jackson ImmunoResearch; West Grove, PA) diluted 1:450 was used as the secondary; all steps for CD45 staining avoided the use of Tween-20.

GFP and Dystrophin Staining Testing

Two C57Bl/6TgN(act-EGFP) animals were used for this testing. One animal was perfused with 0.5% paraformaldehyde (PFA) diluted in PBS and the second was perfused with 4% PFA using the protocol described above. Following perfusion, the tibialis anterior muscles were removed from each mouse and then divided into pieces of equal thickness for further processing. Tissue was processed as follows: 0 min, 15 min, 30 min, 60 min, 120 min, or overnight (~12 hours) incubation at 4ºC in respective concentrations of PFA (0.5% or 4%). After incubation was finished, tissues were washed three times with PBS and then snap frozen in liquid nitrogen cooled isopentane. Tissues were sectioned at 10μM and then washed in PBS and subsequently stained with rabbit anti-dystrophin diluted 1:200 (Abcam, Cambridge, MA). Anti-rabbit AlexaFluor 594 (Invitrogen, Carlsbad, CA) diluted 1:500 was used as the secondary antibody and Hoechst as the counterstain. Double fluorescence was visualized and recorded using an Axiovert 200M microscope and AxioVision 4.3 software (Carl Zeiss, Inc., Thornwood, NY), with careful attention to make exposure times equal for all slides.

Results

Dystrophin Staining Optimization on Fixed Tissues

In an effort to optimize retention of GFP protein in isolated muscle and to visualize dystrophin, we tested different fixation conditions (see methods), as well as 5 different dystrophin antibodies, and 3 different antigen retrieval solutions. We present data for 3 of the 5 fixation conditions using two different concentrations of paraformaldehyde (Figure 3.1), whereas additional fixation periods (15, 30 and 60 min) are not shown. These results suggest that conditions that allow retention of the GFP signal make evaluation of dystrophin expression difficult.

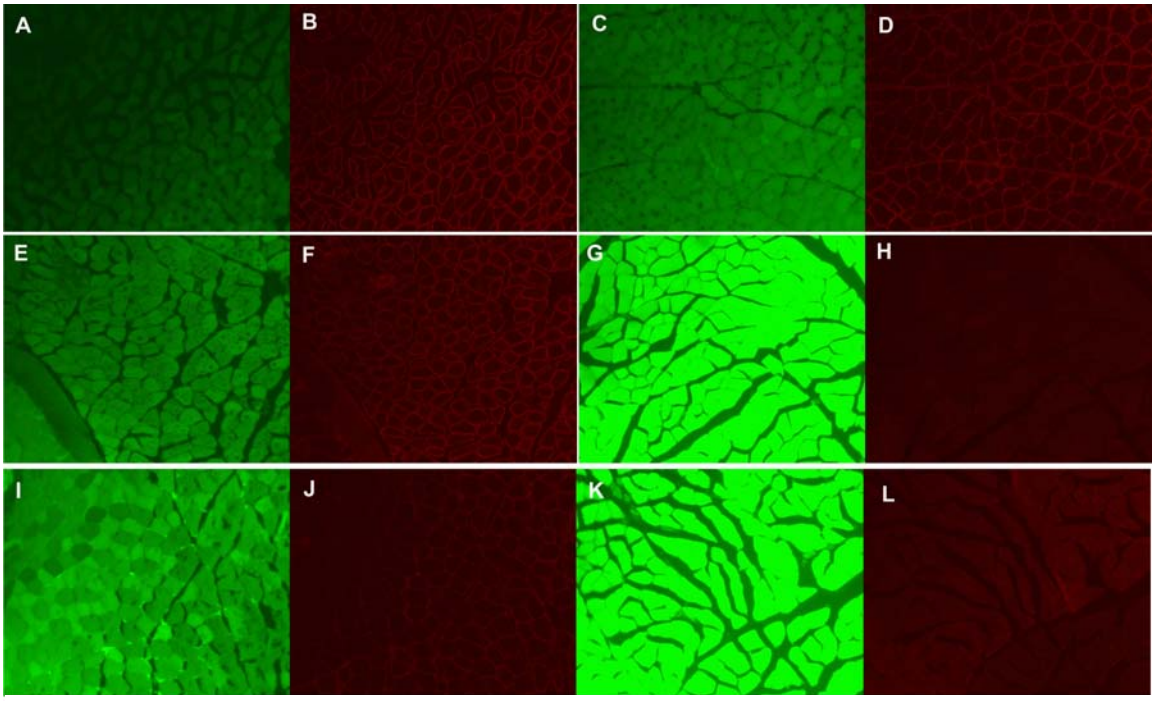

Figure 3.1. Effect of tissue fixation on GFP retention and subsequent dystrophin staining. A, C, E, G, I, and K GFP fluorescence; B, D, F, H, J, L dystrophin staining. A, B) 0.5% PFA used to perfuse and no further fixation; C, D) 4% PFA used to perfuse and no further fixation; E, F) 0.5% PFA for 2 hours; G, H) 4% PFA for 2 hours; I, J) 0.5% PFA overnight (~12 hours); K, L) 4% PFA overnight. Magnification 40X.

Figure 3.2 is an example of a MAPC injected muscle wherein we did not detect dystrophin staining in a GFP^+ fiber from an animal that was treated with cardiotoxin and then exerted by swimming. Similar to the animal shown in figure 3.7A, revertant fibers were found upon dystrophin staining, as well as in our negative control (PBS) animal (data not shown).

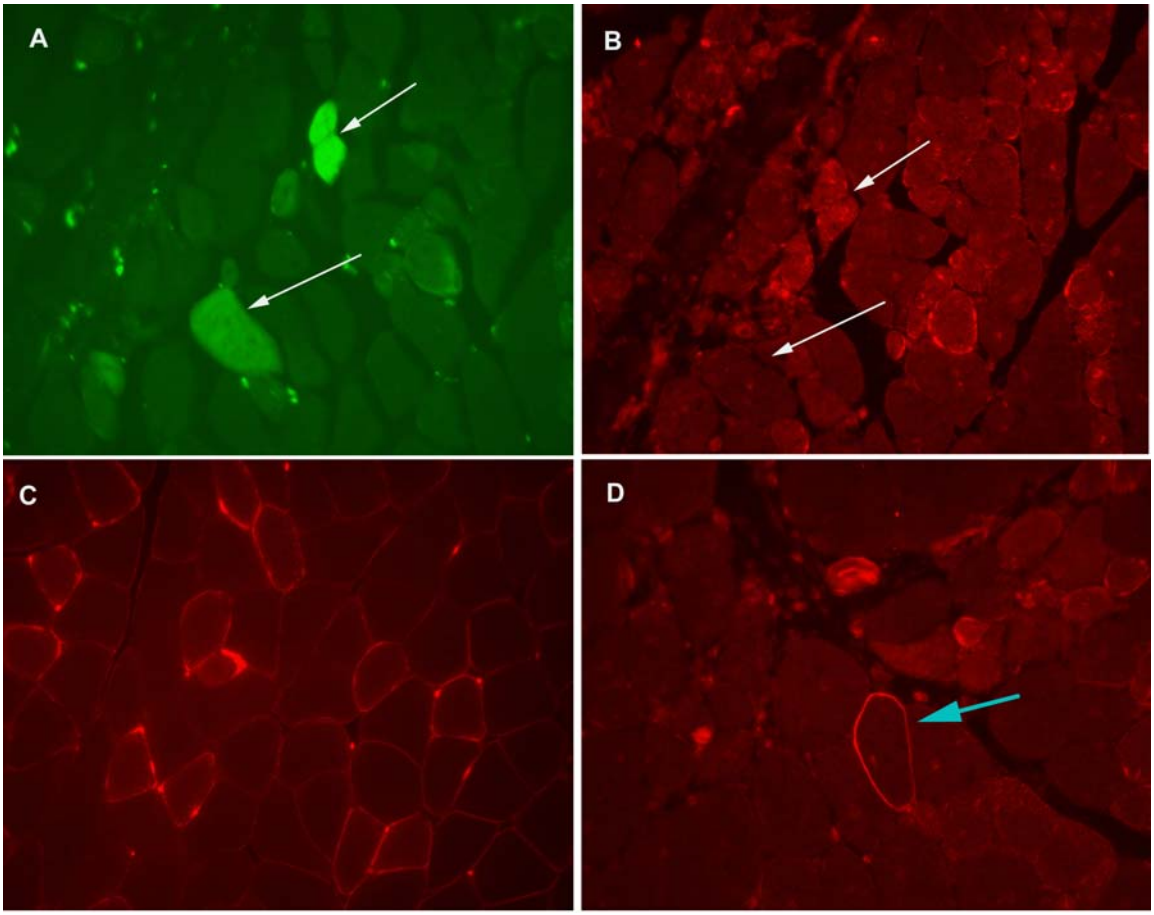

Figure 3.2. Dystrophin staining in muscle of an animal exerted by swimming and subsequently injected with cardiotoxin prior to MAPC grafting. A) GFP+ fiber; B) Sequential slide with no staining of dystrophin for GFP+ fibers (white arrows point to same fibers from A); C) Example of dystrophin staining on fixed normal tissue; D) Example of revertant fiber (blue arrow) staining for dystrophin. Magnification at 20X.

Systemic Delivery of mMAPC into Sublethally Irradiated Immunodeficient Mice without Muscle Damage Does Not Lead to Contribution of mMAPC to Skeletal Muscle

Our lab recently reported [24] robust hematopoietic reconstitution following systemic delivery of mMAPC into sublethally irradiated immunocompromised hosts. Non-hematopoietic tissues were also analyzed, including skeletal muscle.

Mouse	# cells injected	%Oct-4 mRNA	% aneuploid	Time (weeks)	Marrow %	Blood %	Muscles Collected	GFP
M6	1 x 10^6	ND	10	13	64.2	46.2	GAST	+
M10	0.3 x 10^6	64.2	10	21	23	63.1	TA, B	-
M13	0.1 x 10^6	64.2	10	21	1.9	ND	TA, B, GAST	-
M14	0.1 x 10^6	64.2	10	21	2.1	6.2	TA, B, GAST	-
M16	0.3 x 10^6	64.2	10	18	1.9	31.8	TA	+

M23	1 x 10^6	29.5	35	12	84.4	94.4	TA, B, GAST	+
B228	1 x 10^6	13	20	8	50*	ND	TRI	+
B229	1 x 10^6	13	20	8	50*	ND	TRI	+
B230	1 x 10^6	13	20	8	50*	ND	TRI	+

Table 3.1. Summary of NOD/SCID Animals Tested. Abbeviations: Gastrocnemius (GAST); Tibialis Anterior (TA); Biceps (B); Triceps (TRI); Not Determined (ND). Chart adapted from Serafini et al. [24]. *: engraftment level in spleen

Of the 9 animals we tested, we detected GFP positive cells in skeletal muscle tissue of 6; however no GFP positive fibers were observed in any of the animals (Table 3.1 and Figure 3.3). In an effort to determine the nature of the GFP positive cells, we conducted staining for Pax7, MyoD, CD45, and BS-I Lectin. Pax7 and MyoD staining was not compatible with fixed tissue (data not shown). Very few GFP^+ cells co-expressed CD45, and some co-labeled with BS-I Lectin (Figure 3.4); however a number of GFP^+ cells did not co-label with any of the tissue markers tested. These findings were similar to what was seen in other organs, where a significant portion of the GFP^+ cells did not co-label with anti-CD45 but whose lineage fate could not be determined.

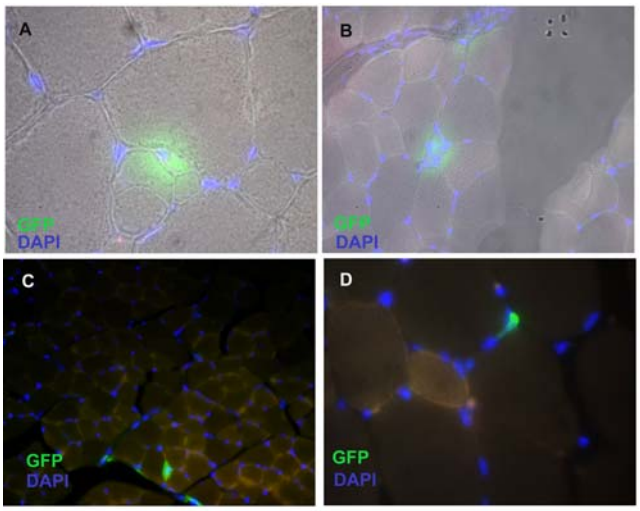

Figure 3.3. Localization of GFP+ cells in NOD/SCID transplants. A, B) M6 mouse gastrocnemius muscle; C) M16 mouse tibialis anterior muscle; D) M23 mouse biceps brachii muscle. Magnification: A, D 40X oil; B, C 20X

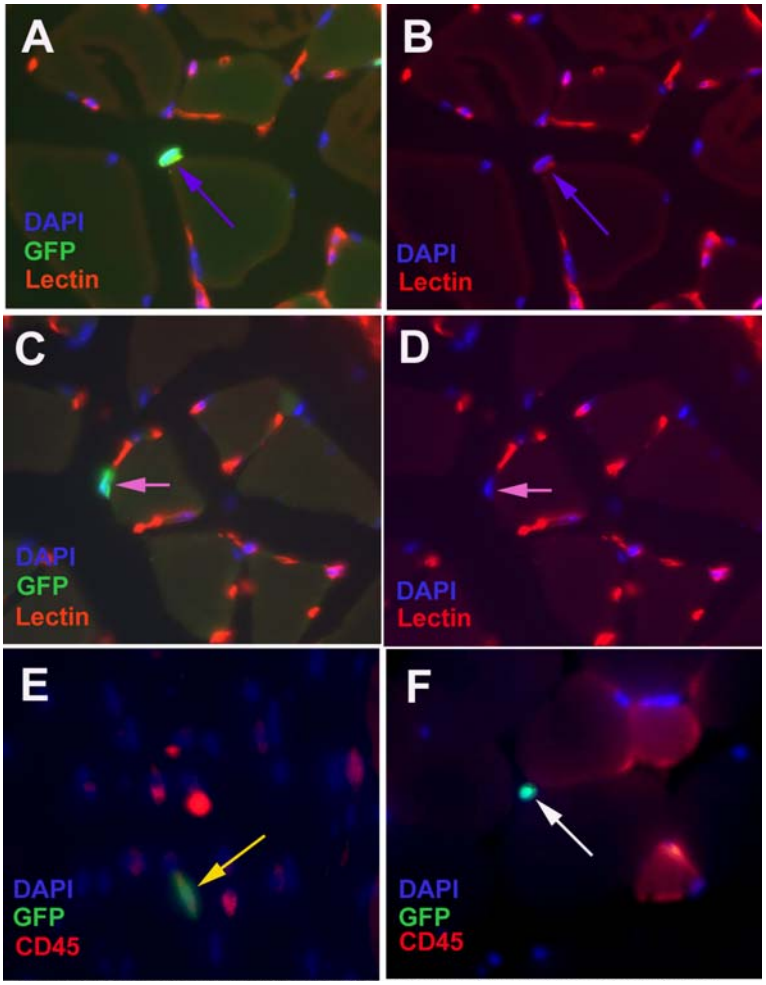

Figure 3.4. GFP co-staining with BS-I Lectin or CD45 in NOD/SCID transplants. A, B) B228 mouse; GFP+ cell co-stains with BS-I Lectin (purple arrows). C, D) B230 mouse; GFP+ cell does not co-stain for BS-I Lectin (pink arrows). E) B229 mouse; GFP+ cell co-stains with CD45 (yellow arrow), and F) B229 mouse; GFP+ cell does not stain for CD45 (white arrow). Magnification: A-F 40X oil.

mMAPC Can Contribute to Muscle Fibers, But Do Not Make Dystrophin

Induced Injury Type	**n**	**Animals with GFP$^+$ Fibers**	**Dystrophin$^+$ GFP$^+$ Fibers**
No Injury	3	0	ND
Cardiotoxin	3	0	ND
X-Ray 10Gy	5	0	ND
5-FU	7	0	ND
Swim	2	0	ND
Swim + 5-FU	10	2	0
5-FU +cardiotoxin	2	0	ND
Swim + cardiotoxin	2	1	0
Swim + 5-FU +cardiotoxin	2	1	0

Femoral Artery Ligation	8	2	ND

Table 3.2. Summary of induced injuries on mdx5cv mice and number per group. The number of animals with GFP+ fibers and dystrophin+/GFP+ fibers is also summarized. Abbreviations: 5-Fluorouracil (5-FU); Not determined (ND).

We also tested whether undifferentiated mMAPC injected directly into muscle would contribute to skeletal muscle. For this a number of different models were used, all in the *mdx*5cv background. Table 3.2 is a summary of our findings. Injection of mMAPC in uninjured mice did not lead to contribution of the mMAPC to skeletal muscle fibers. Likewise in the 2 animals treated with cardiotoxin no contribution of mMAPC to skeletal muscle was observed. In two animals treated with 10Gy X-irradiation, GFP^+ cells were not detected among the muscle fibers, however, collections of GFP^+ cells could be seen in scar tissue (Figure 3.5). The presence of GFP^+ cells in scar tissue was verified through Sirius Red staining for collagen (data not shown).

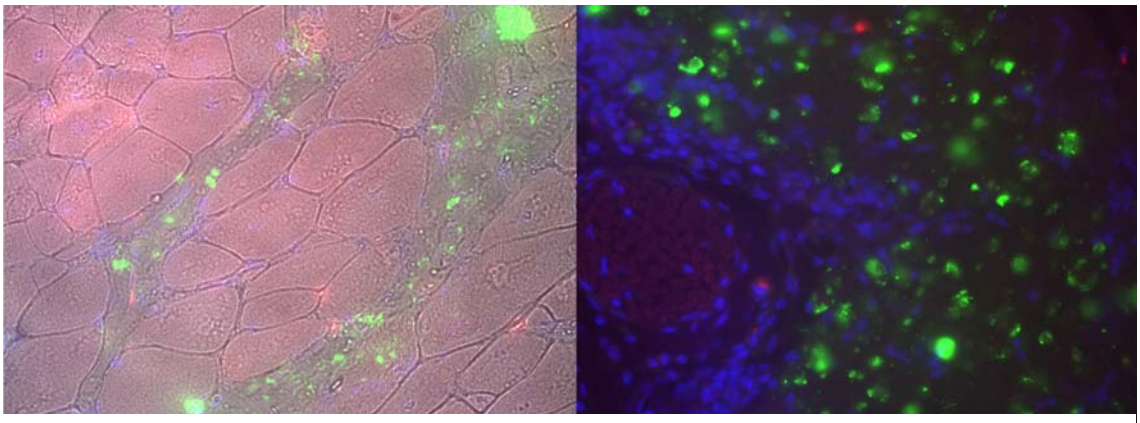

Figure 3.5. GFP localization in muscle from limb irradiated *mdx*5cv mice. GFP detection in muscle from two *mdx*5cv mice in where the hindlimb had been irradiated at 10Gy x-irradiation prior to mMAPC injection. Magnification: A, 20X; B, 40X oil. GFP (green); DAPI (blue); Background (red).

We next tested whether exercise alone or combined with 5-FU, which we hypothesized may eliminate a number of cycling satellite cells induced by the physical exertion, would allow for mMAPC contribution to skeletal muscle. One animal that underwent physical exertion by swimming and received 5-FU had evidence of robust engraftment in the skeletal muscle compartment, as shown in figure 3.6; however no dystrophin staining could be detected. Figure 3.7 shows GFP^+ fibers detected in 3 different injury induced animals. In two additional animals that had been exercised and then treated with cardiotoxin alone or cardiotoxin and 5-FU we found GFP positive muscle fibers. However, again no dystrophin could be detected in the GFP+ fibers even though revertant fibers were present (Figures 3.2A, B, and D).

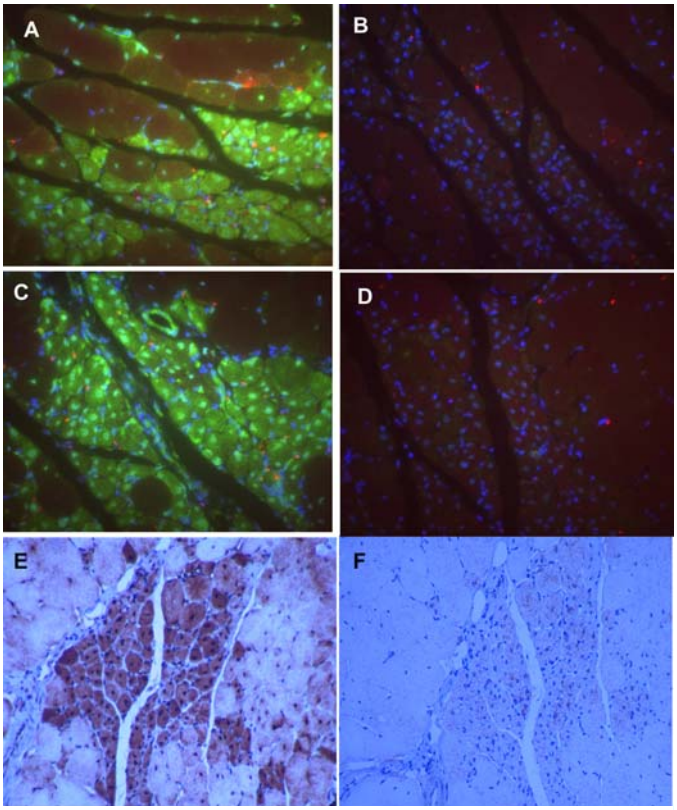

Figure 3.6. Muscle from *mdx*5cv mouse treated with 5-FU following swimming. Muscle from one *mdx*5cv mouse treated with 5-FU after rigorous swimming contained large patches of GFP+ fibers. A, C) GFP fluorescence staining using rabbit anti-GFP and Alexa 488; and B, D) sequential section for A and C, respectively stained with IgG control antibody; E) GFP staining using DAB; F) IgG control for E. Magnification 20X. GFP (green or brown (DAB)), DAPI (blue), background (red).

Finally, as we have evidence that transplantation of MAPC in wild type C57Bl/6 animals with ischemic limb injury leads to contribution of MAPC to regenerating muscle fibers (Aernout Luttun et al, under revision), we tested whether ischemia established by femoral artery ligation in *mdx*5cv mice would lead to contribution of mMAPC to skeletal muscle fibers. In 2 animals we found rare GFP positive muscle fibers (Figures 3.7C and E); however, dystrophin staining has not yet been performed on these tissues.

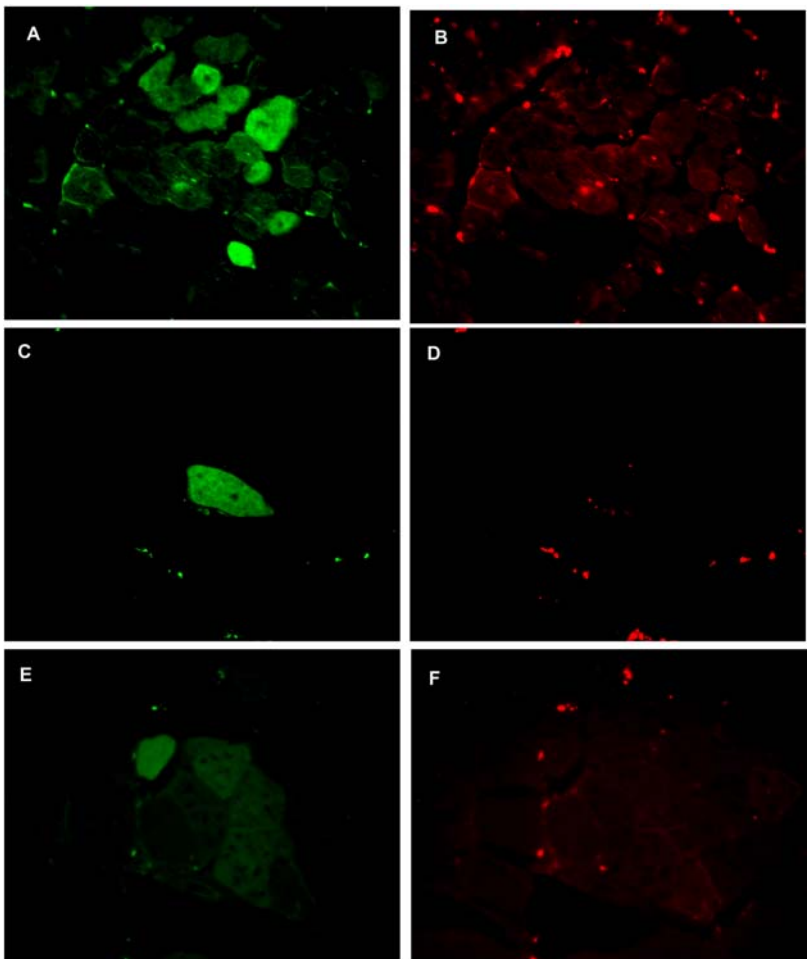

Figure 3.7. Localization of GFP+ fibers. A, B) 5-FU + Cardiotoxin + swimming animal; C-F) Ligation animals. A, C, E are GFP (green); B, D, F are respective red channel images showing background. Magnification 40X.

These studies suggest therefore that under certain damage conditions MAPC contribute at low levels to skeletal muscle fibers in *mdx*5cv mice. However, in none of these MAPC derived fibers have we detected dystrophin expression.

Discussion

In this chapter we evaluated whether undifferentiated MAPC could serve as a cell source for therapy of DMD. We demonstrate that although MAPC can contribute to skeletal muscle fibers when injected in injured muscle of *mdx*5cv animals, levels of contribution are general low, and we have not been able to detect dystrophin expression in donor derived fibers.

Due to the aqueous nature of GFP, we found it necessary to strongly fix our tissues to detect GFP expression[17,25]; however most dystrophin antibodies are not compatible with formalin fixed tissues. There were no published protocols addressing dystrophin staining on highly fixed tissues, therefore we developed our own protocol. In total, five different anti-dystrophin antibodies were tested, and of those only two detected dystrophin in fixed tissue following antigen retrieval (data not shown); however the need for antigen retrieval makes co-localization of GFP with dystrophin impossible, as antigen retrieval destroys the GFP signal and the best tested GFP and dystrophin antibodies on antigen retrieved tissues are both raised in rabbit.

We chose two different concentrations of PFA; 4% is standard in histology protocols and 0.5% was suggested by a couple of investigators (M. Reyes and M. Labarge, personal communications); in addition, 6 different fixation periods were assessed. It can clearly be seen from figure 3.1 that there is an inverse relationship between GFP retention in tissues and intensity of dystrophin staining, suggesting that there is a narrow window for fixation periods that investigators must adhere to if optimal GFP retention and dystrophin staining without antigen retrieval is desired.

Despite the fact that MAPC grafted into sublethally irradiated non-dystrophic animals generate hematopoietic cells[24], we did not detect contribution to skeletal muscle fibers. This is not surprising, as in this model there was no muscle injury. However, in some of these animals some contribution to cardiac muscle was seen [24]. The discovery of GFP^+ cells residing in between fibers of both forelimbs and hindlimbs may nevertheless suggest that MAPC might be exploited as a cell therapy for DMD as this demonstrates that MAPC themselves or their progeny can readily migrate in between muscle fibers. Many of the GFP^+ cells did not co-stain with CD45 or BS-I lectin, a marker for nucleated hematopoietic cells or endothelium, respectively. A few $GFP^+/CD45^-/Lectin^-$ cells appeared to be located in a satellite cell position (figures 3.3D and 3.4C-D); unfortunately Pax7 and MyoD staining was not possible on our tissues due to the degree of fixation and so this observation could not be verified. Grafting of MAPC derived from Pax7-promoter-fluorophore or MyoD-promoter fluorophore could answer this question. In addition, intravenous delivery of undifferentiated MAPC in *mdx* animals, or wild-type animals wherein the skeletal muscle has been injured will be of interest to determine if contribution to skeletal muscle fibers can be seen.

We performed a series of studies wherein undifferentiated MAPC were injected in the muscle of *mdx*5cv animals to assess whether contribution skeletal muscle fibers could be seen. Previous reports on stem cell contribution to skeletal muscle in *mdx* mice have noted low percent contribution from donor cells when using the *mdx* mouse as the model. Reasons for poor contribution include immune rejection of donor cells based on expression of either a marker gene to trace the donor cells, which might be more pronounced

in *mdx* animals than wild type animals due to the inflammatory microenvironment in *mdx* mice, or expression of dystrophin. Another possible reason for low levels of engraftment in *mdx* mice is the mild phenotype exhibited by this mouse model[26].

The uses of myotoxic agents and/or high dose irradiation[27,28] are previously described methods to impose a more severe phenotype in *mdx* mice. Myotoxic agents cause acute damage whereas high-dose irradiation causes long-term damage by arresting satellite cell proliferation. Using these methods, other investigators have observed engraftment into muscle; however we did not observe any.

LaBarge et al. reported up to 12% contribution of donor bone marrow cells to the satellite cell compartment in animals that had undergone whole body irradiation and subsequent exercise[17]; it should be noted that exercise was of voluntary effort. We observed that although *mdx* mice had a mild phenotype, they were less active than age-matched wild type animals. When considering the differences between the *mdx* mouse and their larger counterparts (humans and dogs), lab mice do not experience the same degree of forced physical exertion (i.e. exertion used to get food, play etc.). This observation and the study by Labarge et al. led us to consider what effects forced exercise had on engraftment. When animals were exerted through swimming in combination with another treatment (5-FU and/or cardiotoxin), we detected engraftment in muscle fibers. This is consistent with a study from the Blau group in follow-up to the LaBarge article, demonstrating that forced exercise increases contribution of bone marrow cells to the skeletal muscle compartment[29]. A more recent study reported improved engraftment levels in *mdx* mice after chronic exertion through swimming[30], further supporting our observations. Although we observed GFP^+ fibers, we could not detect any dystrophin through staining. This was disappointing as others have reported numbers of dystrophin positive fibers above the level seen due to revertant fibers[15,31]. However it should be noted that tissue from our best engrafted animal (see figure 3.6) was collected before we optimized dystrophin staining and was fixed for ~24 hours, which decreased the ability to detect dystrophin by antibody staining (patchy staining even after antigen retrieval, data not shown) which could explain the absence of dystrophin staining.

A. Luttun et al., from our group has demonstrated that undifferentiated MAPC contribute, albeit at low levels, to the regenerating skeletal muscle compartment of mice who sustained hindlimb ischemia (paper under revision). We determined if hindlimb ischemia would improve engraftment levels of mMAPC in *mdx*5cv mice. We did notice GFP+ fibers in some animals, although not more than the other injury methods we tested; dystrophin staining has yet to be determined.

Overall we did not see significant engraftment levels, for reasons that are unclear. Immune rejection of the GFP foreign protein could be a significant factor due to the highly immunogenic environment of dystrophic muscle. Future studies will have to test the effect of immunosuppression on MAPC engraftment in *mdx*5cv mice. As the phenotype of *mdx5cv* mice is mild, increasing swimming duration to include the post-injection period may cause more muscle damage and induce greater levels of engraftment[30]. Alternatively, transplantation into a sicker model such as the *mdx/Utr-/-* mouse may yield higher levels of engraftment.

No dystrophin could be detected in the tissues we analyzed. This was surprising in view of the fact that we demonstrate in chapter 3 that MAPC can be induced to express early myogenic transcription factors as well as dystrophin when treated with Activin, IGF, and bFGF. One would therefore expect that following fusion with muscle fibers a normal myogenic program can be activated. As most of the dystrophin identification was done in animals sacrificed at <21 days following grafting, it is possible although not highly likely, that the myogenic program was not activated in a timely manner. It is possible that histology may not be the best method due to the need to highly fix tissue for GFP detection. One possible solution that we are developing is isolating mRNA from fixed tissues and subsequently using quantitative RT-PCR with primers designed to flank the mutated exon to detect donor derived dystrophin (data not shown). A logical next step, if dystrophin expression can not be demonstrated would be to graft the myogenic committed MAPC-progeny described in Chapter 3

Acknowledgments

The authors would like to thank David Abts, Erica Delin, Priya Muthu, and Arjun Menon for their work on this project. The authors also thank Yves Heremans for his invaluable histology advice. Additionally, we would like to thank Robert J.Griffin for his help with X-Irradiation of mouse hindlimbs. Finally, we would like to thank Jonathan McCue, MD for his help with femoral artery ligations. SAF was funded by a NASH Grant, NIH Muscle Training Grant, and NIH Musculoskeletal Training Grant. The work was also supported by R01 DK58295 to CMV.

References

1. McArdle, A., Edwards, R. H. & Jackson, M. J. How does dystrophin deficiency lead to muscle degeneration?--evidence from the mdx mouse. *Neuromuscul Disord* **5**, 445-56 (1995).
2. Judge, L. M., Haraguchiln, M. & Chamberlain, J. S. Dissecting the signaling and mechanical functions of the dystrophin-glycoprotein complex. *J Cell Sci* **119**, 1537-46 (2006).
3. Brenman, J. E. et al. Interaction of nitric oxide synthase with the postsynaptic density protein PSD-95 and alpha1-syntrophin mediated by PDZ domains. *Cell* **84**, 757-67 (1996).
4. Emery, A. E. The muscular dystrophies. *Lancet* **359**, 687-95 (2002).
5. Alter, J. et al. Systemic delivery of morpholino oligonucleotide restores dystrophin expression bodywide and improves dystrophic pathology. *Nat Med* **12**, 175-7 (2006).
6. Lu, Q. L. et al. Functional amounts of dystrophin produced by skipping the mutated exon in the mdx dystrophic mouse. *Nat Med* **9**, 1009-14 (2003).
7. Sampaolesi, M. et al. Mesoangioblast stem cells ameliorate muscle function in dystrophic dogs. *Nature* **444**, 574-9 (2006).
8. Straub, V. & Campbell, K. P. Muscular dystrophies and the dystrophin-glycoprotein complex. *Curr Opin Neurol* **10**, 168-75 (1997).
9. Straub, V., Rafael, J. A., Chamberlain, J. S. & Campbell, K. P. Animal models for muscular dystrophy show different patterns of sarcolemmal disruption. *J Cell Biol* **139**, 375-85 (1997).
10. O'Brien, K. F. & Kunkel, L. M. Dystrophin and muscular dystrophy: past, present, and future. *Mol Genet Metab* **74**, 75-88 (2001).
11. Mann, C. J. et al. Antisense-induced exon skipping and synthesis of dystrophin in the mdx mouse. *Proc Natl Acad Sci U S A* **98**, 42-7 (2001).
12. Lu, Q. L. et al. Massive idiosyncratic exon skipping corrects the nonsense mutation in dystrophic mouse muscle and produces functional revertant fibers by clonal expansion. *J Cell Biol* **148**, 985-96 (2000).
13. Kessler, P. D. et al. Gene delivery to skeletal muscle results in sustained expression and systemic delivery of a therapeutic protein. *Proc Natl Acad Sci U S A* **93**, 14082-7 (1996).
14. Xiao, X., Li, J. & Samulski, R. J. Efficient long-term gene transfer into muscle tissue of immunocompetent mice by adeno-associated virus vector. *J Virol* **70**, 8098-108 (1996).
15. Gussoni, E. et al. Dystrophin expression in the mdx mouse restored by stem cell transplantation. *Nature* **401**, 390-4 (1999).
16. Bittner, R. E. et al. Recruitment of bone-marrow-derived cells by skeletal and cardiac muscle in adult dystrophic mdx mice. *Anat Embryol (Berl)* **199**, 391-6 (1999).
17. LaBarge, M. A. & Blau, H. M. Biological progression from adult bone marrow to mononucleate muscle stem cell to multinucleate muscle fiber in response to injury. *Cell* **111**, 589-601 (2002).
18. Ferrari, G. et al. Muscle regeneration by bone marrow-derived myogenic progenitors. *Science* **279**, 1528-30 (1998).

19. Torrente, Y. et al. Human circulating AC133(+) stem cells restore dystrophin expression and ameliorate function in dystrophic skeletal muscle. *J Clin Invest* **114**, 182-95 (2004).
20. Gussoni, E., Blau, H. M. & Kunkel, L. M. The fate of individual myoblasts after transplantation into muscles of DMD patients. *Nat Med* **3**, 970-7 (1997).
21. Lee, J. Y. et al. Clonal isolation of muscle-derived cells capable of enhancing muscle regeneration and bone healing. *J Cell Biol* **150**, 1085-100 (2000).
22. Bachrach, E. et al. Muscle engraftment of myogenic progenitor cells following intraarterial transplantation. *Muscle Nerve* **34**, 44-52 (2006).
23. Jiang, Y. et al. Pluripotency of mesenchymal stem cells derived from adult marrow. *Nature* **418**, 41-9 (2002).
24. Serafini, M. et al. Hematopoietic reconstitution by multipotent adult progenitor cells: precursors to long-term hematopoietic stem cells. *J Exp Med* **204**, 129-39 (2007).
25. Jockusch, H., Voigt, S. & Eberhard, D. Localization of GFP in frozen sections from unfixed mouse tissues: immobilization of a highly soluble marker protein by formaldehyde vapor. *J Histochem Cytochem* **51**, 401-4 (2003).
26. Stedman, H. H. et al. The mdx mouse diaphragm reproduces the degenerative changes of Duchenne muscular dystrophy. *Nature* **352**, 536-9 (1991).
27. Quinlan, J. G. et al. Radiation inhibition of mdx mouse muscle regeneration: dose and age factors. *Muscle Nerve* **18**, 201-6 (1995).
28. Yokota, T. et al. Expansion of revertant fibers in dystrophic mdx muscles reflects activity of muscle precursor cells and serves as an index of muscle regeneration. *J Cell Sci* **119**, 2679-87 (2006).
29. Palermo, A. T., Labarge, M. A., Doyonnas, R., Pomerantz, J. & Blau, H. M. Bone marrow contribution to skeletal muscle: a physiological response to stress. *Dev Biol* **279**, 336-44 (2005).
30. Bouchentouf, M., Benabdallah, B. F., Mills, P. & Tremblay, J. P. Exercise improves the success of myoblast transplantation in mdx mice. *Neuromuscul Disord* **16**, 518-29 (2006).
31. Wernig, G. et al. The vast majority of bone-marrow-derived cells integrated into mdx muscle fibers are silent despite long-term engraftment. *Proc Natl Acad Sci U S A* **102**, 11852-7 (2005).

CHAPTER 4

DETERMINING DIFFERENCES IN MURINE PLANTARFLEXION MUSCLE CONTRACTILE PROPERTIES USING A NOVEL *IN VIVO* ASSESSMENT DEVICE

Sarah A. Frommer[1,2], Jihan M. Jacobs[3], Dawn Qiu[3], Gary Williams[3], Charles Soule[3], Catherine M. Verfaillie[2], and Paul A. Iaizzo[1,3,4]

Biomedical Engineering Department[1], Stem Cell Institute[2], Department of Surgery[3], and Department of Physiology[4], University of Minnesota, Minneapolis, Minnesota

Abstract

Duchenne muscular dystrophy (DMD) is a devastating and fatal genetic disease which is primarily characterized by the degeneration of striated muscle due to the absence of the protein dystrophin[1]. Experimental therapies aimed at replacing the dystrophin protein, such as exon skipping[2-4], cell therapy[5-10], and/or gene therapy[11-15] are being evaluated. The ultimate goal of any such approach is to restore striated muscle functionality, which is being evaluated most commonly using murine models of DMD. Yet, current methods to assess murine muscle function are highly invasive and do not allow for long-term testing in a given animal. Here we describe a novel murine assessment system developed to measure skeletal muscle contractile properties on multiple occasions over time in intact animals. In normal mice, employing this approach we measured less than an 8% day-to-day variability and also could detect a significant difference ($p < 0.003$) in twitch tension (TT) due to cardiotoxin-induced muscle damage. When muscle properties of normal mice were compared to dystrophic mice of similar weight and age, significant differences in normalized torque and TT per body weight were detected ($p < 0.0005$ and $p < 0.003$, respectively); however no significant differences for fatigue profiles were found. This device will be useful for investigators testing the efficacy of novel therapies for DMD because it is non-invasive, was designed to take measurements at different time-points, and has been shown to be sensitive enough to detect differences in muscle functionality due to pathology.

Introduction

Duchenne muscular dystrophy (DMD) is an X-linked genetic disease that affects approximately 1/3500 newborn males. The etiology of this disease is a mutation of the dystrophin gene, which results in an absence or near absence of dystrophin within the patient[1,16]. Dystrophin links the inner cell structure to the basal lamina by binding to F-actin and a protein complex on the sarcolemma called the dystrophin-glycoprotein complex (DGC), which links to laminin in the basement membrane of striated muscle. This link is believed to be important for stabilizing the sarcolemma during contraction. Thus, an absence of dystrophin leads to destruction of muscle fibers and eventual muscle deterioration. DMD is a progressive degenerative disease which in general, follows a predictable course. Male patients present in early childhood with muscle weakness, elevated creatine kinase levels, and pseudohypertrophic calf muscles. By age 12, patients are typically wheel-chair bound and usually die from respiratory failure and/or cardiomyopathy in their mid-twenties. Unfortunately to date, there are still no cures or even effective treatments to delay the progression of DMD. Yet, there have been many positive outcomes from experimental therapies tested in animal models, such as gene replacement[11,12], exon skipping[2-4], cell therapy[5-10], or pharmaceuticals[17-23,24,25].

Importantly, the ultimate goal of any therapy should be to restore muscle function. In the clinical setting, functionality of voluntary efforts is subjectively assessed by a trained physician; on a scale from 0-5. Yet, it is generally accepted that to truly measure the efficacy of any such therapy, more objective, yet non-invasive tests need to be developed so that quantitative outcomes values can be obtained repeatedly over the lifetime of the patient. However, before any such testing can be conducted in human subjects, efficacy and safety of future therapies have to be critically evaluated by employing similar assessment approaches used in animal models.

To date, the two most useful mammalian animal models of DMD for research are canine (GRMD) and murine (*mdx*). It should be noted that generally, the canine models are considered superior models for DMD because they exhibit more severe phenotypes that are more similar to those of DMD patients. Unfortunately the use of this model has been limited due to: 1) Expressed variability in phenotypes of litters, 2) the high expense associated with maintaining large animals, and/or 3) limited access to colonies by the majority of investigators. As a result, murine models have been the most widely used to investigate expressed pathologies and possible therapies for DMD. The *mdx* mouse exhibits a mild phenotype throughout a near normal life span, and only undergoes two major phases of degeneration and regeneration during 3-6 weeks and after 15 months of age[26,27]. Despite its mild phenotype, traditional *mdx* mice have been invaluable to researchers in this field by offering a consistent and readily available dystrophin deficient animal model. However, assessment of efficacy of innovative therapies has until now not yet been possible on a routine basis in *mdx* mice, as a quantitative, non-invasive measurement systems have not been described that can detect changes in contractile properties due to pathology and in addition, detect any functional amelioration from experimental therapies.

Here we present such an approach and system capable of detecting quantitative differences not only in cardiotoxin-injured normal muscle function, but also differences between dystrophic and normal muscle properties. Traditional methods to evaluate murine contractile properties have been highly invasive; e.g., utilizing *in vitro* methods or measuring the muscle *in situ*. To our knowledge, only one associated *in vivo* study has been described[28] and although similar concepts are used, our device differs significantly in several ways: 1) it can be employed to measure contractile properties in very young mice weighing less than 20 grams, 2) it is non-invasive, in that we use motor point stimulation via the skin (versus percutaneous nerve stimulation), 3) a wide range of stimulation protocols can be used, and 4) animals routinely recover from a recording session and thus the same parameters can be tracked for months.

Materials and Methods

Animal Groups

These experimental protocols were prior approved and conducted in accordance with guidelines of the Institutional Animal Care Usage Committee at the University of Minnesota. Two male C57Bl/6 mice, approximately 2 months old were used to test the device variability and for the cardiotoxin damage study. 9 male and 2 female B6Ros.Cg-DMD*mdx*-5cv (*mdx*5cv) mice with ages ranging from 25 to 31 days, and 10 male C57Bl/6 mice with ages ranging from 20 to 24 days were used for the comparison study. All animals were originally obtained from Jackson Laboratories (Bar Harbor, ME) and housed in specific pathogen-free Research Animal Resources facilities at the University of Minnesota.

In vivo force assessment device and animal set up

Each animal was placed in an induction chamber and anesthetized using an air flow of 1000mL/min and 3% isoflurane. After this brief induction period (1-2 min), the animal was taken out of the induction chamber and its head was placed in an anesthesia chamber on the force assessment device itself. The relative isoflurane concentration was then lowered to 1.5% during animal setup in the device and adjusted accordingly (usually between 0.8-2%) throughout the experiment by observing the animal's respiration. A vacuum was used to salvage extra isoflurane from the anesthesia chamber. Next, lotion was applied to the animal's hindlegs and the legs were shaved using an eyebrow shaver. The legs were then cleansed three times with alcohol wipes. To measure the left leg, the animal was placed on its right side and the left leg was stabilized at the knee and the ankle; to measure the right leg the animal was placed on its left side (see Figure 4.1A). The desired foot pad was attached to a force displacement transducer (Grass Technologies model FT03, West Warwick, RI; employing red and black isometric springs: Maximum working range 0.2 kg) using Velcro® Ultra-Mate fasteners and Velcro® Sticky-Back tape. A thin layer of Signa electrode gel (Parker Laboratories, Fairfield, NJ) was applied to the skin over the belly of the gastrocnemius muscle. Two self-adhering reusable skin electrodes (Empi, St. Paul, MN) were placed over two platinum electrodes (Grass Technologies model E2, West Warwick, RI) and a liberal amount of electrode gel was applied to the skin electrodes. The electrodes were placed on the leg with the positive electrode most distally and the ground electrode over the belly of the gastrocnemius muscle; this electrode placement elicited the best isolation and stimulation of the hindlimb plantarflexion muscles (see figure 4.1B). The platinum electrodes were connected to a Grass Stimulator, which was itself connected to a LabVIEW data acquisition board (National Instruments, Austin, TX). The acquisition board was connected to a desktop PC and a customized LabVIEW program was used to control stimulation. Signals from the force transducer were conditioned by a Gould amplifier (Valley View, OH), which was connected to the LabVIEW data acquisition board. The customized LabVIEW program was employed to display the online force measurements (Figure 4.1C).

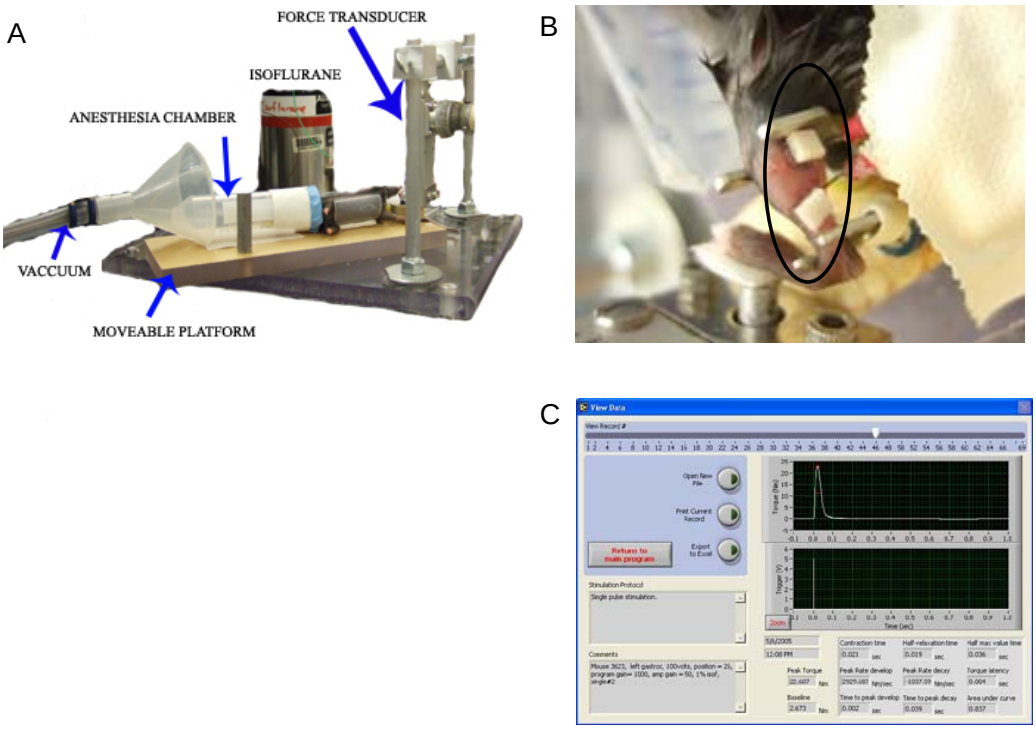

Figure 4.1. Device and animal setup. A) Device setup; B) Animal leg setup and electrode placement (black oval); C) LabVIEW program display of measured force

Stimulation Protocol

Prior to each study, the force transducer was calibrated by applying 20 gram and 50 gram weights. Next, the animal was positioned in the device, and the hindlimb plantarflexion muscles were slightly stretched by rotating the moveable platform. The supramaximal pulse (each were 0.25 milliseconds in duration) stimulation voltage was determined by initially setting the stimulator at 60 volts which was then increased incrementally up until the evoked twitch tension plateaued. After the supramaximal voltage was set, optimal muscle length was defined by performing a length-tension relationship; this was established by rotating the moveable platform so that the ankle angle was ~20º which was increased incrementally by ~2.5º until the maximum twitch tension was reached, and the process was repeated again to verify the optimal ankle position.

The following stimulation protocol was performed on each muscle studied: A single pulse stimuli at supramaximal voltage, 90 seconds rest; double pulse stimulation with 5ms interpulse interval, 90 seconds rest; triple pulses with 5ms interpulse intervals, 90 seconds rest; quadruple pulses with 5ms interpulse intervals, 90 seconds rest; after which this same protocol was performed a second time. If the fatigue protocol was to be performed the following stimulation protocol was utilized: 1) Elicitation of several control single twitch responses, 2) a rest period of 10 seconds, 3) stimulation at 0.2 Hz for 1 minute, 4) 120 second rest, 5) stimulation at 0.5 Hz for 1 minute, 6) 120 second rest, 7) stimulation at 1 Hz for 1 minute, 8)

120 second rest, 9) stimulation at 2 Hz for 1 minute, 10) 120 second rest, 11) stimulation at 3 Hz for 1 minute, 12) 120 second rest, and finally 12) stimulation at 5 Hz for 1 minute.

Experimental Setup

Twitch tensions from two ~2 month old C57Bl/6 mice (called mice 193 and 194) were assessed by employing the aforementioned stimulation protocol on 2-4 different days to evaluate device variability and to establish baseline elicited forces for the subsequent cardiotoxin study. After the last baseline data set was obtained, 25ng of cardiotoxin (Latoxan, Rosans, France) in 75μL of sterile PBS was injected into either the left or right gastrocnemius muscle. Subsequently, contractile properties were assessed on days 7, 8, and 10 post-injection of cardiotoxin.

Twitch torque and fatigue properties were compared in ten C57Bl/6 and eleven *mdx*5cv mice of similar weights and ages. We first performed the stimulation protocol randomly on either the right or left leg, followed by performing the stimulation protocol followed by the fatigue protocol on the second limb. After all measurements were collected, muscle diameters were determined by plantarflexing the foot so that the muscles were fully compressed and subsequently by taking a digital picture of the leg next to a ruler as a reference scale using the macro function of a F10 model Fujitsu digital camera. The foot length was determined by inking the bottom of the foot at the heel and foot pad, and then an imprint was made on paper. Both foot imprints were measured and averaged. Finally, the weight of the animal following each study session was measured on an electric scale.

Data Analysis and Statistics

All secondary calculations were performed using Microsoft Excel. Torque was calculated by taking the force values from the LabVIEW program and multiplying by the gravitational acceleration constant and the measured foot length. The flexed leg images were then analyzed for muscle diameter by using ImageJ (National Institutes of Health, Bethesda, MD). Muscle cross-sectional area was estimated to be circular and calculated using the measured diameter. Torque was then divided by the calculated cross-sectional area (CSA) to obtain torque/CSA (specific torque). To calculate torque per percent of weight, the absolute force values from the program (in grams) were divided by the relative animal weights. Fatigue profiles were obtained by dividing the last measured tension by the first for each fatigue segment (0.2 Hz segment, 0.5 Hz segment, etc). A student's t-test was used to compare the *mdx*5cv group with the C57Bl/6 group's torque/CSA values, percent weight values, and fatigue values. Measurements from the cardiotoxin damage groups were analyzed with a paired t-test to determine differences in TT within the same animal. Significance was set at 5% for all t-tests.

Results

Length-Tension Relationships

During animal setup in the device, the optimal muscle lengths were identified from derived length-tension relationships. Figure 4.2 shows an example of the obtained length-tension relationship from a 24 day old C57Bl/6 mouse. In figure 4.2A, there is an appropriate change in TT when the ankle angle is varied from 20° to 90°. Figure 4.2B shows the change in TT with ankle angle 25° to 37.5° for trials 1 and 2, revealing a similar trend in change of TT versus ankle angle between the two trials and a maximum value of TT when the ankle angle was positioned at ~30°.

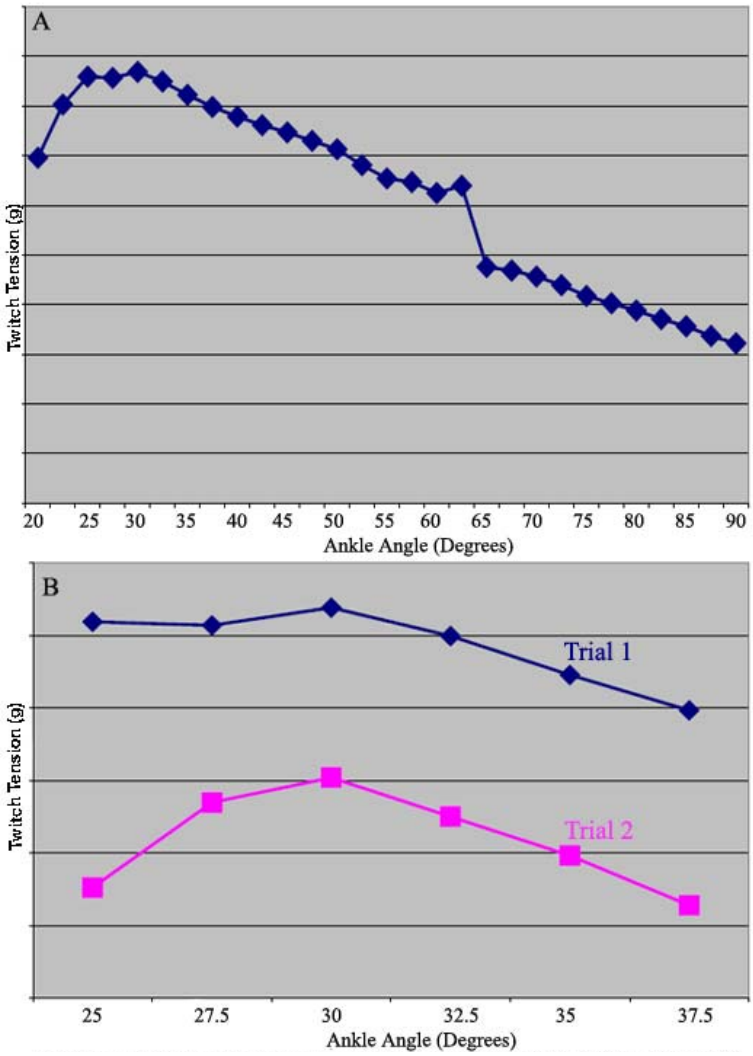

Figure 4.2. Measured length-tension relationship for 24 day old C57Bl/6 male mouse. A) Length-tension trial 1 for ankle angles 20-90°. B) Comparison of trials 1 and 2.

Detection of Muscle Damage Induced by Cardiotoxin

Two young adult C57Bl/6 mice were used to measure device variability and to establish baseline values for the cardiotoxin study. Baseline TT is summarized in tables 4.1 and 4.2 for each induced contraction. Analysis of all four stimulation parameters revealed that for the two animals measured, day-to-day variability ranged from only 1.9 – 7.3%.

TT collected on days 7, 8, and 10 post-injection are shown in tables 4.1 and 4.2 for mouse 193 and 194, respectively. In mouse 193, there were significant differences in TT when compared to baseline for days 7, 8, and 10 after cardiotoxin injection (p-value < 0.005). The measured TT for the injured leg did not change significantly from day 7 to 10. Interestingly, the TT in the uninjured leg of mouse 193 was significantly increased from baseline on days 7 and 8 and returned toward baseline values on day 10. For mouse 194, the injured leg also showed significant decreases in TT on days 7-10 following cardiotoxin

injection, with p-values < 0.005; additionally, the TT values increased toward baseline from day 7 to 10. In contrast to mouse 193, there were no significant TT increases in the uninjured leg of mouse 194.

Mouse 193	**Single TT (g)**	**Double TT (g)**	**Triple TT (g)**	**Quadruple TT (g)**
Left Leg Baseline	31.803 ± 0.69	46.525 ± 1.09	54.191 ± 1.69	59.428 ± 2.08
Right Leg Baseline	30.697 ± 2.23	46.293 ± 2.62	53.805 ± 3.34	58.703 ± 3.68
Left Leg 7 day PI (I) **	16.162	25.326	30.143	34.261
Right Leg 7 day PI (U) *	38.379	56.624	65.104	67.676
Left Leg 8 day PI (I) **	13.916	23.779	28.434	31.787
Right Leg 8 day PI (U) ‡	36.523	57.585	69.190	75.733
Left Leg 10 day PI (I) ***	16.976	25.830	30.843	34.245
Right Leg 10 day PI (U)	33.187	46.485	54.492	59.326

Table 4.1. Mouse 193 twitch tension values following muscle damage of left leg. Abbreviations: Injured (I), Uninjured (U). Significance values compared to baseline using paired t-test: p = 0.001 (*), p = 0.002 (**), p = 0.003 (***), p = 0.01 (‡).

Mouse 194	**Single TT (g)**	**Double TT (g)**	**Triple TT (g)**	**Quadruple TT (g)**
Left Leg (from 4 days)	32.390 ± 1.05	46.944 ± 2.97	53.723 ± 3.13	57.499 ± 3.26
Right Leg (from 2 days)	29.492 ± 1.52	42.635 ± 0.83	49.683 ± 1.21	54.899 ± 1.58
Left Leg 7 day PI (U)	33.545	47.135	54.069	59.050
Right Leg 7 day PI (I) ‡	17.890	29.134	35.710	39.633
Left Leg 8 day PI (U)	30.176	45.426	52.539	61.035

Right Leg 8 day PI (I)*	19.580	30.827	37.581	40.041
Left Leg 10 day (U)	31.673	49.007	56.934	60.091
Right Leg 10 day (I) †	21.924	35.726	43.180	47.119

Table 4.2. Mouse 194 twitch tension values following muscle damage of right leg. Abbreviations: Injured (I), Uninjured (U). Significance values compared to baseline using paired t-test: p = 0.001 (*), p = 0.0002 (†), p = 0.0004 (‡).

Normal and Dystrophic Murine Hindlimb Torques

Table 4.3 is a summary of the measured morphometric and contractile parameters from each animal group. Note that the weights, muscle diameters and foot lengths were lower in the younger C57Bl/6 animals than the older *mdx*5cv animals. The mean torques per CSA were significantly higher for single, double, triple, and quadruple pulses (p-values < 0.0005) in wild type (WT) compared with *mdx*5cv animals. We also normalized the TT based on body weight. Again, the means were significantly higher in WT than *mdx*5cv for single, double, triple and quadruple pulse induced contractile responses (p < 0.003).

	Age (days)	**Weight (g)**	**Diameter (cm)**	**Foot Length (cm)**
C57Bl/6 (n=10)	20-24	11.48 ± 2.21	0.665 ± 0.0540	1.24 ± 0.18
***mdx*5cv (n=11)**	25-31	13.25 ± 1.39	0.734 ± 0.062	1.26± 0.08

Table 4.3. Measured parameters for normal and *mdx* mice groups

	Average Torque/CSA (N/m)			
	Single Pulse*	**Double Pulse***	**Triple Pulse***	**Quad Pulse***
C57Bl/6 (n = 10)	34.321 ± 7.32	50.780 ± 9.85	58.629 ± 11.34	63.145 ± 12.38
***mdx*5cv (n = 11)**	24.89 ± 3.50	39.867 ± 4.99	46.928 ± 5.76	51.288 ± 6.29

Table 4.4. Specific torque values and standard deviations. Abbreviation: Cross-sectional area (CSA). Significance values: p ≤ 0.0003 (*)

	Average % Weight			
	Single Pulse‡	**Double Pulse‡**	**Triple Pulse‡**	**Quad Pulse‡**
C57Bl/6 (n = 10)	87.6 ± 19	129.5 ± 26	149.4 ± 29	160.9 ± 32
***mdx*5cv (n = 11)**	63.7 ± 13	103.8 ± 19	123.0 ± 22	135.0 ± 23

Table 4.5. Percent of weight values and standard deviations. Significance values: p < 0.003 (‡)

Fatique Response Assessment

Fatigue properties of these stimulated muscles were evaluated for each of the two aforementioned groups of animals. Although fatigue response values were slightly lower for *mdx*5cv compared to C57Bl/6 animals, these differences were not statistically significant when comparing the groups for the 0.2 Hz, 0.5 Hz, 1 Hz, 2 Hz, 3 Hz, or 5 Hz stimulation segments; additionally, the fatigue profiles for both groups followed very similar trends (Figure 4.3).

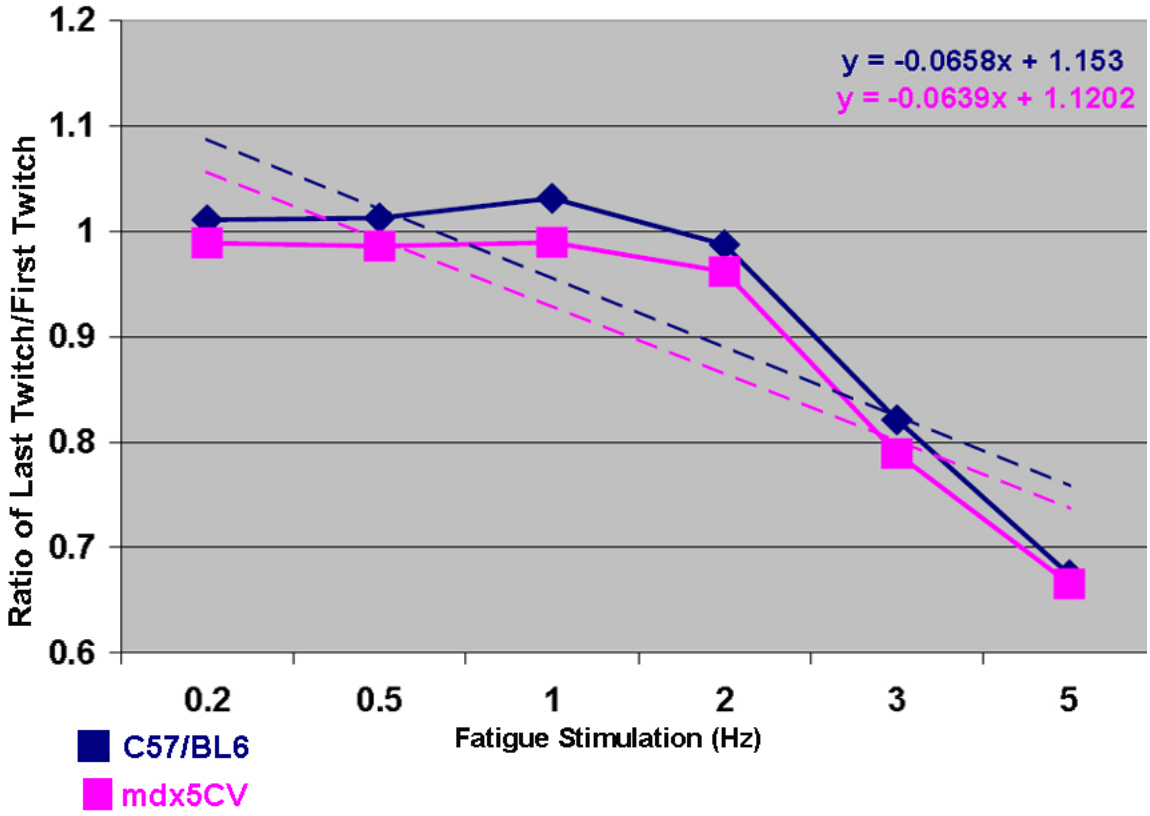

Figure 4.3. Plot of fatigue in WT and *mdx* mice. Trendlines and corresponding equations are shown. WT (blue diamonds) and *mdx* (pink squares).

Discussion

The assessment system and experimental stimulation protocols that we developed allow for the repeated and non-invasive evaluation of muscle strength in mice. Furthermore, this outcomes approach should be a useful tool for investigators to gauge long-term therapy responses for DMD. The leg torque device can appropriately and consistently detect changes in muscle length so to identify the optimal limb position to obtain maximum tension; as repeated testing demonstrated that the same ankle angle yielded highest twitch torque tensions. Although we only presented data for the length-tension relationship in a single animal, the best angle for maximum tension in every animal tested demonstrated that the ankle angle that yielded the maximum tension was very similar (within ± 2.5º), when such testing was repeated in the same animal. In figure 4.2B, the effect of passive tension can be seen in trial 1 by the higher overall TT values and the similar level of TT for angles 25º and 27.5º; it would be expected that the TT value for 25º would be lower than 27.5º, but passive tension is a factor since the muscle was highly stretched. Appropriately, in the second trial the TT value for 25º was lower than the one for 27.5º after the muscle had time to stretch.

To test the feasibility of this device as an outcomes assessment tool to measure muscle pathology, TT differences due to muscle damage were assessed. Daily variations in recorded TT were a <8%. Although variability of less than 5% would be desirable, the use of young adult mice (~2 months of age) was considered to explain this increased variability; C57Bl/6 mice on average increase in weight approximately 1 gram/week after 5 weeks of age[29]. Our measurements were taken over a two week period during which the animals approximately increased their weight by ~10%; this weight increase could explain the increased variability. Snake venom-derived cardiotoxin was used to specifically induce injury of these muscles due to its specificity for muscle, and because it has also been used to model degeneration and regeneration cycles associated with DMD where there is no direct neural or vascular necrosis. In normal mice, cardiotoxin causes myonecrosis 1 to 2 days after injection; nascent myofibers become most noticeable at day 5; by day 14 no myonecrosis is present and the tissue looks indistinguishable from uninjected muscle except for the presence of some centralized nuclei (a hallmark of regeneration); and by day 21 the muscle is completely indistinguishable from uninjured muscle[30]. Days 7-10 post-injection were chosen as time points for the torque assessment studies because it was the most representative of the degeneration and regeneration cycle. For mouse 193, significant decreases in TT from baseline were detected in the injured leg on all three days for all four stimulation protocols; additionally, the uninjected leg showed significant increases in TT from baseline for days 7 and 8 for contractile responses. This increase could be explained if the uninjected leg was compensating for the decreased function of the injured leg. For mouse 194, there were also significant decreases in TT compared to baseline for all three days and all four stimulations; however for the uninjected leg no significant increases in TT could be detected. Possibly, the differences between the two animals can be explained by a varied level of injury. For mouse 193, the decrease in TT was approximately 50% of baseline value and did not change over the three days measured; whereas for mouse 194, at post-injection day 7 TT was ~68% of baseline, post-

injection day 8 was ~72% of baseline, and post-injection day 10 it was ~83% of baseline. Therefore between the two mice, mouse 194 appeared to have a lower degree of injury and recover faster than mouse 193 and hence would not need as much compensation from the uninjured leg. We consider that this degree of sensitivity makes this approach especially useful for phenotype and/or outcomes assessment.

Once our initial feasibility studies showed that this approach could be used to detect differences in muscle function due to pathology, we evaluated whether these torque measurements and stimulation protocols could be used to test the decreased function of the muscles in *mdx* mice. As exact cross-sectional area was not used to calculate specific tension, slightly younger normal mice were chosen to rule out differences in measured force due to size, because at this early age *mdx*5cv mice tend to be smaller than age-matched controls. This observation corresponds to previous findings for this age group of 3-5 weeks[31]. This age group was chosen because it is when the first degeneration and regeneration cycle occurs in the *mdx* mouse and would be most likely the time when investigators test therapies. Highly significant differences in specific torque were detected; however no significant differences in absolute tension could be detected. This correlates with findings from previous *in vitro* and *in situ* studies looking at specific and absolute tension in 3-5 week old *mdx* and normal mice[31,32]. Tension as a percent of body weight was also evaluated and showed highly significant differences between the two groups. This further strengthens the specific torque data because no subjective measurements, specifically, diameter and foot length, were used to calculate percent of body weight; therefore any bias is reduced.

Interestingly, fatigue measurements were not significantly different between the two groups, which does not correlate with findings from previous *in vitro* and *in situ* studies[31,32]. However, the *in vitro* study evaluated extensor digitorum longus and soleus muscles, and the *in situ* study evaluated tibialis anterior muscles. Here we evaluated the plantarflexion muscles, which primarily consist of the very large gastrocnemius muscle. Additionally, the fatigue protocol used by the previous studies was more intensive than the one used here. The combination of a larger muscle and a less intense fatigue protocol might explain for the differences between our study and the previous ones. Nevertheless, this may also indicate that caution should be used if one were to employ a functional assessment to make one such comparison.

To date, we are unaware of any studies involving *in vivo* force assessment of *mdx* mice and comparison with normal mice; however there are numerous articles about the contractile properties of dystrophic versus normal muscle utilizing *in vitro* methods such as whole muscle[32,33] and/or skinned fiber baths[10,34,35], and from studies utilizing *in situ*[31,36,37] methods. Furthermore, very few studies have compared *mdx* and control mice at age 3-5 weeks. With the exception of our fatigue data, our *in vivo* data seems to correlate well with previous findings. We should note again that only one *in vivo* device for mice has been described[28,38,39] from the Faulkner lab, but the previously reported device and our device we report here have important differences. The reason for these differences is that each device was made for different goals. The goal of the device made by the Faulkner group was to measure contractile properties on a physiological level over a short-term basis and to induce precise eccentric contraction injury[40,38], whereas our goal was to measure contractile properties to gauge therapy over a long-term basis. Our described

system and approach for measuring the contractile properties of skeletal muscle in intact animals has been demonstrated here as being a potentially useful tool for investigators assessing therapies for DMD.

Acknowledgements

The authors would like to thank Neda Shahghasemi for her help beginning this project; Andy McCullough and Dan Geoffrion for their help testing the device. Keriann Schulkers for volunteering her time. Additionally, Monica Mahre and Bill Gallagher from the PAI lab for administrative support. SAF was funded by a NASH Grant, NIH Muscle Training Grant, and NIH Musculoskeletal Training Grant.

References

1. Straub, V. & Campbell, K. P. Muscular dystrophies and the dystrophin-glycoprotein complex. *Curr Opin Neurol* **10**, 168-75 (1997).
2. Mann, C. J. et al. Antisense-induced exon skipping and synthesis of dystrophin in the mdx mouse. *Proc Natl Acad Sci U S A* **98**, 42-7 (2001).
3. Lu, Q. L. et al. Massive idiosyncratic exon skipping corrects the nonsense mutation in dystrophic mouse muscle and produces functional revertant fibers by clonal expansion. *J Cell Biol* **148**, 985-96 (2000).
4. Lu, Q. L. et al. Functional amounts of dystrophin produced by skipping the mutated exon in the mdx dystrophic mouse. *Nat Med* **9**, 1009-14 (2003).
5. Gussoni, E. et al. Dystrophin expression in the mdx mouse restored by stem cell transplantation. *Nature* **401**, 390-4 (1999).
6. Bittner, R. E. et al. Recruitment of bone-marrow-derived cells by skeletal and cardiac muscle in adult dystrophic mdx mice. *Anat Embryol (Berl)* **199**, 391-6 (1999).
7. LaBarge, M. A. & Blau, H. M. Biological progression from adult bone marrow to mononucleate muscle stem cell to multinucleate muscle fiber in response to injury. *Cell* **111**, 589-601 (2002).
8. Ferrari, G. et al. Muscle regeneration by bone marrow-derived myogenic progenitors. *Science* **279**, 1528-30 (1998).
9. Sampaolesi, M. et al. Mesoangioblast stem cells ameliorate muscle function in dystrophic dogs. *Nature* **444**, 574-9 (2006).
10. Torrente, Y. et al. Human circulating AC133(+) stem cells restore dystrophin expression and ameliorate function in dystrophic skeletal muscle. *J Clin Invest* **114**, 182-95 (2004).
11. Kessler, P. D. et al. Gene delivery to skeletal muscle results in sustained expression and systemic delivery of a therapeutic protein. *Proc Natl Acad Sci U S A* **93**, 14082-7 (1996).
12. Xiao, X., Li, J. & Samulski, R. J. Efficient long-term gene transfer into muscle tissue of immunocompetent mice by adeno-associated virus vector. *J Virol* **70**, 8098-108 (1996).
13. Yamamoto, K. et al. Immune response to adenovirus-delivered antigens upregulates utrophin and results in mitigation of muscle pathology in mdx mice. *Hum Gene Ther* **11**, 669-80 (2000).
14. Rybakova, I. N., Patel, J. R., Davies, K. E., Yurchenco, P. D. & Ervasti, J. M. Utrophin binds laterally along actin filaments and can couple costameric actin with sarcolemma when overexpressed in dystrophin-deficient muscle. *Mol Biol Cell* **13**, 1512-21 (2002).
15. Tinsley, J. M. et al. Amelioration of the dystrophic phenotype of mdx mice using a truncated utrophin transgene. *Nature* **384**, 349-53 (1996).
16. Judge, L. M., Haraguchiln, M. & Chamberlain, J. S. Dissecting the signaling and mechanical functions of the dystrophin-glycoprotein complex. *J Cell Sci* **119**, 1537-46 (2006).
17. Pulido, S. M. et al. Creatine supplementation improves intracellular Ca2+ handling and survival in mdx skeletal muscle cells. *FEBS Lett* **439**, 357-62 (1998).

18. Zeman, R. J., Zhang, Y. & Etlinger, J. D. Clenbuterol, a beta 2-agonist, retards wasting and loss of contractility in irradiated dystrophic mdx muscle. *Am J Physiol* **267**, C865-8 (1994).
19. Barton, E. R., Morris, L., Musaro, A., Rosenthal, N. & Sweeney, H. L. Muscle-specific expression of insulin-like growth factor I counters muscle decline in mdx mice. *J Cell Biol* **157**, 137-48 (2002).
20. Bogdanovich, S. et al. Functional improvement of dystrophic muscle by myostatin blockade. *Nature* **420**, 418-21 (2002).
21. Gregorevic, P., Plant, D. R., Leeding, K. S., Bach, L. A. & Lynch, G. S. Improved contractile function of the mdx dystrophic mouse diaphragm muscle after insulin-like growth factor-I administration. *Am J Pathol* **161**, 2263-72 (2002).
22. Minetti, G. C. et al. Functional and morphological recovery of dystrophic muscles in mice treated with deacetylase inhibitors. *Nat Med* **12**, 1147-50 (2006).
23. Granchelli, J. A., Avosso, D. L., Hudecki, M. S. & Pollina, C. Cromolyn increases strength in exercised mdx mice. *Res Commun Mol Pathol Pharmacol* **91**, 287-96 (1996).
24. Hodgetts, S., Radley, H., Davies, M. & Grounds, M. D. Reduced necrosis of dystrophic muscle by depletion of host neutrophils, or blocking TNFalpha function with Etanercept in mdx mice. *Neuromuscul Disord* **16**, 591-602 (2006).
25. Brunelli, S. et al. Nitric oxide release combined with nonsteroidal antiinflammatory activity prevents muscular dystrophy pathology and enhances stem cell therapy. *Proc Natl Acad Sci U S A* **104**, 264-9 (2007).
26. Stedman, H. H. et al. The mdx mouse diaphragm reproduces the degenerative changes of Duchenne muscular dystrophy. *Nature* **352**, 536-9 (1991).
27. Khurana, T. S. & Davies, K. E. Pharmacological strategies for muscular dystrophy. *Nat Rev Drug Discov* **2**, 379-90 (2003).
28. Ashton-Miller, J. A., He, Y., Kadhiresan, V. A., McCubbrey, D. A. & Faulkner, J. A. An apparatus to measure in vivo biomechanical behavior of dorsi- and plantarflexors of mouse ankle. *J Appl Physiol* **72**, 1205-11 (1992).
29. Weight Chart for the C57BL/6NCrl Mouse (Charles River Laboratories).
30. Yan, Z. et al. Highly coordinated gene regulation in mouse skeletal muscle regeneration. *J Biol Chem* **278**, 8826-36 (2003).
31. Dangain, J. & Vrbova, G. Muscle development in mdx mutant mice. *Muscle Nerve* **7**, 700-4 (1984).
32. Anderson, J. E., Bressler, B. H. & Ovalle, W. K. Functional regeneration in the hindlimb skeletal muscle of the mdx mouse. *J Muscle Res Cell Motil* **9**, 499-515 (1988).
33. Lynch, G. S., Hinkle, R. T., Chamberlain, J. S., Brooks, S. V. & Faulkner, J. A. Force and power output of fast and slow skeletal muscles from mdx mice 6-28 months old. *J Physiol* **535**, 591-600 (2001).

34. Williams, D. A., Head, S. I., Lynch, G. S. & Stephenson, D. G. Contractile properties of skinned muscle fibres from young and adult normal and dystrophic (mdx) mice. *J Physiol* **460**, 51-67 (1993).

35. Sampaolesi, M. et al. Cell therapy of alpha-sarcoglycan null dystrophic mice through intra-arterial delivery of mesoangioblasts. *Science* **301**, 487-92 (2003).

36. Sacco, P., Jones, D. A., Dick, J. R. & Vrbova, G. Contractile properties and susceptibility to exercise-induced damage of normal and mdx mouse tibialis anterior muscle. *Clin Sci (Lond)* **82**, 227-36 (1992).

37. Lovering, R. M. & De Deyne, P. G. Contractile function, sarcolemma integrity, and the loss of dystrophin after skeletal muscle eccentric contraction-induced injury. *Am J Physiol Cell Physiol* **286**, C230-8 (2004).

38. Lesniewski, L. A., Miller, T. A. & Armstrong, R. B. Mechanisms of force loss in diabetic mouse skeletal muscle. *Muscle Nerve* **28**, 493-500 (2003).

39. Ingalls, C. P., Warren, G. L., Lowe, D. A., Boorstein, D. B. & Armstrong, R. B. Differential effects of anesthetics on in vivo skeletal muscle contractile function in the mouse. *J Appl Physiol* **80**, 332-40 (1996).

40. Lowe, D. A., Warren, G. L., Ingalls, C. P., Boorstein, D. B. & Armstrong, R. B. Muscle function and protein metabolism after initiation of eccentric contraction-induced injury. *J Appl Physiol* **79**, 1260-70 (1995).

CONCLUSION

As a future physician scientist, my desire was to choose a subject matter that could be developed into a translational project for future clinical use. The choice of DMD as a disease model was appealing to me because of its prevalence and severity. The overall goal of this research was to test the possibility that MAPC could be used to treat DMD. Although such a conclusion can definitely not yet be reached based on the work I have done, a number of important findings are summarized in this thesis that should be invaluable for investigators interested in further developing possible therapies for DMD from MAPC or other stem cell populations.

My *in vitro* work can be applied by researchers investigating development of skeletal muscle from (more) pluripotent stem cells not yet committed to mesoderm or the myotome, by providing a framework for directed myogenic induction without need for toxic agents, sera or co-culture with muscle cell populations. In addition, as I have shown that the culture conditions that allow early myogenic commitment also induce early osteoblast or chondroblast commitment, this culture system can form the basis to induce these lineages from (more) pluripotent stem cells not yet committed to mesoderm. Importantly, the *in vitro* work presented can be applied to stem cells intended for clinical therapies because in addition to directing myogenesis and thereby increasing the target cell yield, the use of cytokines reduces/abolishes the need for sera, toxic agents like 5-azacytidine or co-culture with other cell populations.

Future studies of this *in vitro* work should aim to further direct a more mature myogenic phenotype and to verify at the protein level what has been observed so far at the transcriptional level. Finally, cells committed using this protocol to early myogenic committed cells are being tested for their ability to engraft in muscle, and regenerate dystrophin lacking in muscle of patients (and mice) with DMD.

The use of stem cells as a clinical therapy treat holds immense potential, as long as investigators define which cells (stem cells, progenitors, mature cells) should be used for a certain disease, and what the best method is to induce long-term engraftment followed by appropriate differentiation *in vivo*. My *in vivo* work aimed to test if undifferentiated MAPC could be used to treat DMD and to test methods to increase long-term persistence and obtain a high engraftment level. Although I learned that very few undifferentiated MAPC contributed to muscle fibers in the mouse model used, valuable lessons were learned from the study. These include difficulties with combined GFP and dystrophin detection, for which I developed an optimized staining protocol. This study also provided insight as to what methods can be used to obtain proof of principle that stem cells can contribute to skeletal muscle *in vivo*. Interestingly our data suggest that exertion and hence activation of the satellite cell compartment (which occurs spontaneously in boys with DMD but not in *mdx* mice) combined with a cell cycle active chemotherapeutic agent commonly used clinically that we hypothesize may temporally deplete the satellite cell compartment, may be a good and clinically applicable method to encourage stem cell engraftment. Ongoing studies are confirming that the additive effect of 5-FU with exercise is as hypothesized, i.e. elimination of part of the satellite cell compartment, and determining the reasons that may underlie poor MAPC engraftment.

The last part of my project will be a useful tool for investigators researching contractile properties in mice. The *in vivo* force system can significantly detect differences in contractile properties due to pathology. This system is of particular interest to researchers evaluating experimental therapies for DMD because it is quantitative, sensitive and non-invasive which allows for repeated testing within the same animal. Not only could this system be useful for DMD studies, but any study involving the use of myopathic mouse models. Interest of using this device has already been voiced from a couple of well known investigators in the stem cell/DMD field and work is currently underway to make a portable system as well as to modify the setup to reduce variability.

References

Weight Chart for the C57BL/6NCrl Mouse, Charles River Laboratories**:** Weight Chart for the C57BL/6NCrl Mouse.

Alter, J., F. Lou, et al. (2006). "Systemic delivery of morpholino oligonucleotide restores dystrophin expression bodywide and improves dystrophic pathology." Nat Med **12**(2): 175-7.

Alvarez-Dolado, M., R. Pardal, et al. (2003). "Fusion of bone-marrow-derived cells with Purkinje neurons, cardiomyocytes and hepatocytes." Nature **425**(6961): 968-73.

Anderson, J. E., B. H. Bressler, et al. (1988). "Functional regeneration in the hindlimb skeletal muscle of the mdx mouse." J Muscle Res Cell Motil **9**(6): 499-515.

Anjos-Afonso, F. and D. Bonnet (2007). "Nonhematopoietic/endothelial SSEA-1+ cells define the most primitive progenitors in the adult murine bone marrow mesenchymal compartment." Blood **109**(3): 1298-306.

Asakura, A., M. Komaki, et al. (2001). "Muscle satellite cells are multipotential stem cells that exhibit myogenic, osteogenic, and adipogenic differentiation." Differentiation **68**(4-5): 245-53.

Asakura, A. and M. A. Rudnicki (2002). "Side population cells from diverse adult tissues are capable of in vitro hematopoietic differentiation." Exp Hematol **30**(11): 1339-45.

Asakura, A., P. Seale, et al. (2002). "Myogenic specification of side population cells in skeletal muscle." J Cell Biol **159**(1): 123-34.

Ashton-Miller, J. A., Y. He, et al. (1992). "An apparatus to measure in vivo biomechanical behavior of dorsi- and plantarflexors of mouse ankle." J Appl Physiol **72**(3): 1205-11.

Bachrach, E., A. L. Perez, et al. (2006). "Muscle engraftment of myogenic progenitor cells following intraarterial transplantation." Muscle Nerve **34**(1): 44-52.

Badalamente, M. A. and A. Stracher (2000). "Delay of muscle degeneration and necrosis in mdx mice by calpain inhibition." Muscle Nerve **23**(1): 106-11.

Barohn, R. J., E. J. Levine, et al. (1988). "Gastric hypomotility in Duchenne's muscular dystrophy." N Engl J Med **319**(1): 15-8.

Barton, E. R., L. Morris, et al. (2002). "Muscle-specific expression of insulin-like growth factor I counters muscle decline in mdx mice." J Cell Biol **157**(1): 137-48.

Beauchamp, J. R., L. Heslop, et al. (2000). "Expression of CD34 and Myf5 defines the majority of quiescent adult skeletal muscle satellite cells." J Cell Biol **151**(6): 1221-34.

Belcastro, A. N., L. D. Shewchuk, et al. (1998). "Exercise-induced muscle injury: a calpain hypothesis." Mol Cell Biochem **179**(1-2): 135-45.

Bertorini, T. E., G. M. Palmieri, et al. (1991). "Effect of dantrolene in Duchenne muscular dystrophy." Muscle Nerve **14**(6): 503-7.

Bhagavati, S. and W. Xu (2005). "Generation of skeletal muscle from transplanted embryonic stem cells in dystrophic mice." Biochem Biophys Res Commun **333**(2): 644-9.

Bialek, P., B. Kern, et al. (2004). "A twist code determines the onset of osteoblast differentiation." Dev Cell **6**(3): 423-35.

Bittner, R. E., C. Schofer, et al. (1999). "Recruitment of bone-marrow-derived cells by skeletal and cardiac muscle in adult dystrophic mdx mice." Anat Embryol (Berl) **199**(5): 391-6.

Blau, H. M., G. K. Pavlath, et al. (1985). "Plasticity of the differentiated state." Science **230**(4727): 758-66.

Blomberg, M., S. Rao, et al. (1998). "Repetitive bone marrow transplantation in nonmyeloablated recipients." Exp Hematol **26**(4): 320-4.

Bogdanovich, S., T. O. Krag, et al. (2002). "Functional improvement of dystrophic muscle by myostatin blockade." Nature **420**(6914): 418-21.

Bouchentouf, M., B. F. Benabdallah, et al. (2006). "Exercise improves the success of myoblast transplantation in mdx mice." Neuromuscul Disord **16**(8): 518-29.

Bradley, A., M. Evans, et al. (1984). "Formation of germ-line chimaeras from embryo-derived teratocarcinoma cell lines." Nature **309**(5965): 255-6.

Brenman, J. E., D. S. Chao, et al. (1996). "Interaction of nitric oxide synthase with the postsynaptic density protein PSD-95 and alpha1-syntrophin mediated by PDZ domains." Cell **84**(5): 757-67.

Breyer, A., N. Estharabadi, et al. (2006). "Multipotent adult progenitor cell isolation and culture procedures." Exp Hematol **34**(11): 1596-601.

Brockes, J. P. and A. Kumar (2002). "Plasticity and reprogramming of differentiated cells in amphibian regeneration." Nat Rev Mol Cell Biol **3**(8): 566-74.

Brohmann, H., K. Jagla, et al. (2000). "The role of Lbx1 in migration of muscle precursor cells." Development **127**(2): 437-45.

Brunelli, S., F. Relaix, et al. (2007). "Beta catenin-independent activation of MyoD in presomitic mesoderm requires PKC and depends on Pax3 transcriptional activity." Dev Biol.

Brunelli, S., C. Sciorati, et al. (2007). "Nitric oxide release combined with nonsteroidal antiinflammatory activity prevents muscular dystrophy pathology and enhances stem cell therapy." Proc Natl Acad Sci U S A **104**(1): 264-9.

Buckingham, M. (2001). "Skeletal muscle formation in vertebrates." Curr Opin Genet Dev **11**(4): 440-8.

Buckingham, M., L. Bajard, et al. (2003). "The formation of skeletal muscle: from somite to limb." J Anat **202**(1): 59-68.

Burdi, R., M. P. Didonna, et al. (2006). "First evaluation of the potential effectiveness in muscular dystrophy of a novel chimeric compound, BN 82270, acting as calpain-inhibitor and anti-oxidant." Neuromuscul Disord **16**(4): 237-48.

Camargo, F. D., R. Green, et al. (2003). "Single hematopoietic stem cells generate skeletal muscle through myeloid intermediates." Nat Med **9**(12): 1520-7.

Cao, B., B. Zheng, et al. (2003). "Muscle stem cells differentiate into haematopoietic lineages but retain myogenic potential." Nat Cell Biol **5**(7): 640-6.

Carpenter, J. L., E. P. Hoffman, et al. (1989). "Feline muscular dystrophy with dystrophin deficiency." Am J Pathol **135**(5): 909-19.

Chapman, V. M., D. R. Miller, et al. (1989). "Recovery of induced mutations for X chromosome-linked muscular dystrophy in mice." Proc Natl Acad Sci U S A **86**(4): 1292-6.

Charge, S. B. and M. A. Rudnicki (2004). "Cellular and molecular regulation of muscle regeneration." Physiol Rev **84**(1): 209-38.

Corbel, S. Y., A. Lee, et al. (2003). "Contribution of hematopoietic stem cells to skeletal muscle." Nat Med **9**(12): 1528-32.

Corti, S., S. Strazzer, et al. (2002). "A subpopulation of murine bone marrow cells fully differentiates along the myogenic pathway and participates in muscle repair in the mdx dystrophic mouse." Exp Cell Res **277**(1): 74-85.

Cossu, G. and U. Borello (1999). "Wnt signaling and the activation of myogenesis in mammals." Embo J **18**(24): 6867-72.

Craig, R. (1986). The Structure of the Contractile Filaments. Myology. B. Q. B. Andrew G. Engel. New York, McGraw-Hill**:** 73-123.

Crawford, G. E., Q. L. Lu, et al. (2001). "Suppression of revertant fibers in mdx mice by expression of a functional dystrophin." Hum Mol Genet **10**(24): 2745-50.

D'Amour, K. A., A. G. Bang, et al. (2006). "Production of pancreatic hormone-expressing endocrine cells from human embryonic stem cells." Nat Biotechnol **24**(11): 1392-401.

Dangain, J. and G. Vrbova (1984). "Muscle development in mdx mutant mice." Muscle Nerve **7**(9): 700-4.

Davis, R. L., H. Weintraub, et al. (1987). "Expression of a single transfected cDNA converts fibroblasts to myoblasts." Cell **51**(6): 987-1000.

De Angelis, L., L. Berghella, et al. (1999). "Skeletal myogenic progenitors originating from embryonic dorsal aorta coexpress endothelial and myogenic markers and contribute to postnatal muscle growth and regeneration." J Cell Biol **147**(4): 869-78.

De Angelis, L., S. Borghi, et al. (1998). "Inhibition of myogenesis by transforming growth factor beta is density-dependent and related to the translocation of transcription factor MEF2 to the cytoplasm." Proc Natl Acad Sci U S A **95**(21): 12358-63.

De Backer, F., C. Vandebrouck, et al. (2002). "Long-term study of Ca(2+) homeostasis and of survival in collagenase-isolated muscle fibres from normal and mdx mice." J Physiol **542**(Pt 3): 855-65.

Deasy, B. M., B. M. Gharaibeh, et al. (2005). "Long-term self-renewal of postnatal muscle-derived stem cells." Mol Biol Cell **16**(7): 3323-33.

Deconinck, A. E., J. A. Rafael, et al. (1997). "Utrophin-dystrophin-deficient mice as a model for Duchenne muscular dystrophy." Cell **90**(4): 717-27.

Dinsmore, J., J. Ratliff, et al. (1996). "Embryonic stem cells differentiated in vitro as a novel source of cells for transplantation." Cell Transplant **5**(2): 131-43.

D'Ippolito, G., S. Diabira, et al. (2004). "Marrow-isolated adult multilineage inducible (MIAMI) cells, a unique population of postnatal young and old human cells with extensive expansion and differentiation potential." J Cell Sci **117**(Pt 14): 2971-81.

D'Ippolito, G., G. A. Howard, et al. (2006). "Isolation and characterization of marrow-isolated adult multilineage inducible (MIAMI) cells." Exp Hematol **34**(11): 1608-10.

Duclos, F., V. Straub, et al. (1998). "Progressive muscular dystrophy in alpha-sarcoglycan-deficient mice." J Cell Biol **142**(6): 1461-71.

Emery, A. E. (2002). "The muscular dystrophies." Lancet **359**(9307): 687-95.

Ervasti, J. M. and K. P. Campbell (1991). "Membrane organization of the dystrophin-glycoprotein complex." Cell **66**(6): 1121-31.

Evans, M. J. and M. H. Kaufman (1981). "Establishment in culture of pluripotential cells from mouse embryos." Nature **292**(5819): 154-6.

Fernandes, K. J., I. A. McKenzie, et al. (2004). "A dermal niche for multipotent adult skin-derived precursor cells." Nat Cell Biol **6**(11): 1082-93.

Ferrari, G., G. Cusella-De Angelis, et al. (1998). "Muscle regeneration by bone marrow-derived myogenic progenitors." Science **279**(5356): 1528-30.

Gaschen, F. and J. M. Burgunder (2001). "Changes of skeletal muscle in young dystrophin-deficient cats: a morphological and morphometric study." Acta Neuropathol (Berl) **101**(6): 591-600.

Gilbert, S. F., Ed. (1997). Developmental Biology. Sunderland, Massachusetts, Sinauer Associates, Inc.

Gordon, A. M., A. F. Huxley, et al. (1966). "The variation in isometric tension with sarcomere length in vertebrate muscle fibres." J Physiol **184**(1): 170-92.

Granchelli, J. A., D. L. Avosso, et al. (1996). "Cromolyn increases strength in exercised mdx mice." Res Commun Mol Pathol Pharmacol **91**(3): 287-96.

Graves, K. H. and R. W. Moreadith (1993). "Derivation and characterization of putative pluripotential embryonic stem cells from preimplantation rabbit embryos." Mol Reprod Dev **36**(4): 424-33.

Gregorevic, P., D. R. Plant, et al. (2002). "Improved contractile function of the mdx dystrophic mouse diaphragm muscle after insulin-like growth factor-I administration." Am J Pathol **161**(6): 2263-72.

Guan, K., K. Nayernia, et al. (2006). "Pluripotency of spermatogonial stem cells from adult mouse testis." Nature **440**(7088): 1199-203.

Gupta, S., C. Verfaillie, et al. (2006). "Isolation and characterization of kidney-derived stem cells." J Am Soc Nephrol **17**(11): 3028-40.

Gussoni, E., H. M. Blau, et al. (1997). "The fate of individual myoblasts after transplantation into muscles of DMD patients." Nat Med **3**(9): 970-7.

Gussoni, E., Y. Soneoka, et al. (1999). "Dystrophin expression in the mdx mouse restored by stem cell transplantation." Nature **401**(6751): 390-4.

Gustafsson, M. K., H. Pan, et al. (2002). "Myf5 is a direct target of long-range Shh signaling and Gli regulation for muscle specification." Genes Dev **16**(1): 114-26.

Guyton, A. and J. Hall, Eds. (1996). Textbook of Medical Physiology. Philadelphia, W.B. Saunders Company.

Hashimoto, N., T. Murase, et al. (2004). "Muscle reconstitution by muscle satellite cell descendants with stem cell-like properties." Development **131**(21): 5481-90.

Hasty, P., A. Bradley, et al. (1993). "Muscle deficiency and neonatal death in mice with a targeted mutation in the myogenin gene." Nature **364**(6437): 501-6.

Heldin, C. H., K. Miyazono, et al. (1997). "TGF-beta signalling from cell membrane to nucleus through SMAD proteins." Nature **390**(6659): 465-71.

Hodgetts, S., H. Radley, et al. (2006). "Reduced necrosis of dystrophic muscle by depletion of host neutrophils, or blocking TNFalpha function with Etanercept in mdx mice." Neuromuscul Disord **16**(9-10): 591-602.

Hong, J. B. and P. A. Iaizzo (2002). "Force assessment of the stimulated arm flexors: quantification of contractile properties." J Med Eng Technol **26**(1): 28-35.

Howell, J. M., H. Lochmuller, et al. (1998). "High-level dystrophin expression after adenovirus-mediated dystrophin minigene transfer to skeletal muscle of dystrophic dogs: prolongation of expression with immunosuppression." Hum Gene Ther **9**(5): 629-34.

Huang, H., M. D. Lane, et al. (2005). "Effect of serum on the down-regulation of CHOP-10 during differentiation of 3T3-L1 preadipocytes." Biochem Biophys Res Commun **338**(2): 1185-8.

Ingalls, C. P., G. L. Warren, et al. (1996). "Differential effects of anesthetics on in vivo skeletal muscle contractile function in the mouse." J Appl Physiol **80**(1): 332-40.

Inoue, K., S. Noda, et al. (2007). "Differential developmental ability of embryos cloned from tissue-specific stem cells." Stem Cells.

Jackson, K. A., T. Mi, et al. (1999). "Hematopoietic potential of stem cells isolated from murine skeletal muscle." Proc Natl Acad Sci U S A **96**(25): 14482-6.

Jensen, H., M. Warburg, et al. (1995). "Duchenne muscular dystrophy: negative electroretinograms and normal dark adaptation. Reappraisal of assignment of X linked incomplete congenital stationary night blindness." J Med Genet **32**(5): 348-51.

Jiang, Y., B. N. Jahagirdar, et al. (2002). "Pluripotency of mesenchymal stem cells derived from adult marrow." Nature **418**(6893): 41-9.

Jiang, Y., B. Vaessen, et al. (2002). "Multipotent progenitor cells can be isolated from postnatal murine bone marrow, muscle, and brain." Exp Hematol **30**(8): 896-904.

Jockusch, H., S. Voigt, et al. (2003). "Localization of GFP in frozen sections from unfixed mouse tissues: immobilization of a highly soluble marker protein by formaldehyde vapor." J Histochem Cytochem **51**(3): 401-4.

Judge, L. M., M. Haraguchiln, et al. (2006). "Dissecting the signaling and mechanical functions of the dystrophin-glycoprotein complex." J Cell Sci **119**(Pt 8): 1537-46.

Kamochi, H., M. S. Kurokawa, et al. (2006). "Transplantation of myocyte precursors derived from embryonic stem cells transfected with IGFII gene in a mouse model of muscle injury." Transplantation **82**(4): 516-26.

Kassar-Duchossoy, L., B. Gayraud-Morel, et al. (2004). "Mrf4 determines skeletal muscle identity in Myf5:Myod double-mutant mice." Nature **431**(7007): 466-71.

Kawakami, Y., M. Tsuda, et al. (2005). "Transcriptional coactivator PGC-1alpha regulates chondrogenesis via association with Sox9." Proc Natl Acad Sci U S A **102**(7): 2414-9.

Keller, G. M. (1995). "In vitro differentiation of embryonic stem cells." Curr Opin Cell Biol **7**(6): 862-9.

Kessler, P. D., G. M. Podsakoff, et al. (1996). "Gene delivery to skeletal muscle results in sustained expression and systemic delivery of a therapeutic protein." Proc Natl Acad Sci U S A **93**(24): 14082-7.

Khan, J., M. L. Bittner, et al. (1999). "cDNA microarrays detect activation of a myogenic transcription program by the PAX3-FKHR fusion oncogene." Proc Natl Acad Sci U S A **96**(23): 13264-9.

Khurana, T. S. and K. E. Davies (2003). "Pharmacological strategies for muscular dystrophy." Nat Rev Drug Discov **2**(5): 379-90.

Khurana, T. S., R. A. Prendergast, et al. (1995). "Absence of extraocular muscle pathology in Duchenne's muscular dystrophy: role for calcium homeostasis in extraocular muscle sparing." J Exp Med **182**(2): 467-75.

Kim, J. H., J. M. Auerbach, et al. (2002). "Dopamine neurons derived from embryonic stem cells function in an animal model of Parkinson's disease." Nature **418**(6893): 50-6.

Kishigami, S., S. Wakayama, et al. (2006). "Cloned mice and embryonic stem cell establishment from adult somatic cells." Hum Cell **19**(1): 2-10.

Klug, M. G., M. H. Soonpaa, et al. (1996). "Genetically selected cardiomyocytes from differentiating embronic stem cells form stable intracardiac grafts." J Clin Invest **98**(1): 216-24.

Kogler, G., S. Sensken, et al. (2004). "A new human somatic stem cell from placental cord blood with intrinsic pluripotent differentiation potential." J Exp Med **200**(2): 123-35.

Konigsberg, I. R. (1986). The Embryonic Origin of Muscle. Myology. A. G. Engel. New York, McGraw-Hill, Inc. **1:** 39-71.

Kubo, A., K. Shinozaki, et al. (2004). "Development of definitive endoderm from embryonic stem cells in culture." Development **131**(7): 1651-62.

Kucia, M., M. Halasa, et al. (2007). "Morphological and molecular characterization of novel population of CXCR4+ SSEA-4+ Oct-4+ very small embryonic-like cells purified from human cord blood: preliminary report." Leukemia **21**(2): 297-303.

Kucia, M., J. Ratajczak, et al. (2004). "Tissue-specific muscle, neural and liver stem/progenitor cells reside in the bone marrow, respond to an SDF-1 gradient and are mobilized into peripheral blood during stress and tissue injury." Blood Cells Mol Dis **32**(1): 52-7.

Kucia, M., R. Reca, et al. (2006). "A population of very small embryonic-like (VSEL) CXCR4(+)SSEA-1(+)Oct-4+ stem cells identified in adult bone marrow." Leukemia **20**(5): 857-69.

LaBarge, M. A. and H. M. Blau (2002). "Biological progression from adult bone marrow to mononucleate muscle stem cell to multinucleate muscle fiber in response to injury." Cell **111**(4): 589-601.

Labeit, S. and B. Kolmerer (1995). "The complete primary structure of human nebulin and its correlation to muscle structure." J Mol Biol **248**(2): 308-15.

Labeit, S. and B. Kolmerer (1995). "Titins: giant proteins in charge of muscle ultrastructure and elasticity." Science **270**(5234): 293-6.

Lagasse, E., H. Connors, et al. (2000). "Purified hematopoietic stem cells can differentiate into hepatocytes in vivo." Nat Med **6**(11): 1229-34.

Lee, J. Y., Z. Qu-Petersen, et al. (2000). "Clonal isolation of muscle-derived cells capable of enhancing muscle regeneration and bone healing." J Cell Biol **150**(5): 1085-100.

Leibovitz, S., A. Meshorer, et al. (2002). "Exogenous Dp71 is a dominant negative competitor of dystrophin in skeletal muscle." Neuromuscul Disord **12**(9): 836-44.

Lesniewski, L. A., T. A. Miller, et al. (2003). "Mechanisms of force loss in diabetic mouse skeletal muscle." Muscle Nerve **28**(4): 493-500.

Li, H. and Y. Capetanaki (1994). "An E box in the desmin promoter cooperates with the E box and MEF-2 sites of a distal enhancer to direct muscle-specific transcription." Embo J **13**(15): 3580-9.

Li, M., D. Zhang, et al. (2003). "Isolation and culture of embryonic stem cells from porcine blastocysts." Mol Reprod Dev **65**(4): 429-34.

Lidov, H. G. and L. M. Kunkel (1997). "Dp140: alternatively spliced isoforms in brain and kidney." Genomics **45**(1): 132-9.

Lodish, H., A. Berk, et al. (2000). Molecular Cell Biology. New York, W.H. Freeman and Company.

Lovering, R. M. and P. G. De Deyne (2004). "Contractile function, sarcolemma integrity, and the loss of dystrophin after skeletal muscle eccentric contraction-induced injury." Am J Physiol Cell Physiol **286**(2): C230-8.

Lowe, D. A., G. L. Warren, et al. (1995). "Muscle function and protein metabolism after initiation of eccentric contraction-induced injury." J Appl Physiol **79**(4): 1260-70.

Lu, Q. L., C. J. Mann, et al. (2003). "Functional amounts of dystrophin produced by skipping the mutated exon in the mdx dystrophic mouse." Nat Med **9**(8): 1009-14.

Lu, Q. L., G. E. Morris, et al. (2000). "Massive idiosyncratic exon skipping corrects the nonsense mutation in dystrophic mouse muscle and produces functional revertant fibers by clonal expansion." J Cell Biol **148**(5): 985-96.

Lynch, G. S., R. T. Hinkle, et al. (2001). "Force and power output of fast and slow skeletal muscles from mdx mice 6-28 months old." J Physiol **535**(Pt 2): 591-600.

Maltsev, V. A., J. Rohwedel, et al. (1993). "Embryonic stem cells differentiate in vitro into cardiomyocytes representing sinusnodal, atrial and ventricular cell types." Mech Dev **44**(1): 41-50.

Mankoo, B. S., N. S. Collins, et al. (1999). "Mox2 is a component of the genetic hierarchy controlling limb muscle development." Nature **400**(6739): 69-73.

Mann, C. J., K. Honeyman, et al. (2001). "Antisense-induced exon skipping and synthesis of dystrophin in the mdx mouse." Proc Natl Acad Sci U S A **98**(1): 42-7.

Manzur, A., T. Kuntzer, et al. (2004). "Glucocorticoid corticosteroids for Duchenne muscular dystrophy." Cochrane Database Syst Rev **2**: CD003725.

Marcelle, C., C. Lesbros, et al. (2002). Somite Patterning: a Few More Pieces of the Puzzle. Vertebrate Myogenesis. B.Brand-Saberi. Berlin, Springer**:** 81-108.

Marques, M. J., R. Ferretti, et al. (2006). "Intrinsic laryngeal muscles are spared from myonecrosis in the mdx mouse model of Duchenne muscular dystrophy." Muscle Nerve.

Martin, B. L. and R. M. Harland (2006). "A novel role for lbx1 in Xenopus hypaxial myogenesis." Development **133**(2): 195-208.

Matsumura, K., F. M. Tome, et al. (1993). "Deficiency of dystrophin-associated proteins in Duchenne muscular dystrophy patients lacking COOH-terminal domains of dystrophin." J Clin Invest **92**(2): 866-71.

McArdle, A., R. H. Edwards, et al. (1995). "How does dystrophin deficiency lead to muscle degeneration?--evidence from the mdx mouse." Neuromuscul Disord **5**(6): 445-56.

McKenzie, J. L., O. I. Gan, et al. (2006). "Individual stem cells with highly variable proliferation and self-renewal properties comprise the human hematopoietic stem cell compartment." Nat Immunol **7**(11): 1225-33.

McKinney-Freeman, S. L., K. A. Jackson, et al. (2002). "Muscle-derived hematopoietic stem cells are hematopoietic in origin." Proc Natl Acad Sci U S A **99**(3): 1341-6.

McNiece, I. K., R. A. Briddell, et al. (1993). "The role of stem cell factor in mobilization of peripheral blood progenitor cells: synergy with G-CSF." Stem Cells **11 Suppl 3**: 83-8.

McPherron, A. C., A. M. Lawler, et al. (1997). "Regulation of skeletal muscle mass in mice by a new TGF-beta superfamily member." Nature **387**(6628): 83-90.

McPherron, A. C. and S. J. Lee (1997). "Double muscling in cattle due to mutations in the myostatin gene." Proc Natl Acad Sci U S A **94**(23): 12457-61.

Mennerich, D., K. Schafer, et al. (1998). "Pax-3 is necessary but not sufficient for lbx1 expression in myogenic precursor cells of the limb." Mech Dev **73**(2): 147-58.

Merlini, L., A. Cicognani, et al. (2003). "Early prednisone treatment in Duchenne muscular dystrophy." Muscle Nerve **27**(2): 222-7.

Minetti, G. C., C. Colussi, et al. (2006). "Functional and morphological recovery of dystrophic muscles in mice treated with deacetylase inhibitors." Nat Med **12**(10): 1147-50.

Moens, P., P. H. Baatsen, et al. (1993). "Increased susceptibility of EDL muscles from mdx mice to damage induced by contractions with stretch." J Muscle Res Cell Motil **14**(4): 446-51.

Montarras, D., J. Morgan, et al. (2005). "Direct isolation of satellite cells for skeletal muscle regeneration." Science **309**(5743): 2064-7.

Muguruma, Y., M. Reyes, et al. (2003). "In vivo and in vitro differentiation of myocytes from human bone marrow-derived multipotent progenitor cells." Exp Hematol **31**(12): 1323-30.

Nabeshima, Y., K. Hanaoka, et al. (1993). "Myogenin gene disruption results in perinatal lethality because of severe muscle defect." Nature **364**(6437): 532-5.

Nakayama, T., T. Momoki-Soga, et al. (2004). "Efficient production of neural stem cells and neurons from embryonic stem cells." Neuroreport **15**(3): 487-91.

O'Brien, K. F. and L. M. Kunkel (2001). "Dystrophin and muscular dystrophy: past, present, and future." Mol Genet Metab **74**(1-2): 75-88.

Odelberg, S. J., A. Kollhoff, et al. (2000). "Dedifferentiation of mammalian myotubes induced by msx1." Cell **103**(7): 1099-109.

Oh, S. H., M. Miyazaki, et al. (2000). "Hepatocyte growth factor induces differentiation of adult rat bone marrow cells into a hepatocyte lineage in vitro." Biochem Biophys Res Commun **279**(2): 500-4.

Olguin, H. C. and B. B. Olwin (2004). "Pax-7 up-regulation inhibits myogenesis and cell cycle progression in satellite cells: a potential mechanism for self-renewal." Dev Biol **275**(2): 375-88.

Osawa, M., K. Hanada, et al. (1996). "Long-term lymphohematopoietic reconstitution by a single CD34-low/negative hematopoietic stem cell." Science **273**(5272): 242-5.

Oyama, T., T. Nagai, et al. (2007). "Cardiac side population cells have a potential to migrate and differentiate into cardiomyocytes in vitro and in vivo." J Cell Biol **176**(3): 329-41.

Palermo, A. T., M. A. Labarge, et al. (2005). "Bone marrow contribution to skeletal muscle: a physiological response to stress." Dev Biol **279**(2): 336-44.

Parker, M. H., P. Seale, et al. (2003). "Looking back to the embryo: defining transcriptional networks in adult myogenesis." Nat Rev Genet **4**(7): 497-507.

Patapoutian, A., J. K. Yoon, et al. (1995). "Disruption of the mouse MRF4 gene identifies multiple waves of myogenesis in the myotome." Development **121**(10): 3347-58.

Patel, K., B. Christ, et al. (2002). Control of Muscle Size During Embryonic, Fetal, and Adult Life. Vertebrate Myogenesis. B. Brand-Saberi. Berlin, Springer. **38:** 163-186.

Pearce, M., D. J. Blake, et al. (1993). "The utrophin and dystrophin genes share similarities in genomic structure." Hum Mol Genet **2**(11): 1765-72.

Perkins, K. J. and K. E. Davies (2002). "The role of utrophin in the potential therapy of Duchenne muscular dystrophy." Neuromuscul Disord **12 Suppl 1**: S78-89.

Petrof, B. J., J. B. Shrager, et al. (1993). "Dystrophin protects the sarcolemma from stresses developed during muscle contraction." Proc Natl Acad Sci U S A **90**(8): 3710-4.

Petropoulos, H. and I. S. Skerjanc (2002). "Beta-catenin is essential and sufficient for skeletal myogenesis in P19 cells." J Biol Chem **277**(18): 15393-9.

Phinney, D. G., G. Kopen, et al. (1999). "Plastic adherent stromal cells from the bone marrow of commonly used strains of inbred mice: variations in yield, growth, and differentiation." J Cell Biochem **72**(4): 570-85.

Phinney, D. G., G. Kopen, et al. (1999). "Donor variation in the growth properties and osteogenic potential of human marrow stromal cells." J Cell Biochem **75**(3): 424-36.

Pittenger, M. F., A. M. Mackay, et al. (1999). "Multilineage potential of adult human mesenchymal stem cells." Science **284**(5411): 143-7.

Pourquie, O., C. M. Fan, et al. (1996). "Lateral and axial signals involved in avian somite patterning: a role for BMP4." Cell **84**(3): 461-71.

Pulido, S. M., A. C. Passaquin, et al. (1998). "Creatine supplementation improves intracellular Ca2+ handling and survival in mdx skeletal muscle cells." FEBS Lett **439**(3): 357-62.

Qu, Z., L. Balkir, et al. (1998). "Development of approaches to improve cell survival in myoblast transfer therapy." J Cell Biol **142**(5): 1257-67.

Quinlan, J. G., S. P. Lyden, et al. (1995). "Radiation inhibition of mdx mouse muscle regeneration: dose and age factors." Muscle Nerve **18**(2): 201-6.

Qu-Petersen, Z., B. Deasy, et al. (2002). "Identification of a novel population of muscle stem cells in mice: potential for muscle regeneration." J Cell Biol **157**(5): 851-64.

Rafael, J. A., G. A. Cox, et al. (1996). "Forced expression of dystrophin deletion constructs reveals structure-function correlations." J Cell Biol **134**(1): 93-102.

Rafael, J. A., E. R. Townsend, et al. (2000). "Dystrophin and utrophin influence fiber type composition and post-synaptic membrane structure." Hum Mol Genet **9**(9): 1357-67.

Ragot, T., N. Vincent, et al. (1993). "Efficient adenovirus-mediated transfer of a human minidystrophin gene to skeletal muscle of mdx mice." Nature **361**(6413): 647-50.

Rando, T. A. and H. M. Blau (1994). "Primary mouse myoblast purification, characterization, and transplantation for cell-mediated gene therapy." J Cell Biol **125**(6): 1275-87.

Ratajczak, M. Z., M. Kucia, et al. (2004). "Stem cell plasticity revisited: CXCR4-positive cells expressing mRNA for early muscle, liver and neural cells 'hide out' in the bone marrow." Leukemia **18**(1): 29-40.

Relaix, F., D. Rocancourt, et al. (2005). "A Pax3/Pax7-dependent population of skeletal muscle progenitor cells." Nature **435**(7044): 948-53.

Reyes, M., T. Lund, et al. (2001). "Purification and ex vivo expansion of postnatal human marrow mesodermal progenitor cells." Blood **98**(9): 2615-25.

Reyes, M. and C. M. Verfaillie (2001). "Characterization of multipotent adult progenitor cells, a subpopulation of mesenchymal stem cells." Ann N Y Acad Sci **938**: 231-3; discussion 233-5.

Ridgeway, A. G. and I. S. Skerjanc (2001). "Pax3 is essential for skeletal myogenesis and the expression of Six1 and Eya2." J Biol Chem **276**(22): 19033-9.

Rippon, H. J. and A. E. Bishop (2004). "Embryonic stem cells." Cell Prolif **37**(1): 23-34.

Rybakova, I. N., J. R. Patel, et al. (2002). "Utrophin binds laterally along actin filaments and can couple costameric actin with sarcolemma when overexpressed in dystrophin-deficient muscle." Mol Biol Cell **13**(5): 1512-21.

Sabourin, L. A. and M. A. Rudnicki (2000). "The molecular regulation of myogenesis." Clin Genet **57**(1): 16-25.

Sacco, P., D. A. Jones, et al. (1992). "Contractile properties and susceptibility to exercise-induced damage of normal and mdx mouse tibialis anterior muscle." Clin Sci (Lond) **82**(2): 227-36.

Salvatori, G., L. Lattanzi, et al. (1995). "Myogenic conversion of mammalian fibroblasts induced by differentiating muscle cells." J Cell Sci **108 (Pt 8)**: 2733-9.

Sampaolesi, M., S. Blot, et al. (2006). "Mesoangioblast stem cells ameliorate muscle function in dystrophic dogs." Nature **444**(7119): 574-9.

Sampaolesi, M., Y. Torrente, et al. (2003). "Cell therapy of alpha-sarcoglycan null dystrophic mice through intra-arterial delivery of mesoangioblasts." Science **301**(5632): 487-92.

Sander, M., B. Chavoshan, et al. (2000). "Functional muscle ischemia in neuronal nitric oxide synthase-deficient skeletal muscle of children with Duchenne muscular dystrophy." Proc Natl Acad Sci U S A **97**(25): 13818-23.

Sarig, R., V. Mezger-Lallemand, et al. (1999). "Targeted inactivation of Dp71, the major non-muscle product of the DMD gene: differential activity of the Dp71 promoter during development." Hum Mol Genet **8**(1): 1-10.

Schmalbruch, H. and D. M. Lewis (2000). "Dynamics of nuclei of muscle fibers and connective tissue cells in normal and denervated rat muscles." Muscle Nerve **23**(4): 617-26.

Seale, P., A. Asakura, et al. (2001). "The potential of muscle stem cells." Dev Cell **1**(3): 333-42.

Seale, P. and M. A. Rudnicki (2000). "A new look at the origin, function, and "stem-cell" status of muscle satellite cells." Dev Biol **218**(2): 115-24.

Seale, P., L. A. Sabourin, et al. (2000). "Pax7 is required for the specification of myogenic satellite cells." Cell **102**(6): 777-86.

Serafini, M., S. J. Dylla, et al. (2007). "Hematopoietic reconstitution by multipotent adult progenitor cells: precursors to long-term hematopoietic stem cells." J Exp Med **204**(1): 129-39.

Shamblott, M. J., J. Axelman, et al. (1998). "Derivation of pluripotent stem cells from cultured human primordial germ cells." Proc Natl Acad Sci U S A **95**(23): 13726-31.

Smith, J. P., P. S. Hicks, et al. (1995). "Quantitative measurement of muscle strength in the mouse." J Neurosci Methods **62**(1-2): 15-9.

Smith, P. J., L. S. Wise, et al. (1988). "Insulin-like growth factor-I is an essential regulator of the differentiation of 3T3-L1 adipocytes." J Biol Chem **263**(19): 9402-8.

Stamataki, D., M. Kastrinaki, et al. (2001). "Homeodomain proteins Mox1 and Mox2 associate with Pax1 and Pax3 transcription factors." FEBS Lett **499**(3): 274-8.

Stedman, H. H., H. L. Sweeney, et al. (1991). "The mdx mouse diaphragm reproduces the degenerative changes of Duchenne muscular dystrophy." Nature **352**(6335): 536-9.

Stein, G. S., J. B. Lian, et al. (2004). "Runx2 control of organization, assembly and activity of the regulatory machinery for skeletal gene expression." Oncogene **23**(24): 4315-29.

Straub, V. and K. P. Campbell (1997). "Muscular dystrophies and the dystrophin-glycoprotein complex." Curr Opin Neurol **10**(2): 168-75.

Straub, V., J. A. Rafael, et al. (1997). "Animal models for muscular dystrophy show different patterns of sarcolemmal disruption." J Cell Biol **139**(2): 375-85.

Tajbakhsh, S. (2002). The Genetics of Murine Skeletal Muscle Biogenesis. Vertebrate Myogenesis. B.Brand-Saberi. Berlin, Springer-Verlag**:** 61-79.

Takahashi, K. and S. Yamanaka (2006). "Induction of pluripotent stem cells from mouse embryonic and adult fibroblast cultures by defined factors." Cell **126**(4): 663-76.

Terada, N., T. Hamazaki, et al. (2002). "Bone marrow cells adopt the phenotype of other cells by spontaneous cell fusion." Nature **416**(6880): 542-5.

Thomson, J. A., J. Itskovitz-Eldor, et al. (1998). "Embryonic stem cell lines derived from human blastocysts." Science **282**(5391): 1145-7.

Thomson, J. A., J. Kalishman, et al. (1995). "Isolation of a primate embryonic stem cell line." Proc Natl Acad Sci U S A **92**(17): 7844-8.

Tinsley, J. M., A. C. Potter, et al. (1996). "Amelioration of the dystrophic phenotype of mdx mice using a truncated utrophin transgene." Nature **384**(6607): 349-53.

Toma, J. G., M. Akhavan, et al. (2001). "Isolation of multipotent adult stem cells from the dermis of mammalian skin." Nat Cell Biol **3**(9): 778-84.

Toma, J. G., I. A. McKenzie, et al. (2005). "Isolation and characterization of multipotent skin-derived precursors from human skin." Stem Cells **23**(6): 727-37.

Torrente, Y., M. Belicchi, et al. (2004). "Human circulating AC133(+) stem cells restore dystrophin expression and ameliorate function in dystrophic skeletal muscle." J Clin Invest **114**(2): 182-95.

Uchida, N., H. L. Aguila, et al. (1994). "Rapid and sustained hematopoietic recovery in lethally irradiated mice transplanted with purified Thy-1.1lo Lin-Sca-1+ hematopoietic stem cells." Blood **83**(12): 3758-79.

Verfaillie, C. M., M. F. Pera, et al. (2002). "Stem cells: hype and reality." Hematology (Am Soc Hematol Educ Program): 369-91.

Wada, M. R., M. Inagawa-Ogashiwa, et al. (2002). "Generation of different fates from multipotent muscle stem cells." Development **129**(12): 2987-95.

Wagers, A. J. and I. L. Weissman (2004). "Plasticity of adult stem cells." Cell **116**(5): 639-48.

Waibler, Z. and A. Starzinski-Powitz (2002). Cadherins in Skeletal Muscle Development. Vertebrate Myogenesis. B.Brand-Saberi. Berlin, Springer-Verlag. **38:** 188-198.

Wakitani, S., T. Saito, et al. (1995). "Myogenic cells derived from rat bone marrow mesenchymal stem cells exposed to 5-azacytidine." Muscle Nerve **18**(12): 1417-26.

Wang, B., J. Li, et al. (2000). "Adeno-associated virus vector carrying human minidystrophin genes effectively ameliorates muscular dystrophy in mdx mouse model." Proc Natl Acad Sci U S A **97**(25): 13714-9.

Wang, X., H. Willenbring, et al. (2003). "Cell fusion is the principal source of bone-marrow-derived hepatocytes." Nature **422**(6934): 897-901.

Wernig, G., V. Janzen, et al. (2005). "The vast majority of bone-marrow-derived cells integrated into mdx muscle fibers are silent despite long-term engraftment." Proc Natl Acad Sci U S A **102**(33): 11852-7.

Williams, D. A., S. I. Head, et al. (1993). "Contractile properties of skinned muscle fibres from young and adult normal and dystrophic (mdx) mice." J Physiol **460**: 51-67.

Wilmut, I., A. E. Schnieke, et al. (1997). "Viable offspring derived from fetal and adult mammalian cells." Nature **385**(6619): 810-3.

Xiao, X., J. Li, et al. (1996). "Efficient long-term gene transfer into muscle tissue of immunocompetent mice by adeno-associated virus vector." J Virol **70**(11): 8098-108.

Yamamoto, K., K. Yuasa, et al. (2000). "Immune response to adenovirus-delivered antigens upregulates utrophin and results in mitigation of muscle pathology in mdx mice." Hum Gene Ther **11**(5): 669-80.

Yan, Z., S. Choi, et al. (2003). "Highly coordinated gene regulation in mouse skeletal muscle regeneration." J Biol Chem **278**(10): 8826-36.

Yang, B., J. M. Verbavatz, et al. (2000). "Skeletal muscle function and water permeability in aquaporin-4 deficient mice." Am J Physiol Cell Physiol **278**(6): C1108-15.

Yin, Y., Y. K. Lim, et al. (2002). "AFP(+), ESC-derived cells engraft and differentiate into hepatocytes in vivo." Stem Cells **20**(4): 338-46.

Ying, Q. L., J. Nichols, et al. (2002). "Changing potency by spontaneous fusion." Nature **416**(6880): 545-8.

Yokota, T., Q. L. Lu, et al. (2006). "Expansion of revertant fibers in dystrophic mdx muscles reflects activity of muscle precursor cells and serves as an index of muscle regeneration." J Cell Sci **119**(Pt 13): 2679-87.

Yoon, Y. S., A. Wecker, et al. (2005). "Clonally expanded novel multipotent stem cells from human bone marrow regenerate myocardium after myocardial infarction." J Clin Invest **115**(2): 326-38.

Yuasa, K., Y. Miyagoe, et al. (1998). "Effective restoration of dystrophin-associated proteins in vivo by adenovirus-mediated transfer of truncated dystrophin cDNAs." FEBS Lett **425**(2): 329-36.

Yuasa, K., M. Sakamoto, et al. (2002). "Adeno-associated virus vector-mediated gene transfer into dystrophin-deficient skeletal muscles evokes enhanced immune response against the transgene product." Gene Ther **9**(23): 1576-88.

Zeman, R. J., Y. Zhang, et al. (1994). "Clenbuterol, a beta 2-agonist, retards wasting and loss of contractility in irradiated dystrophic mdx muscle." Am J Physiol **267**(3 Pt 1): C865-8.

Zhao, L. R., W. M. Duan, et al. (2002). "Human bone marrow stem cells exhibit neural phenotypes and ameliorate neurological deficits after grafting into the ischemic brain of rats." Exp Neurol **174**(1): 11-20.

Zhao, P. and E. P. Hoffman (2004). "Embryonic myogenesis pathways in muscle regeneration." Dev Dyn **229**(2): 380-92.